AC- SU 8

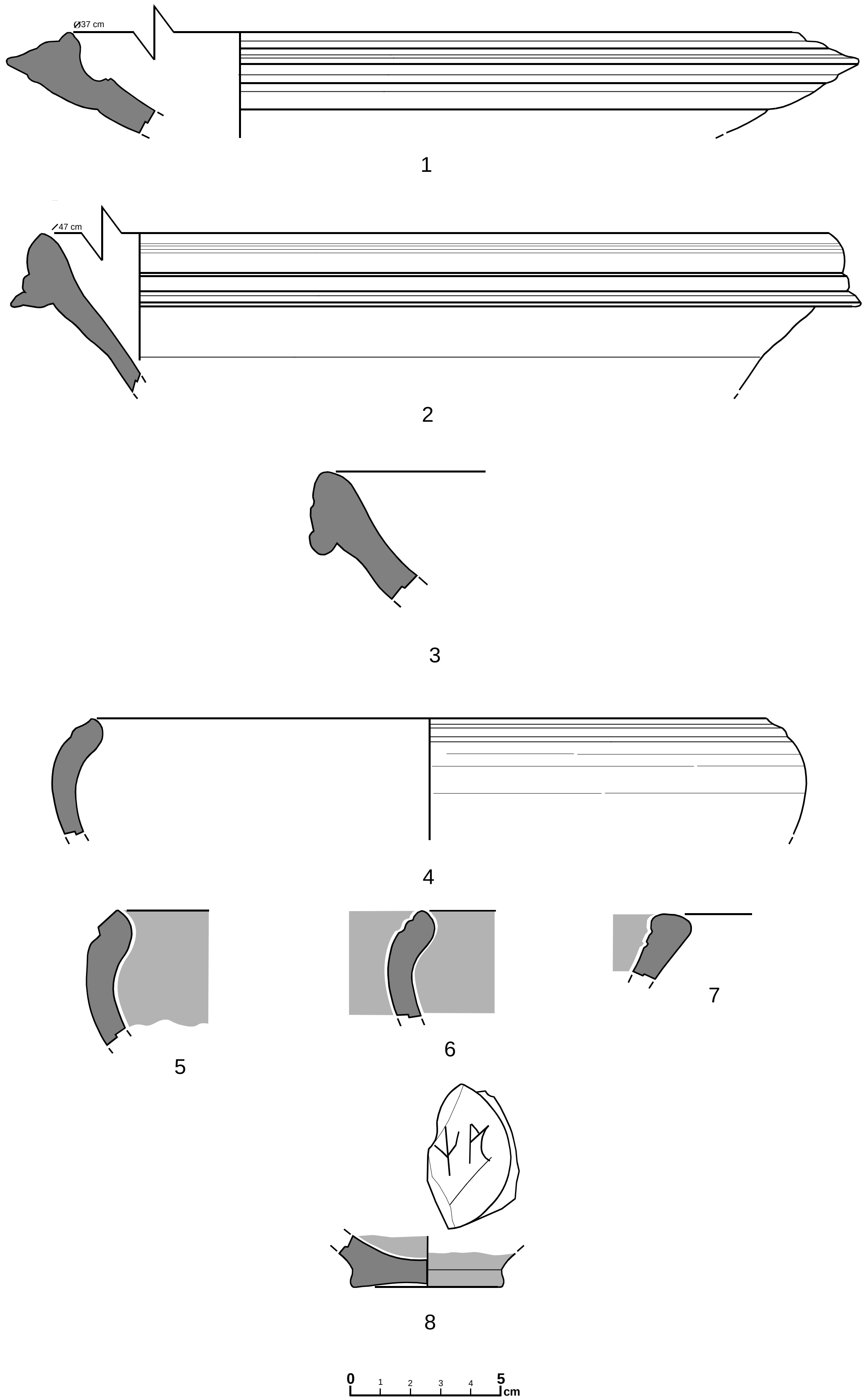

AC - SU 9

Definition: Interface

Interpretation:

Observations: Level of rubble from dwellings.

Material:

Archaeologist: J.M. Gurt

Intersecting (Structure)	3

AC - SU 10

Definition: Interface

Interpretation:

Observations: Level of rubble from dwellings.

Material:

Archaeologist: J.M. Gurt

Intersecting (Structure)	4

AC - SU 11

Definition: Trodden earth floor

Interpretation: Hardened surface serving as a floor to level the terrain.

Observations: Very compact clayey level. Slightly dark brown in colour.

Material: Slip ware: 102 frags.
Common ware: 515 frags.
Cooking ware: 21 frags.
Stone construction elements: 1 frag.
Bone: (0,150 kg)

Archaeologist: S. Dahí

Covered by (Stratum)	8
Covering (Stratum)	12

AC- SU 11

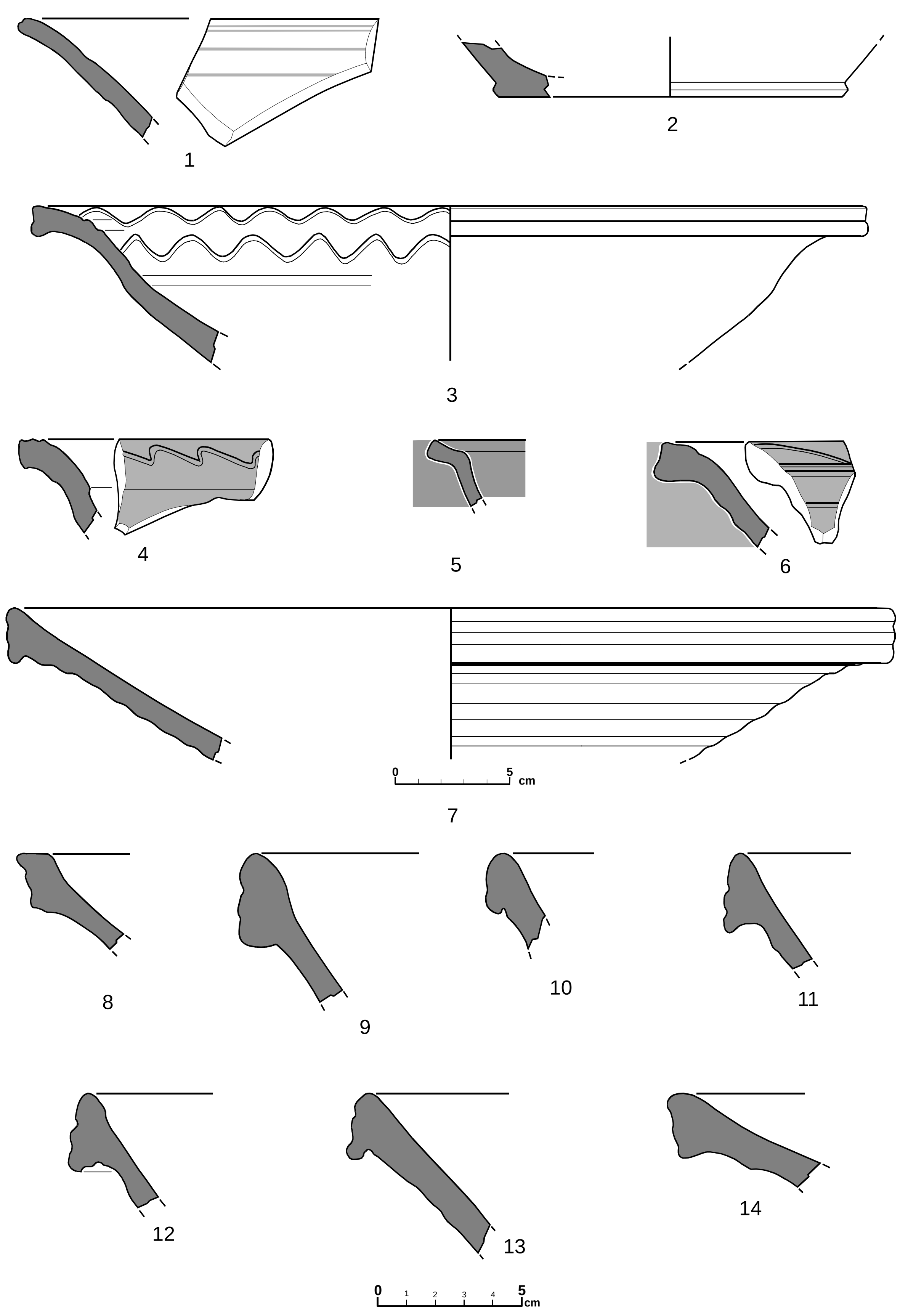

AC- SU 11

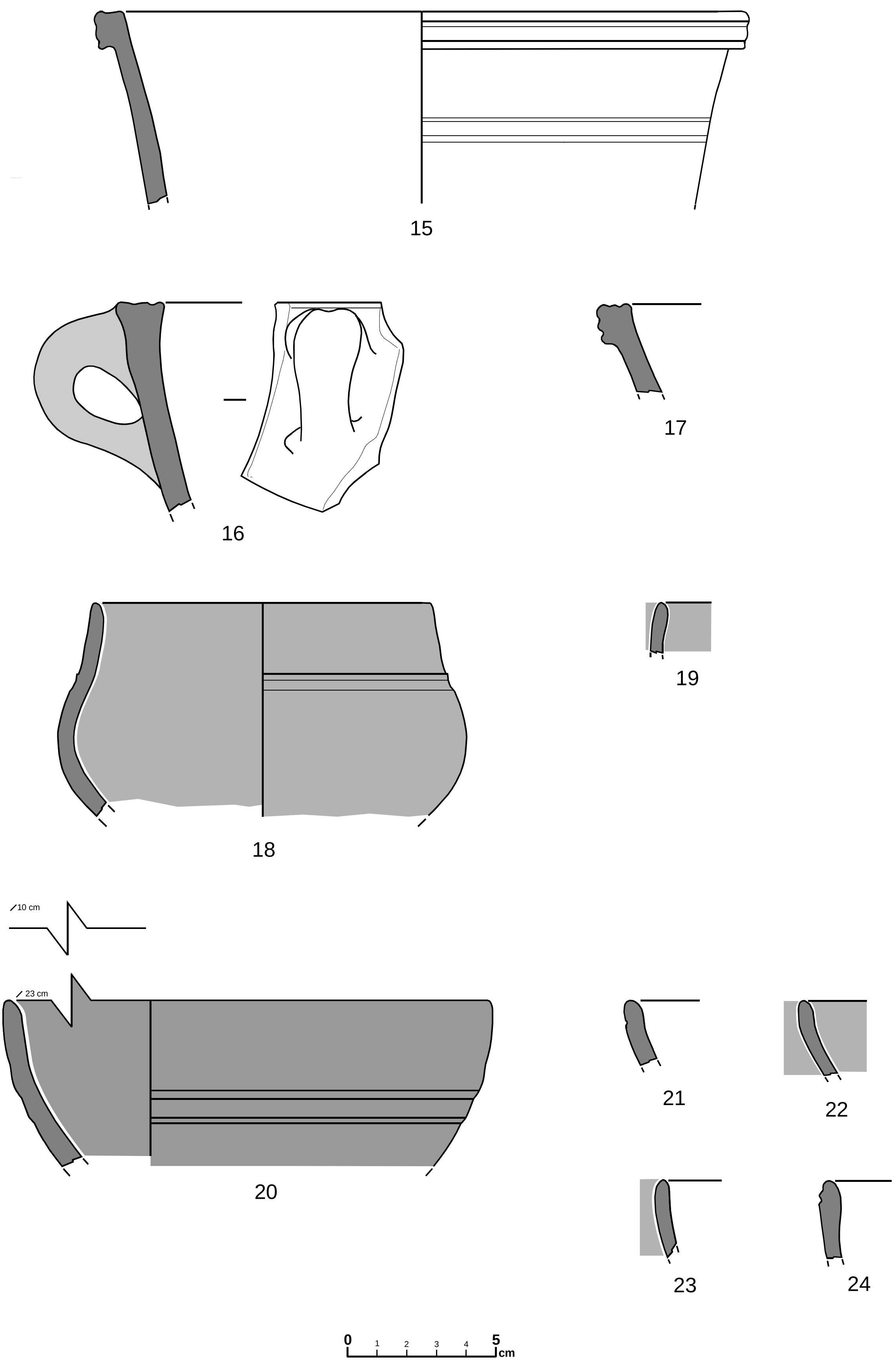

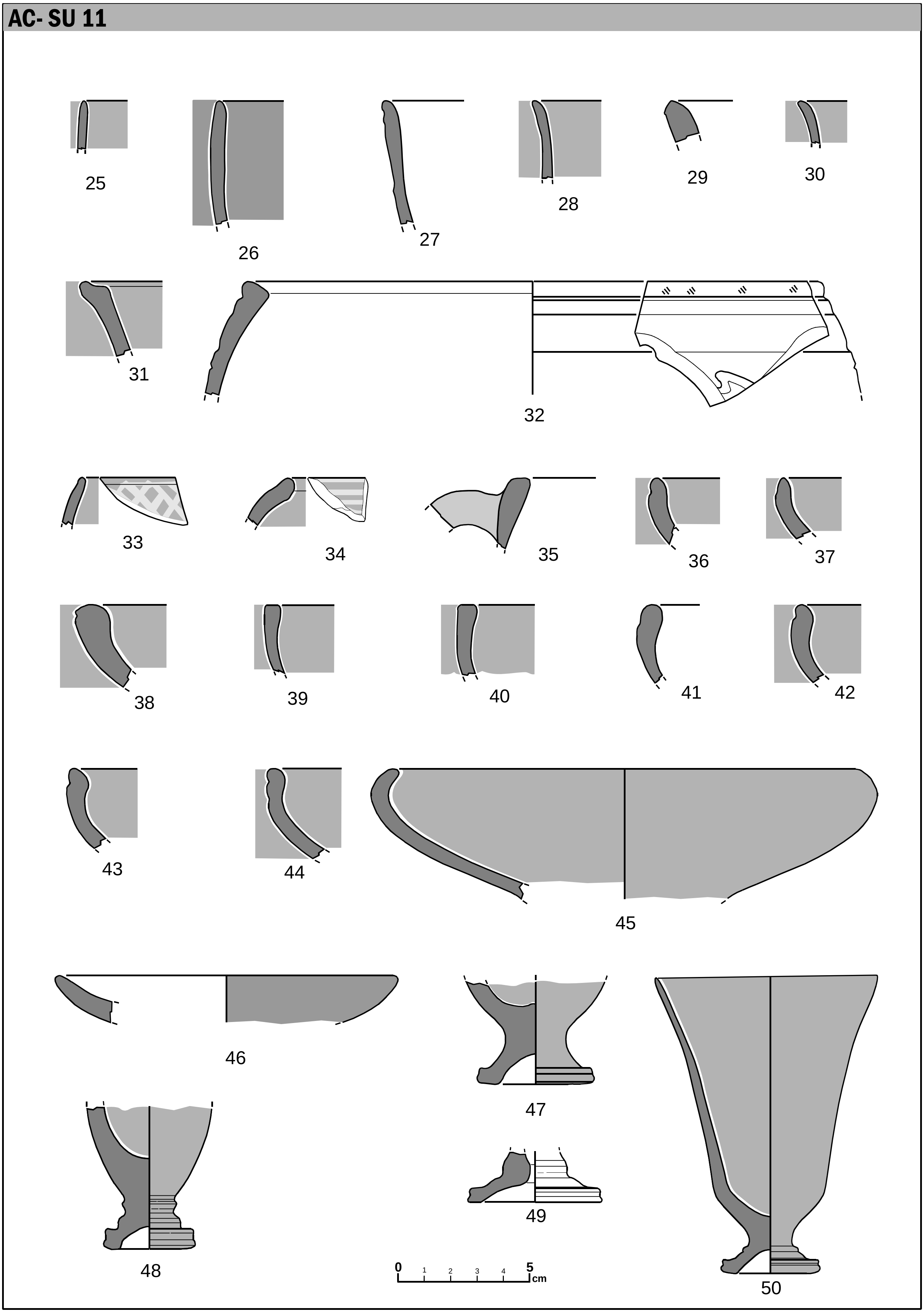
AC- SU 11
25
26
27
28
29
30
31
32
33
34
35
36
37
38
39
40
41
42
43
44
45
46
47
48
49
50
0
1
2
3
4
5
cm

AC- SU 11

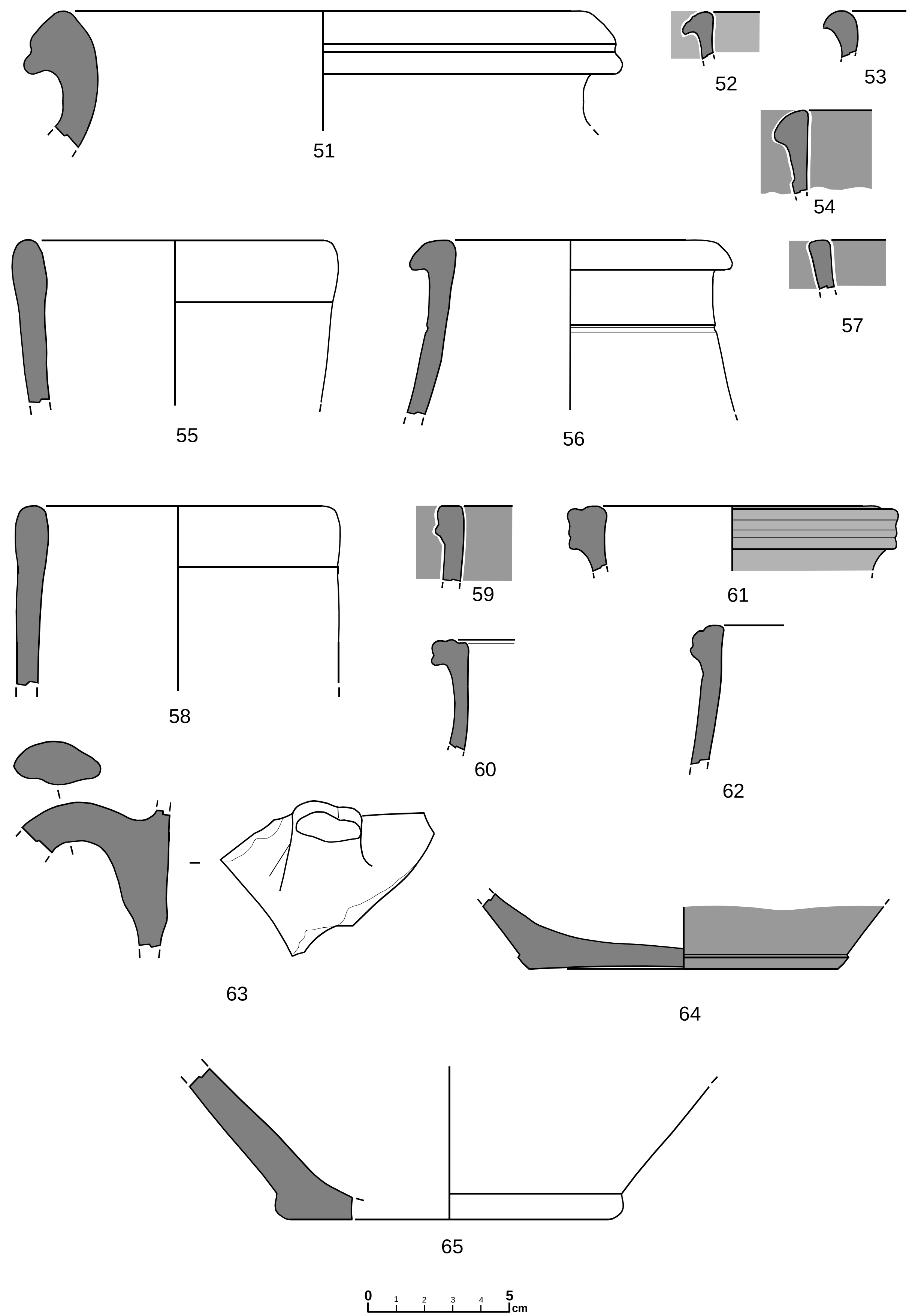

AC- SU 11

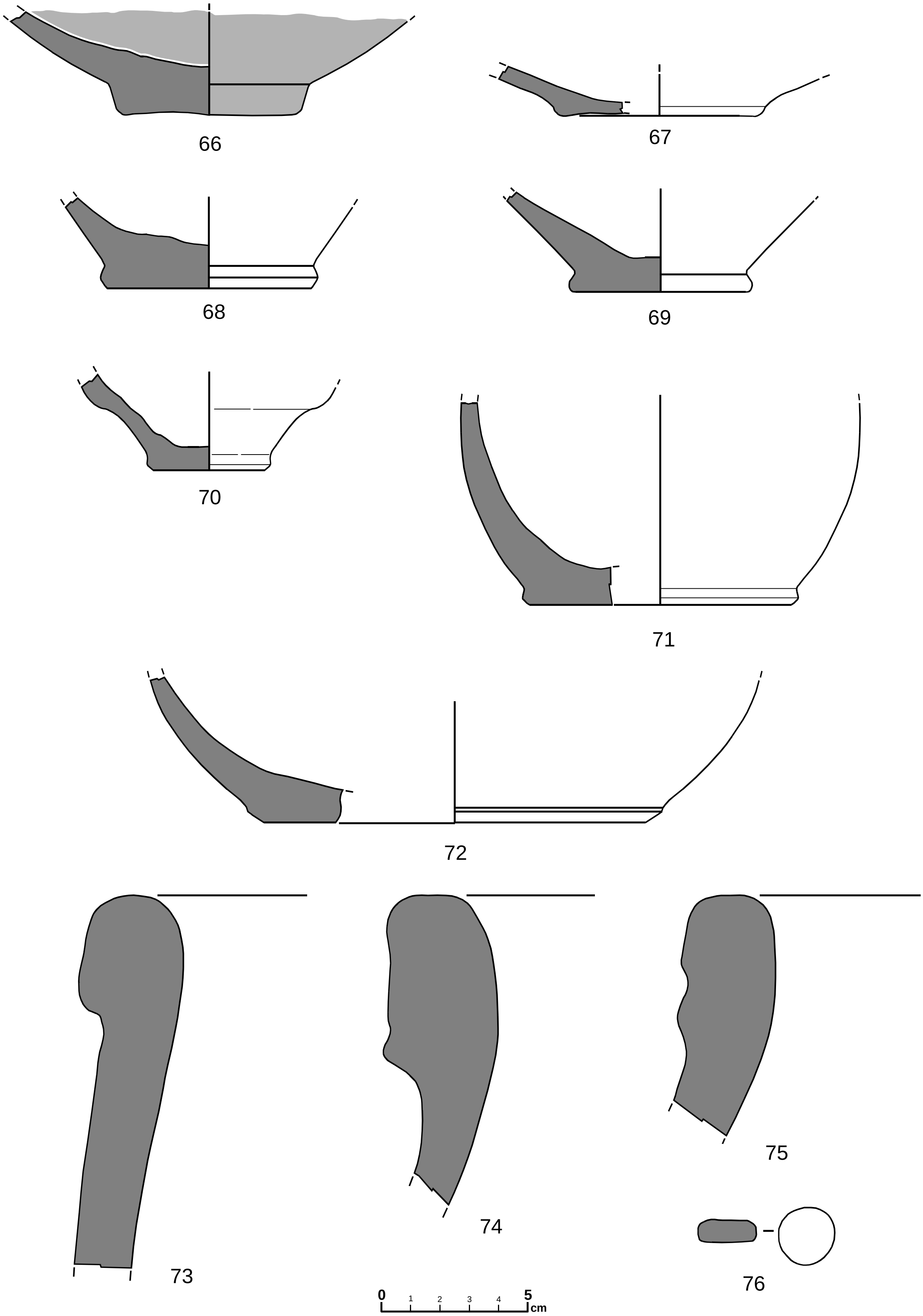

AC - SU 12

Definition: Trodden earth floor

Interpretation: Hardened surface serving as a floor to level the terrain.

Observations: Very compact clayey level. Ochre/dark-brown in colour. Containing a large amount of pottery, practically stuck to the bedrock (SU-13).

Material: Slip ware: 77 frags.
Common ware: 397 frags.
Cooking ware: 10 frags.
Bone: (1 kg)

Archaeologist: J.M. Gurt

Covered by (Stratum)	11
Covering (Stratum)	13
Filling: (Negative)	14
Covering (Structure)	15
Covering (Negative)	16

AC- SU 12

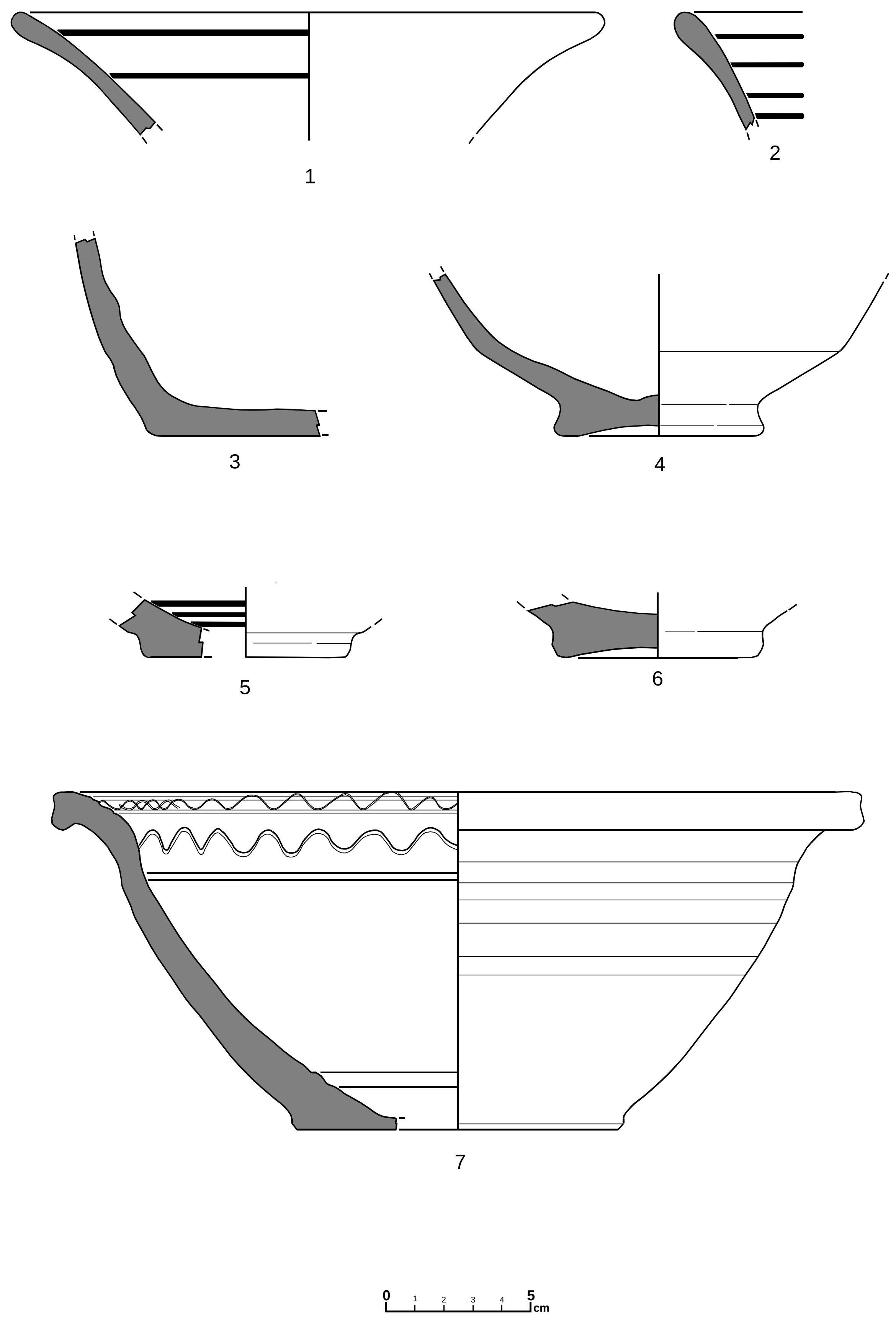

AC- SU 12

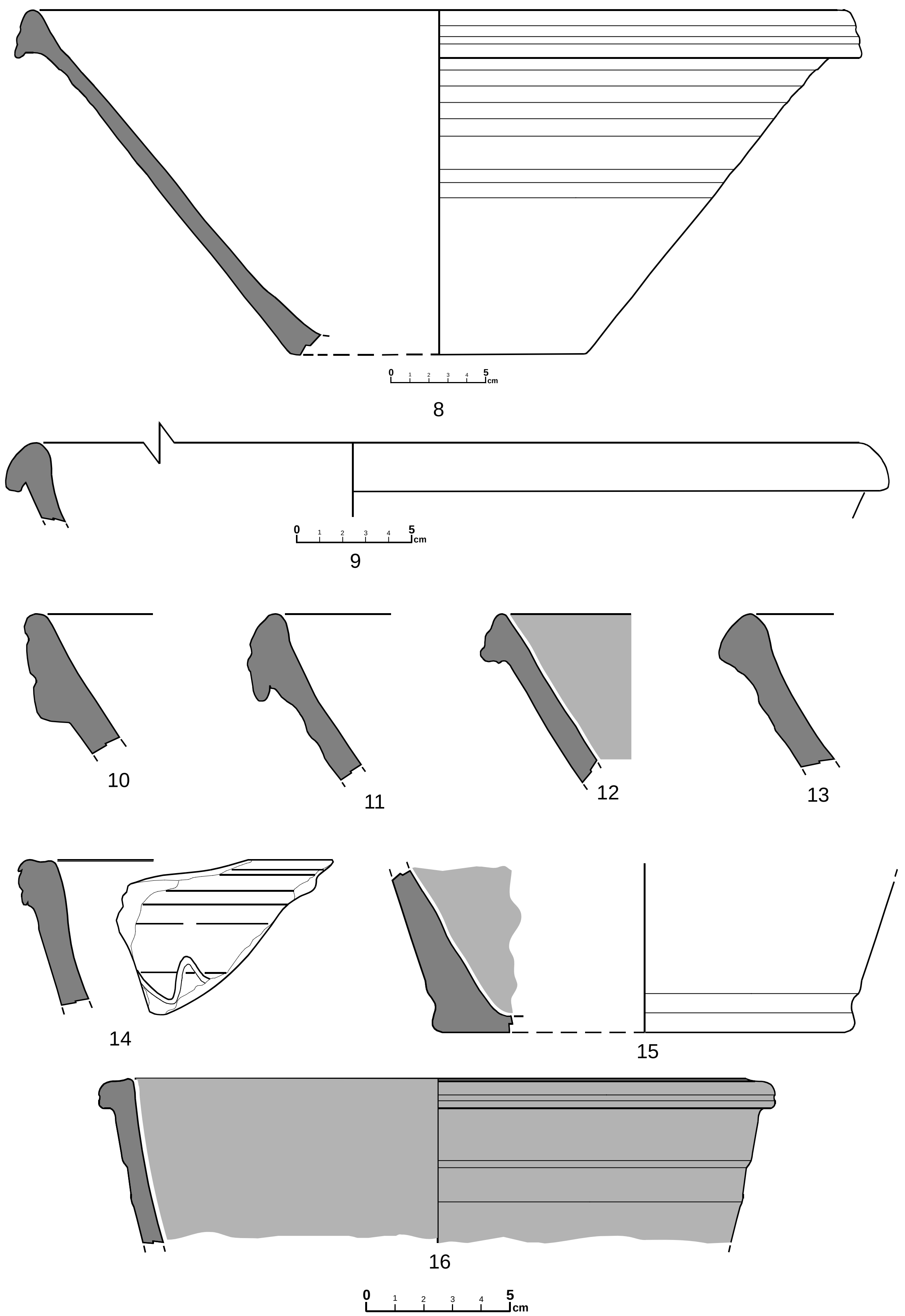

AC- SU 12

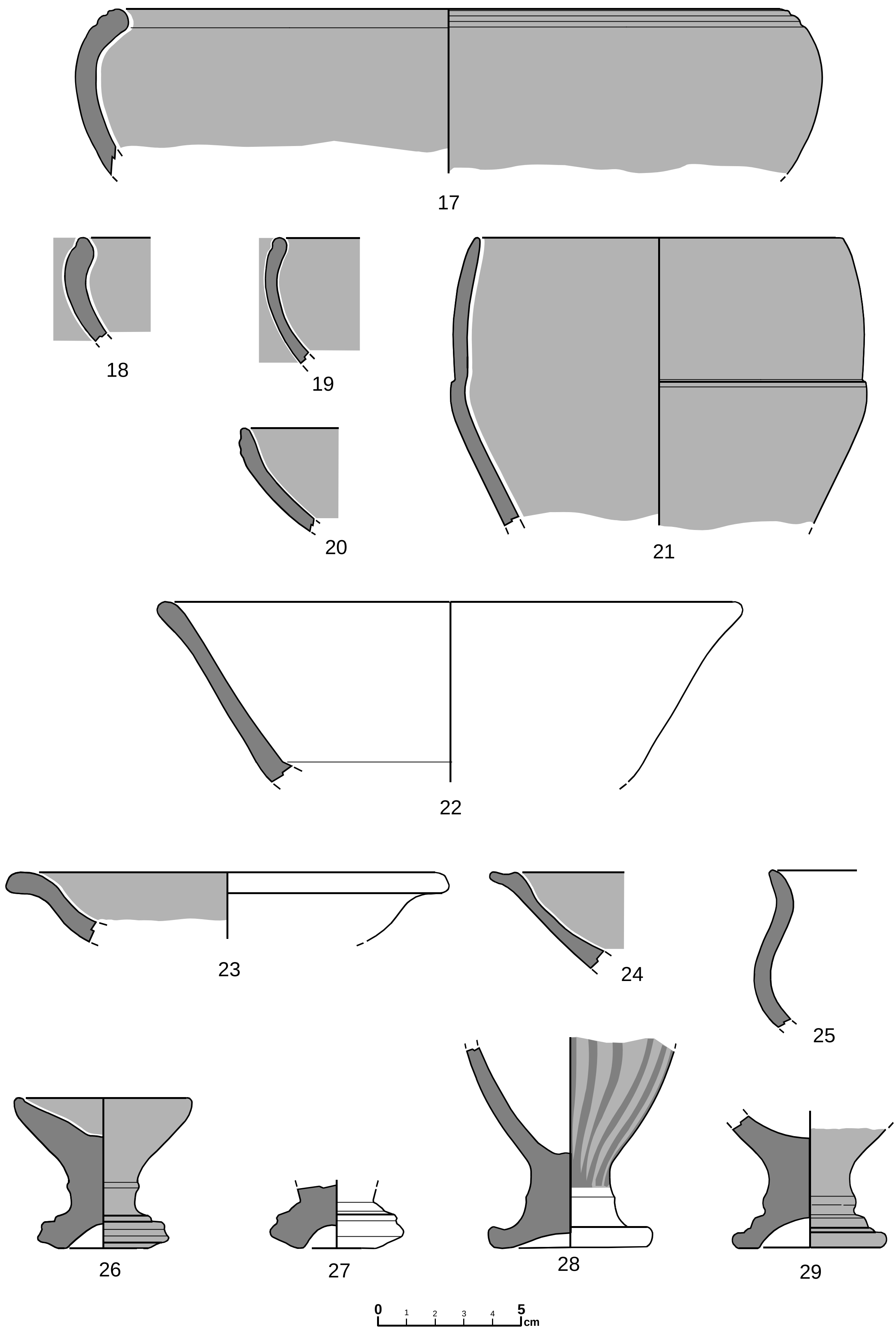

AC- SU 12

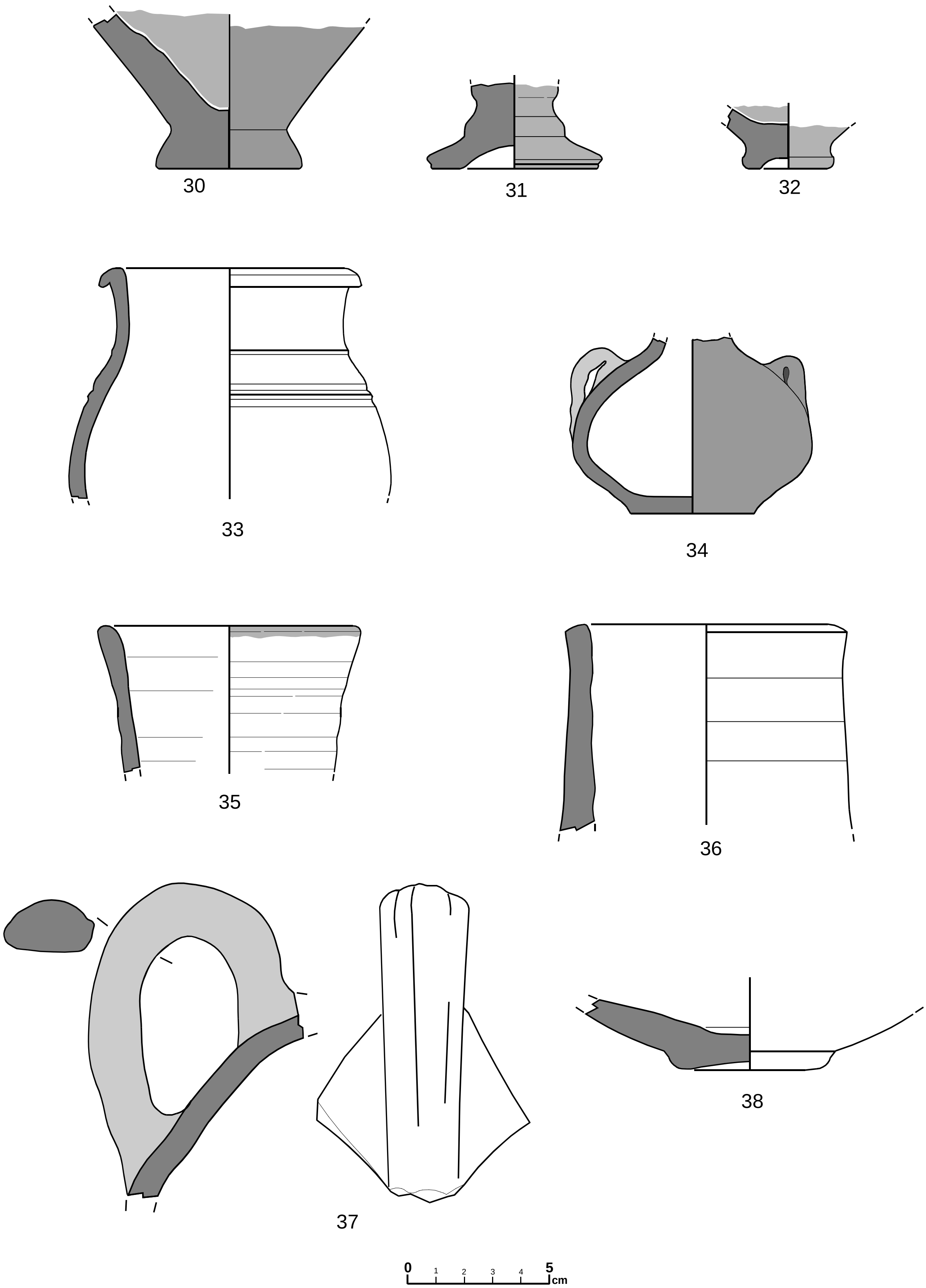

AC- SU 12

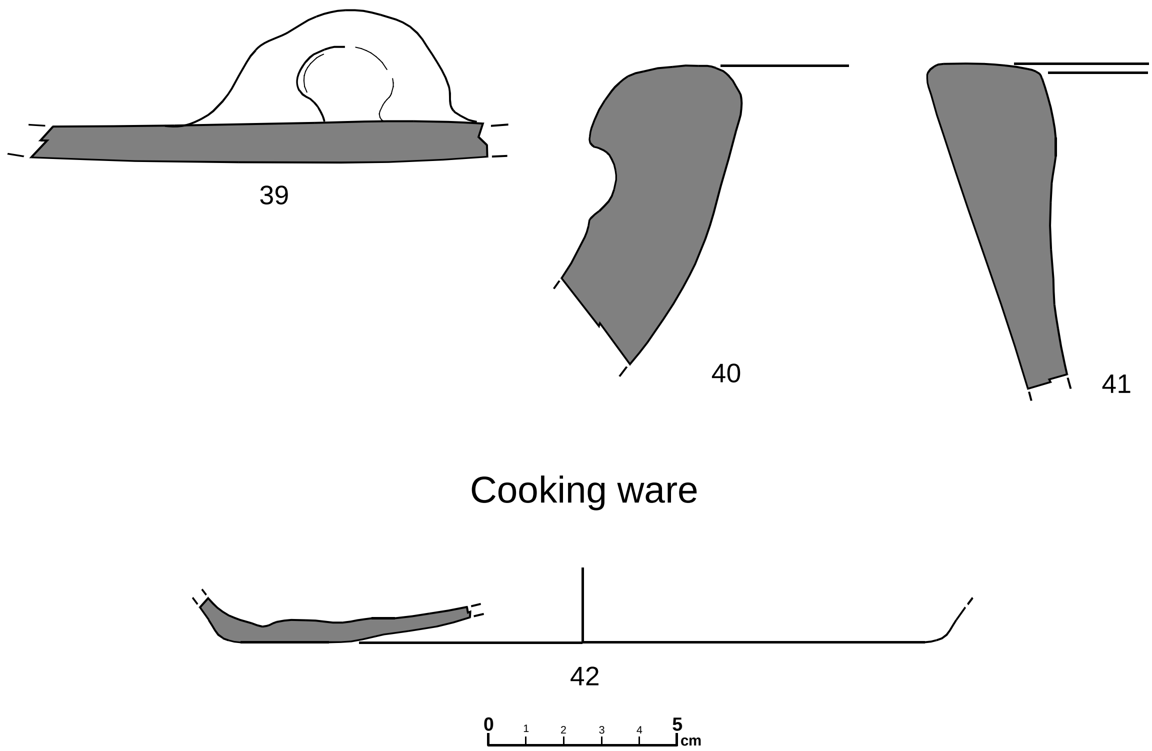

AC - SU 13

Definition: Bedrock

Interpretation:

Observations:

Material:

Archaelogist: J.M. Gurt

Covered by (Stratum)	12
Intersected by (Negative)	16-14

AC - SU 14

Definition: Interface in the bedrock

Interpretation:

Observations: The bedrock bears a cutting to fit a channel made out of standard ceramic pieces.

Material:

Archaeologist: J.M. Gurt

Infill from (Stratum)	12
Supporting (Structure)	15
Intersecting (Stratum)	13
Intersecting (Negative)	16

AC - SU 15

Definition: Ceramic channel

Interpretation: Channel with an interior diameter of roughly 10/12 cms, suggesting its use in the circulation of clean water. It has a marked slope.

Observations: Channel made out of standard ceramic elements.

Material:

Archaeologist: J.M. Gurt

Covered by (Stratum)	12
Resting on (Negative)	16-14

AC - SU 16

Definition: Interface in the bedrock

Interpretation:

Observations: The rock has been carved but the purpose cannot be determined. At one point, the channel (SU-15) passes directly over it.

Material:

Archaeologist: J.M. Gurt

Covered by (Stratum)	12
Intersected by (Negative)	14
Supporting (Structure)	15
Intersecting (Stratum)	13

SU- 13, 14, 15, 16

AC - SU 16

SU- 13, 14, 15, 16

Anthracological Analysis

Raquel Piqué i Huerta
of the UAB's Archaeological Analysis Service

Generally, the remains of carbonised wood found in archaeological sites come from wood burning in domestic fireplaces or specialised structures, such as ovens, which are related to artesanal production. As a result, studying the charcoal serves to identify which species have been used for these purposes, linking them to specific processes found in association with given structures. Dendrological analysis also yields data on the various way the resources were obtained and consumed, making it possible to establish which type of wood was burnt (wood from natural pruning, reusing the product of fruit-tree pruning, etc.), the gathering season, the state of the wood at the time of burning (dry, green), and the morphology of the wood used (branch, trunk). All of these data are critical to understanding the relationships between human groups and their habitats, not only because the charcoal provides evidence of the environment in which human groups developed, but also because it points to the ways they made use of that habitat.

TCH-T, RF, SU 26

It cannot be assumed that all the carbonised wood found in archaeological sites comes from wood burning. In the levels where burning appears, there are numerous remains of furniture, wooden tools and architectural elements (beams and posts). Determining where carbonised wood comes from is not always possible, because the state of fragmentation is typically great. The shapes and interrelationships of identified remains may not be recognisable. Consequently, fire levels require care in interpretation. Architectural elements and furniture may disintegrate as a result of carbonisation, giving rise to large quantities of fragments which may correspond to highly time-specific uses and not necessarily reflect the characteristics of the plant habitat.

TCH-T, RF, SU 26

TCH-T, RF, SU26

In the case of the samples taken from the Termez Tepe and Kampyr Tepe sites, the analysed remains correspond to residues of fuel used in a pottery kiln, in the former case (TCH-T, RF, SU-26), and could relate to architectural elements originating from the collapse of a roof, in the latter case (KP-T, C14-4). The objective of the analysis has been to focus on determining the species consumed, evaluate how they were obtained and attempt to establish their possible uses.

KP-T, C14-4

KP-T, C14-4

Method

The basis of the taxonomic classification of archaeological charcoal is the study of microanatomy and its comparison with current reference material. Anatomical analysis is performed with reflected light microscopy equipped with lenses that enable magnifications from 40X to 400X. The identification requires study of the three sections of the wood (transverse, radial longitudinal and tangential longitudinal), and the anatomical sections are prepared by manual slicing of the charcoal fragment. The keys used in identification are the ones published by Schweingruber (1990) and the comparative materials used were drawn from the reference collection of current carbonised wood at the Archaeological Analysis Service of the Autonomous University of Barcelona.

Material studied and results

The samples of carbonised wood came from three samples: TCH-T, RF, SU-26 and KP-T, C14-4. The first sample was composed of a set of stems of varying lengths and with diameters less than 5 mm. The second sample was composed of charcoal of highly variable size, although most were larger than a centimetre. Analysis proceeded on a sample of the stalks from TCH-T, RF, SU-26, in order to verify whether they were from the same taxon, and on the entirety of the remains from sample KP-T, C14-4. In total, 122 remains were studied, enabling at least six species to be identified. The species consumed were the plane tree (*Platanus sp*), ash tree (*Fraxinus sp*), willow tree (*Salix sp*), common fig tree (*Ficus carica*), common grape vine (*Vitis vinifera*) and a type of grass. As can be seen in Table I, which shows the results for each of the samples, the greatest diversity arises in the sample KPT-C14-4.

Sample	**SU**	Platanus SP	Fraxinus SP	Salix SP	Ficus Carica	Vitis Vinifera	Grasses	**Total**
TCH-T	RF-26						20	20
KP-T	C14-4	39	24	8	20	11		102

Table I. Results of anthracological analysis for Termez sample

Below are set out the main anatomical features observed in the studied remains.

- *Fraxinus* sp. (ash tree)

Anatomy

Transverse section: Porous wood. Isolated and grouped wares, ware size diminishes sharply between the initial wood and final wood (Figure 1). In the final wood wood, the wares are solitary or grouped radially (in groups of two).Vasicentric paratracheal parenchyma.

Tangential and radial longitudinal sections: radii in two and three rows, homogeneous.

Simple perforations.

Ecology

Deciduous tree that lives near rivers and streams.

Wood properties

Very tough and elastic. The leaves are used to feed livestock (Romo, 1997)

Charcoal characteristics

The remains correspond to twigs of one to three years in age and from between 5 and 20 mm in diameter. The twigs were felled before a new growth ring had begun, pointing to cutting in autumn/winter.

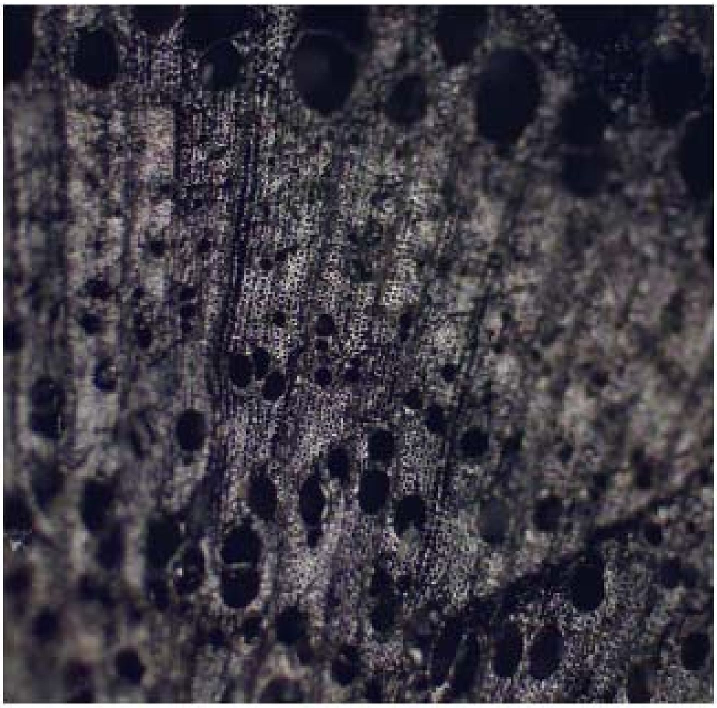

Figure 1. Transverse section of fragment of Fraxinus sp

- ***Platanus* sp** (plane tree)

Anatomy

Anatomy of the transverse section: wood is diffuse to semi-porous. Highly numerous wares, grouped. Very marked growth rings, with thickening radii at this height. Diffuse apotracheal parenchyma (Figures 2 and 3). Tangential and radial longitudinal sections: simple and stepped perforations with a variable number of bands. Homogenous radii, from between 4 and 10 cells in width and up to 2 mm in length (Figure 4).

Ecology

Deciduous tree that lives nears rivers and streams.

Wood properties

Hard wood, difficult to split and not very tough. Used in carpentry.

Charcoal characteristics

Some of the remains clearly correspond to branch fragments, other are shapeless and no original morphology can be seen. In some cases, the bark remains and it is possible to see that new cells had already begun to form in the growth ring at the time of felling, indicating that the remains were felled in the spring. In other cases, cut marks are visible and in one case a truncated conical shape is clearly visible, although we cannot say what kind of artefact was involved.

Figure 2. Transverse section of *Platanus sp*

Figure 3.Transverse section of Platanus sp, detail of last ring in which new wares can be seen forming at the time of cutting.

Figure 4. Tangential longitudinal section of Platanus sp

- ***Vitis vinifera*** (common grapevine)

Anatomy

The anatomical section does not enable the wild variety to be distinguished from the cultivated variety.

Transverse section: Porous wood tending towards semi-porosity. Very large wares, solitary or grouped in radial rows in the final wood (Figure 5). Tangential and radial longitudinal sections: Multiple rows of radii. Wares with stepped perforation showing a large number of bands (Figure 6).

Ecology

In the wild, it lives near woodland riverbanks. Many varieties of the species are cultivated.

Charcoal characteristics

The remains correspond to branches and twigs of variable thickness, up to around 20 mm. In one case, five growth rings could be counted. The moment of cutting cannot clearly be seen.

Figure 5. Transverse section of *Vitis vinifera*

Figure 6. Tangential longitudinal section of *Vitis vinifera*

- *Ficus carica* (common fig tree)

Anatomy

Transverse section: Diffuse wood. Very large wares, solitary or grouped in radial rows. Banded apotracheal parenchyma (Figure 7)

Tangential and radial longitudinal sections: Radii in three to five rows. Wares with simple perforations

Ecology

Many varieties of the species are cultivated and it can be introduced for growth in many places.

Wood properties

The wood of the fig tree is soft and of low quality.

Característiques dels carbons

The remains correspond to branches of between 10 and 20 mm in diameter.

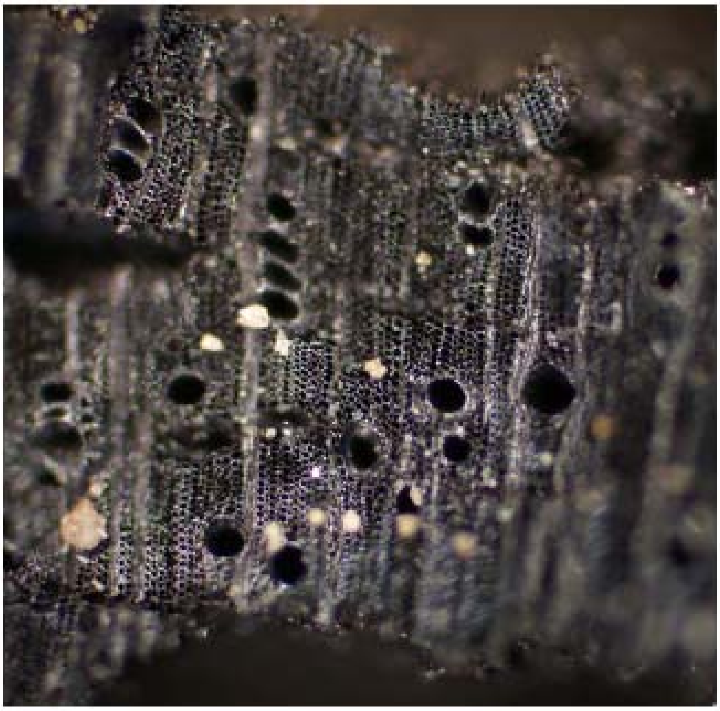

Figure 7. Transverse section of *Ficus carica*

- *Salix* sp (willow tree)

Anatomy

Transverse section: Diffuse wood. Principally solitary wares or grouped in short radial rows (Figure 8). Tangential and radial longitudinal section: Radii in single rows and heterogeneous (Figure 9). Wares with simple perforations.

Ecology

Several species of the Salix genus grow close to rivers and watercourses where they mix with other woodland species.

Wood properties

Willow wood is soft and pliable. Some species are used in basket weaving.

Charcoal characteristics

The remains clearly correspond to fragments of a trunk, because growth rings show very little curve and the fragments are generally very large. The trunk grew rapidly. There are traces of work, as some of the fragments shows sign of being split.

Figure 8. Transverse section of *Salix sp*

Figure 9. Tangential longitudinal section of *Salix sp*

- *Monocotyledon*

The branch remains present anatomical characteristics typical of monocotyledons, with primary xylem and phloem (Figure 10). The distribution of the anatomical elements in the transverse section is similar to what is observed in the grass family, but we are unable to determine which precise type it is.

Figure 10. Transverse section of grasses.

Discussion of results

The predominant taxa in the anthracological samples grow wild largely in woodlands near water. However, some of the species have been cultivated in the Mediterranean area since the first millennium of our era, i.e. grapes and figs. The anatomical characteristics do not enable wild varieties to be distinguished from cultivated varieties.

The ecological similarities of the given taxa raise the likelihood that the wood may have been gathered in woodlands that grow near watercourses. The riverside woodlands of Uzbekistan, known as “tugai” (CAREC 2006), are composed primarily of willows (Populus ssp, Salix ssp), although there are also other trees such as the ash (Fraxinus ssp) and the plane (Platanus orientalis) as well as vines (including the common grapevine). We may therefore consider that this type of woodland was intensively used to obtain wood for a variety of purposes (e.g., wood or raw material for construction). On the other hand, the presence of fig wood raises the possibility that the species was cultivated or brought from a greater distance, which does not seem likely in light of its poor quality. The use of the products of pruning may have been one of the reasons for the presence of this taxon.

Lastly, the monocotyledons encompass a large number of herbaceous species including grasses, which are in great abundance in steppe areas. Several species are represented and they may have been collected easily in the vicinity of the settlement.

We find it interesting to note the morphological differences observed in the studied taxa. As pointed out in the introduction to the results, many of the remains clearly correspond to branches and twigs of small diameters up to 20 mm (ash, grape, fig) or medium-sized diameters (plane). This points to a predominant use of branches and twigs and, in particular, a rigorous selection of young ones (between 1 and 5 years of age in the case of the ash and fig). The selection may stem from the purpose to which the wood was destined. It may have been used jointly with the grasses to cover the roof of the structure. However, we cannot rule out the practice of pruning, which would have enabled trees and bushes to be used over the longer term. In this respect, it is notable that the season of felling could be determined in two cases. It was spring in the case of the plane tree and autumn/winter in the case of the ash, which would indicate two distinct times for gathering the wood.

The only taxon for which the trunk was used is the willow (Salix sp), perhaps because it was used as a structural element to support the rest of the aerial structure.

We cannot state with certainty that the remains come from architectural elements, but the regularity of the shapes used (small branches and twigs) appears to point to a very careful selection. In addition, the presence of cut marks on the fragments of willow and plane would be consistent with a use of the wood as a construction element or in the use of furniture or tools.

Works cited

CENTRAL ASIA REGIONAL ECONOMIC COOPERATION (CAREC) 2006 *Non Wood Forest Products in Central Asia and Caucasus.* Roma: FAO

ROMO, A. (1997) *Árboles y arbustos de la Península Ibèrica y Baleares*. Barcelona: Planeta

SCHWEINGRUBER, F. (1990) *Anatomy of European Woods*. Bern/Stuttgart: Paul Haupt

Provenience and Technological study of the ceramics coming from the archaeological sites of Termez, Kampyr Tepe and Zar Tepe in Uzbekistan

Verònica Martínez, Evanthia Tsantini, Josep Maria Gurt i Shakir Pidaev

Introduction

In Uzbekistan a number of archaeometrical studies were done during the 1980's and early 90's using chemical and mineralogical analysis, notably by S. V. Vivdenko and A. Abdurazakov. The first analysed sherds from a number of sites mostly dated to the Iron Age but also from the Kushan period at Jalangtush Tepe [Vivdenko 1987, 1987a, 1990, 1992, 1993, 1994 and 1996]. Abdurazakov also

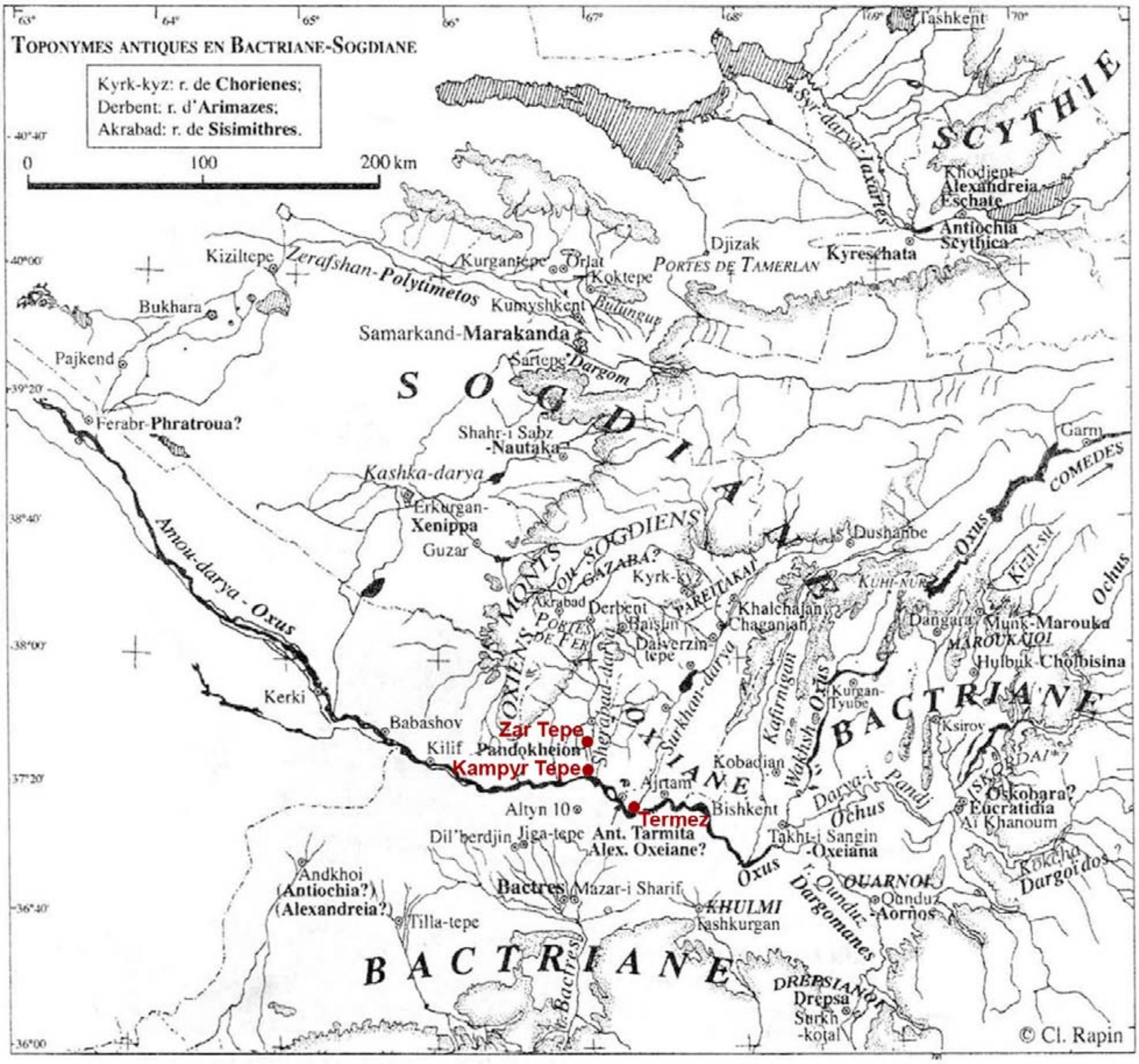

Figure 1: Localization of the studied archaeological sites
The cartographic base used corresponds to the figure number 1 (p. 30) published by:
Rapin, C. 2007, Nomads and the Shaping of Central Asia: from the Early Iron Age to the Kushan period. After Alexander. Central Asia before Islam (Joe Cribb and Georgina Herrmann edits.) in Proceedings of the British Academy 133, pp. 29-72.

analysed a few sherds, mainly dated to the Bronze Age but including some from the Kushan period at sites such as Mirzakul' Tepe and Talashkan Tepe [Abdurazakov, Bezborodov *et al.* 1963, Abdurazakov 1988, Abdurazakov 1996, Abdurazakov, Dzhalalova 1986, Abdurazakov 1987]. None of this work had the necessary continuation neither was based on the definition of Reference Groups (RG) of Paste Compositional Reference Units (PCRU) which is a fundamental process in the mark of provenience studies in order to attempt to locate the *origin* or the *production site* where the pottery was made [Picon, 1984; Buxeda *et al.*,1995].

The present work is centred on the archaeometrical study of 299 individuals sampled at different locations at the archaeological site of ***Termez*** (Uzbekistan), at the archaeological site of ***Kampir Kampyr Tepe*** (Uzbekistan) and finally coming from the superficial prospection of the archaeological site of ***Zar Tepe.*** (Uzbekistan) (Figure 1).

The selection of the new material for analysis was based on the already obtained results from the archaeometrical and archaeological study of the 144 (2006/2007) ceramic individuals recovered at different areas of ***Termez*** (basically from ***Kara Tepe***, ***Tchinguiz Tepe,*** the ***Ciutadelle*** and the ***Monasteries***), taking into consideration these results, which meant to compare the different productions from ***Kara Tepe's Kiln Nº2*** and ***Kiln Nº1***, the ***Monasteries***, which are located in the close proximities of both Kiln sites, as well the materials coming from ***Tchinguiz Tepe*** and the ***Ciutadelle***, which seems to be the chronologically eldest between the excavated sites. In the frame of this year's work 58 new samples coming from a new kiln site and other areas of ***Tchinguiz Tepe*** have been incorporated in the study thus to be able to compare and expand the information upon pottery making at the city of ***Termez*** and 88 samples from two new sites ***Kampyr Tepe*** and ***Zar Tepe*** are included in the study to expand our knowledge upon pottery making in the broader territory. ***Kampyr Tepe*** (Long 67º01'38'' Lat 37º24'38'') (Stride 2004 Uz-SD-226) and ***Zar Tepe*** (Long 67º09'18'' Lat 37º24'46'') (Stride 2004 Uz-SD-223), both situated to a short distance from ***Termez***. The first one is located upon the border of the river ***Amu Darya***, 30 kms to the West from ***Termez***. The second one is located within the delta of ***Sherobood***.

At ***Kampyr Tepe***, the samples selected according to the previous work of the archaeologists of the Oriental Museum of Moscow, with whom we established collaboration to be able to carry out this study. The sampling is centered on material that can be dated by C^{14} and for that reason we also obtained organic samples from the stratigrafical units where the ceramics comes from. On the other hand, at ***Zar Tepe*** the sampling carried out by some of the members of our archaeological mission after a superficial prospecting. In this case, the proper typologies will be based upon the chronology obtained from the C^{14} and by comparing with the other ceramic types identified at the rest of the sites.

Kampyr Tepe is a city situated at the site of the river ***Amu Darya,*** surrounded by a wall with defence towers exactly like the one found at ***Tchinguiz Tepe*** within the modern city of ***Termez.*** Inside the city walls the citadel's area protected by a wall that has 4 hectares of extension, although the total extension of the archaeological site is 15 hectares. The lifelong excavation showed that the city of ***Kampyr Tepe*** must have been occupied during the Hellenistic period and throughout the first phase of the Kushan period.

Zar Tepe corresponds to a rectangular urban structure also surrounded by a defence wall supported by towers and a moat of 17 hectares of extension. The citadel's area estimated to 14 400 m^2 (120 x120 m) and it is located at the North East of city separated by the moat. At the South East there is another possible citadel. The excavations carried out up to now date the citadel to the Kushan or Sassano-Kushan period.

MATERIAL FROM TERMEZ			
Analytical code	**Number of inventory**	**Site**	**Type of ceramic**
TRZ001	TZ06-UE 11-4	KARA TEPE KILN 2	Open rim, painted common ware
TRZ002	TZ06-UE 12-9	KARA TEPE KILN 2	Open rim, painted common ware
TRZ003	TZ06-UE 12-7	KARA TEPE KILN 2	Open rim, painted common ware
TRZ004	TZ06-UE 11-2	KARA TEPE KILN 2	Base
TRZ005	TZ06-UE 9-2	KARA TEPE KILN 2	Base of a painted common ware
TRZ006	TZ06-UE 12-4	KARA TEPE KILN 2	Open rim, painted common ware
TRZ007	TZ06-UE 1-2	KARA TEPE KILN 2	Base
TRZ008	TZ06-UE 9-16	KARA TEPE KILN 2	Closed rim, painted common ware
TRZ009	TZ06-UE 9-1	KARA TEPE KILN 2	Open rim, common ware
TRZ010	TZ06-UE 9-9	KARA TEPE KILN 2	Open rim, common ware
TRZ011	TZ06-UE 1-7	KARA TEPE KILN 2	Open rim, common ware
TRZ012	TZ06-UE 1-3	KARA TEPE KILN 2	Open rim, painted common ware
TRZ013	TZ06-UE 1-5	KARA TEPE KILN 2	Open rim, painted common ware
TRZ014	TZ06-UE 11-3	KARA TEPE KILN 2	Open rim, painted common ware
TRZ015	TZ06-UE 9-17	KARA TEPE KILN 2	Open rim, painted common ware
TRZ016	TZ06-UE 12-8	KARA TEPE KILN 2	Closed rim, common ware
TRZ017	TZ06-UE 9-8	KARA TEPE KILN 2	Closed rim, common ware
TRZ018	TZ06-UE 12-10	KARA TEPE KILN 2	Open rim, painted common ware
TRZ019	TZ06-UE 9-10	KARA TEPE KILN 2	Top of painted common ware
TRZ020	TZ06-UE 12-5	KARA TEPE KILN 2	Open rim, common ware
TRZ021	TZ06-UE 9-15	KARA TEPE KILN 2	Open rim, common ware
TRZ022	TZ06-UE 11-5	KARA TEPE KILN 2	Open rim, common ware
TRZ023	TZ06-UE 9-19	KARA TEPE KILN 2	Base of a painted common ware
TRZ024	TZ06-UE 9-3	KARA TEPE KILN 2	?
TRZ025	TZ06-UE 11-1	KARA TEPE KILN 2	Closed rim, painted common ware
TRZ026	TZ06-UE 9-18	KARA TEPE KILN 2	Base
TRZ027	TZ06-UE 9-4	KARA TEPE KILN 2	Open rim, painted common ware
TRZ028	TZ06-UE 9-7	KARA TEPE KILN 2	Closed rim, painted common ware
TRZ029	TZ06-UE 9-5	KARA TEPE KILN 2	Open rim, common ware
TRZ030	TZ06-UE 12-3	KARA TEPE KILN 2	Open rim, painted common ware
TRZ031	TZ06-UE 9-11	KARA TEPE KILN 2	Open rim, common ware
TRZ032	TZ06-UE 9-20	KARA TEPE KILN 2	Open rim, painted common ware
TRZ033	TZ06-UE 9-13	KARA TEPE KILN 2	Closed rim, common ware
TRZ034	TZ06-UE 1-6	KARA TEPE KILN 2	Open rim, common ware
TRZ035	TZ06-UE 11-6	KARA TEPE KILN 2	Base
TRZ036	TZ06-UE 9-12	KARA TEPE KILN 2	Closed rim, painted common ware
TRZ037	TZ06-UE 12-2	KARA TEPE KILN 2	Open rim, common ware
TRZ038	TZ06-UE 1-1	KARA TEPE KILN 2	Open rim, common ware
TRZ039	TZ06-UE 12-6	KARA TEPE KILN 2	Open rim, common ware
TRZ040	TZ06-UE 1-4	KARA TEPE KILN 2	Open rim, common ware
TRZ041	TZ06-UE 12-1	KARA TEPE KILN 2	Open rim, common ware
TRZ042	TZ06-UE 9-14	KARA TEPE KILN 2	Open rim, common ware
TRZ043	TZ06-UE 9-6	KARA TEPE KILN 2	Closed rim, common ware
TRZ044	TZ06P-6E-1	KARA TEPE - Prospection	Open rim, common ware
TRZ045	TZ06P-7D-1	KARA TEPE - Prospection	Open rim, painted common ware
TRZ046	TZ06P-8D-1	KARA TEPE - Prospection	Open rim, painted common ware
TRZ047	TZ06P-4E-1	KARA TEPE - Prospection	Open rim, painted common ware
TRZ048	TZ06P-9F-1	KARA TEPE - Prospection	Open rim, painted common ware
TRZ049	TZ06P-12A-1	KARA TEPE - Prospection	Open rim, painted common ware
TRZ050	TZ06P-3E-1	KARA TEPE - Prospection	Open rim, common ware
TRZ051	TZ07-RC-10-1	TCHINGUIZ TEPE - RC	Open rim, painted common ware
TRZ052	TZ07-RC-10-2	TCHINGUIZ TEPE - RC	Open rim, painted common ware
TRZ053	TZ07-RC-10-3	TCHINGUIZ TEPE - RC	Open rim, common ware
TRZ054	TZ07-RC-10-4	TCHINGUIZ TEPE - RC	Closed rim, painted common ware
TRZ055	TZ07-RC-10-5	TCHINGUIZ TEPE - RC	Open rim, painted common ware
TRZ056	TZ07-RC-10-6	TCHINGUIZ TEPE - RC	Open rim, painted common ware
TRZ057	TZ07-RC-10-7	TCHINGUIZ TEPE - RC	Open rim, painted common ware
TRZ058	TZ07-RC-10-8	TCHINGUIZ TEPE - RC	Open rim, painted common ware
TRZ059	TZ07-RC-10-9	TCHINGUIZ TEPE - RC	Open rim, painted common ware
TRZ060	TZ07-RC-10-10	TCHINGUIZ TEPE - RC	Base
TRZ061	TZ07-RC-10-11	TCHINGUIZ TEPE - RC	Close rim, cooking ware
TRZ062	TZ07-RC-10-12	TCHINGUIZ TEPE - RC	Open rim, painted common ware
TRZ063	TZ07-RC-10-13	TCHINGUIZ TEPE - RC	Walls of painted common ware
TRZ064	TZ07-RC-10-14	TCHINGUIZ TEPE - RC	Open rim, painted common ware
TRZ065	TZ07-RC-10-15	TCHINGUIZ TEPE - RC	Open rim, painted common ware
TRZ066	TZ07-RC-10-16	TCHINGUIZ TEPE - RC	Open rim, painted common ware
TRZ067	TZ07-5D-17	TCHINGUIZ TEPE - Prospection	Walls of common ware
TRZ068	TZ07-5D-18	TCHINGUIZ TEPE - Prospection	Open rim, common ware
TRZ069	TZ07-5D-19	TCHINGUIZ TEPE - Prospection	Open rim, common ware
TRZ070	TZ07-5D-20	TCHINGUIZ TEPE - Prospection	Rim of common ware
TRZ071	TZ07-5D-21	TCHINGUIZ TEPE - Prospection	Rim of common ware
TRZ072	TZ07-5D-22	TCHINGUIZ TEPE - Prospection	Closed rim, common ware

Table 1: The analysed individuals

MATERIAL FROM TERMEZ			
Analytical code	**Number of inventory**	**Site**	**Type of ceramic**
TRZ073	TZ07-RC-6-23	TCHINGUIZ TEPE - RC	Walls of common ware
TRZ074	TZ07-RC-5-24	TCHINGUIZ TEPE - RC	Base
TRZ075	TZ07-RC-5-25	TCHINGUIZ TEPE - RC	Open rim, painted common ware
TRZ076	TZ07-RC-5-26	TCHINGUIZ TEPE - RC	Open rim, painted common ware
TRZ077	TZ07-RC-5-27	TCHINGUIZ TEPE - RC	Walls of common ware
TRZ078	TZ07-RC-5-28	TCHINGUIZ TEPE - RC	Walls of painted common ware
TRZ079	TZ07-RC-5-29	TCHINGUIZ TEPE - RC	Walls of common ware
TRZ080	TZ07-RC-5-30	TCHINGUIZ TEPE - RC	Open rim, painted common ware
TRZ081	TZ07-RC-5-31	TCHINGUIZ TEPE - RC	Open rim, painted common ware
TRZ082	TZ07-RC-5-32	TCHINGUIZ TEPE - RC	Walls of common ware
TRZ083	TZ07-RC-5-33	TCHINGUIZ TEPE - RC	Open rim, common ware
TRZ084	TZ07-RC-5-34	TCHINGUIZ TEPE - RC	Closed rim, common ware
TRZ085	TZ07-RC-5-35	TCHINGUIZ TEPE - RC	Top of cooking ware
TRZ086	TZ07-RC-5-36	TCHINGUIZ TEPE - RC	Walls of painted common ware
TRZ087	TZ07-RC-5-37	TCHINGUIZ TEPE - RC	Walls of painted common ware
TRZ088	TZ07-RB-5-38	TCHINGUIZ TEPE - RC	Open rim, common ware
TRZ089	TZ07-RB-5-39	TCHINGUIZ TEPE - RC	Walls of painted common ware
TRZ090	TZ07-RB-5-40	TCHINGUIZ TEPE - RC	Base
TRZ091	TZ07-RB-5-41	TCHINGUIZ TEPE - RC	Open rim, common ware
TRZ092	TZ07-RB-5-42	TCHINGUIZ TEPE - RC	Closed rim, common ware
TRZ093	TZ07-4-43	CIUTADELLE	Open rim, common ware
TRZ094	TZ07-4-44	CIUTADELLE	Open rim, common ware
TRZ095	TZ07-4-45	CIUTADELLE	Open rim, common ware
TRZ096	TZ07-4-46	CIUTADELLE	Open rim, common ware
TRZ097	TZ07-4-47	CIUTADELLE	Open rim, painted common ware
TRZ088	TZ07-4-48	CIUTADELLE	Open rim, painted common ware
TRZ099	TZ07-4-49	CIUTADELLE	Open rim, painted common ware
TRZ100	TZ07-4-50	CIUTADELLE	Open rim, common ware
TRZ101	TZ07-4-51	CIUTADELLE	Base of painted common ware
TRZ102	TZ07-4-52	CIUTADELLE	Open rim, painted common ware
TRZ103	TZ07-4-53	CIUTADELLE	Open rim, painted common ware
TRZ104	TZ07-54	CIUTADELLE	Closed rim, common ware
TRZ105	TZ07-4-55	CIUTADELLE	Base of painted common ware
TRZ106	TZ07-56	CIUTADELLE	Walls of painted common ware
TRZ107	TZ07-4-57	CIUTADELLE	Open rim, painted common ware
TRZ108	TZ07-4-58	CIUTADELLE	Base of painted common ware
TRZ109	TZ07-4-59	CIUTADELLE	Open rim, common ware
TRZ110	TZ07-4-60	CIUTADELLE	Closed rim, common ware
TRZ111	TZ07-4-61	CIUTADELLE	Open rim, common ware
TRZ112	TZ07-4-62	CIUTADELLE	Open rim, common ware
TRZ113	TZ07-4-63	CIUTADELLE	Open rim, common ware
TRZ114	TZ07-5-64	CIUTADELLE	Open rim, common ware
TRZ115	TZ07-65	CIUTADELLE	Open rim, common ware
TRZ116	TZ07-66	CIUTADELLE	Closed rim, common ware
TRZ117	TZ07-67	CIUTADELLE	Open rim, common ware
TRZ118	TZ07-68	CIUTADELLE	Base
TRZ119	TZ07-69	CIUTADELLE	Open rim, common ware
TRZ120	TZ07-70	CIUTADELLE	Open rim, common ware
TRZ121	TZ07-4-71	CIUTADELLE	Open rim, common ware
TRZ122	TZ07-72	CIUTADELLE	Closed rim, common ware
TRZ123	TZ07-73	KARA TEPE KILN 1	Open rim, painted common ware
TRZ124	TZ07-74	KARA TEPE KILN 1	Base
TRZ125	TZ07-75	KARA TEPE KILN 1	Open rim, painted common ware
TRZ126	TZ07-76	KARA TEPE KILN 1	Closed rim, common ware
TRZ127	TZ07-77	KARA TEPE KILN 1	Kiln material
TRZ128	TZ07-78	KARA TEPE Monasteries	Closed rim, painted common ware
TRZ129	TZ07-79	KARA TEPE Monasteries	Open rim, painted common ware
TRZ130	TZ07-80	KARA TEPE Monasteries	Open rim, painted common ware
TRZ131	TZ07-81	KARA TEPE Monasteries	Lantern
TRZ132	TZ07-82	KARA TEPE Monasteries	Closed rim, common ware
TRZ133	TZ07-83	KARA TEPE Monasteries	Walls of painted common ware
TRZ134	TZ07-84	KARA TEPE Monasteries	Closed rim, painted common ware
TRZ135	TZ07-85	KARA TEPE Monasteries	Open rim, painted common ware
TRZ136	TZ07-86	KARA TEPE Monasteries	Closed rim, painted common ware
TRZ137	TZ07-87	KARA TEPE Monasteries	Open rim, common ware
TRZ138	TZ07-88	KARA TEPE Monasteries	Closed rim, common ware
TRZ139	TZ07-89	KARA TEPE Monasteries	Closed rim, painted common ware
TRZ140	TZ07-90	KARA TEPE Monasteries	Closed rim, painted common ware
TRZ141	TZ07-91	KARA TEPE Monasteries	Open rim, painted common ware
TRZ142	TZ07-92	KARA TEPE Monasteries	Open rim, painted common ware
TRZ143	TZ07-93	KARA TEPE Monasteries	Open rim, painted common ware
TRZ144	TZ07-94	KARA TEPE Monasteries	Open rim, painted common ware

Table 1: The analysed individuals

MATERIAL FROM TERMEZ			
Analytical code	**Number of inventory**	**Site**	**Type of ceramic**
TRZ145	TZ08-AC-11-1	Antic Military Quarters	Open rim, painted common ware
TRZ146	TZ08-AC-11-2	Antic Military Quarters	Open rim, painted common ware
TRZ147	TZ08-AC-11-3	Antic Military Quarters	Painted cup
TRZ148	TZ08-AC-11-4	Antic Military Quarters	Base of a painted cup
TRZ149	TZ08-AC-12-1	Antic Military Quarters	Open rim, painted common ware / gray int
TRZ150	TZ08-AC-12-2	Antic Military Quarters	Angular grey base
TRZ151	TZ08-AC-12-3	Antic Military Quarters	Angular grey base
TRZ152	TZ08-AC-12-4	Antic Military Quarters	Angular grey base
TRZ153	TZ08-AC-12-5	Antic Military Quarters	Open rim, painted common ware
TRZ154	TZ08-AC-12-6	Antic Military Quarters	Base of a painted cup
TRZ155	TZ08-AC-12-7	Antic Military Quarters	Open rim, decorated by impression common ware
TRZ156	TZ08-AC-12-8	Antic Military Quarters	Base of a cooking ware
TRZ157	TZ08-RC-2-1	TCHINGUIZ TEPE - RC	Open rim, painted common ware
TRZ158	TZ08-RC-2-2	TCHINGUIZ TEPE - RC	Open rim, painted common ware
TRZ159	TZ08-RC-2-3	TCHINGUIZ TEPE - RC	Open rim, painted common ware
TRZ160	TZ08-RC-2-4	TCHINGUIZ TEPE - RC	Base of a painted cup
TRZ161	TZ08-RC-2-5	TCHINGUIZ TEPE - RC	Closed rim, cooking ware
TRZ162	TZ08-RC-3-1	TCHINGUIZ TEPE - RC	Base of a cooking ware
TRZ163	TZ08-RC-4-1	TCHINGUIZ TEPE - RC	Open rim, cooking ware
TRZ164	TZ08-RC-5-1	TCHINGUIZ TEPE - RC	Closed rim, painted common ware
TRZ165	TZ08-RC-5-2	TCHINGUIZ TEPE - RC	Open rim, painted common ware - gray paste
TRZ166	TZ08-RC-5-3	TCHINGUIZ TEPE - RC	Closed rim, painted common ware - gray paste
TRZ167	TZ08-RC-5-4	TCHINGUIZ TEPE - RC	High base of common ware
TRZ168	TZ08-RC-5-5	TCHINGUIZ TEPE - RC	Angular base of common ware
TRZ169	TZ08-RC-5-6	TCHINGUIZ TEPE - RC	Rim of a lantern
TRZ170	TZ08-RC-5-7	TCHINGUIZ TEPE - RC	Open rim, cooking ware-like african type
TRZ171	TZ08-RC-5-8	TCHINGUIZ TEPE - RC	Open rim, cooking ware
TRZ172	TZ08-RC-5-9	TCHINGUIZ TEPE - RC	Base of cooking ware
TRZ173	TZ08-RC-18-1	TCHINGUIZ TEPE - RC	Open rim, painted common ware
TRZ174	TZ08-RC-18-2	TCHINGUIZ TEPE - RC	Open rim, painted common ware wiht impressed decoration
TRZ175	TZ08-RC-18-3	TCHINGUIZ TEPE - RC	Open rim, painted common ware
TRZ176	TZ08-RC-18-4	TCHINGUIZ TEPE - RC	Open rim, painted common ware
TRZ177	TZ08-RC-21-1	TCHINGUIZ TEPE - RC	Open rim, painted common ware
TRZ178	TZ08-RC-21-2	TCHINGUIZ TEPE - RC	Open rim, painted common ware
TRZ179	TZ08-RC-21-3	TCHINGUIZ TEPE - RC	Closed rim, painted common ware wiht impressed decoration
TRZ180	TZ08-RC-21-4	TCHINGUIZ TEPE - RC	Open rim, painted common ware wiht impressed decoration (overfired)
TRZ181	TZ08-RC-21-5	TCHINGUIZ TEPE - RC	Closed rim, painted common ware wiht impressed decoration in the rim
TRZ182	TZ08-RC-21-6	TCHINGUIZ TEPE - RC	Open rim, cooking ware
TRZ183	TZ08-RC-21-7	TCHINGUIZ TEPE - RC	Tap of cooking ware
TRZ184	TZ08-RF-2-1	TCHINGUIZ TEPE - kiln RF	Open rim, common ware
TRZ185	TZ08-RF-11-1	TCHINGUIZ TEPE - kiln RF	Open rim, painted common ware with stamped decoration
TRZ186	TZ08-RF-11-2	TCHINGUIZ TEPE - kiln RF	Base of painted common ware
TRZ187	TZ08-RF-11-3	TCHINGUIZ TEPE - kiln RF	Rim of cooking ware
TRZ188	TZ08-RF-15-1	TCHINGUIZ TEPE - kiln RF	Base of a cip (overfired)
TRZ189	TZ08-RF-20-1	TCHINGUIZ TEPE - kiln RF	Cooking ware
TRZ190	TZ08-RF-20-2	TCHINGUIZ TEPE - kiln RF	Open rim, painted common ware
TRZ191	TZ08-RF-20-3	TCHINGUIZ TEPE - kiln RF	Open rim, painted common ware
TRZ192	TZ08-RF-22-1	TCHINGUIZ TEPE - kiln RF	Open rim, painted common ware wiht impressed decoration (overfired)
TRZ193	TZ08-RF-22-2	TCHINGUIZ TEPE - kiln RF	Open rim, painted common ware
TRZ194	TZ08-RF-22-3	TCHINGUIZ TEPE - kiln RF	Open rim, painted common ware with stamped decoration
TRZ195	TZ08-RF-23-1	TCHINGUIZ TEPE - kiln RF	Base of a painted common ware
TRZ196	TZ08-RF-23-2	TCHINGUIZ TEPE - kiln RF	Open rim, common ware
TRZ197	TZ08-RF-23-3	TCHINGUIZ TEPE - kiln RF	Open rim, common ware
TRZ198	TZ08-RF-23-4	TCHINGUIZ TEPE - kiln RF	Walls and rim of open rim, painted common ware with impr. decoration
TRZ199	TZ08-RF-27-1	TCHINGUIZ TEPE - kiln RF	Open rim, painted common ware
TRZ200	TZ08-RF-27-2	TCHINGUIZ TEPE - kiln RF	Open rim, painted common ware
TRZ201	TZ08-RC-23-1	TCHINGUIZ TEPE - RC	Open rim, painted common ware
TRZ202	TZ08-RF-29-1	TCHINGUIZ TEPE - kiln RF	Open rim, painted common ware

Table 1: The analysed individuals

MATERIAL FROM KAMPIR TEPE			
Analytical code	**Number of inventory**	**Site /SU**	**Type of ceramic**
TRZ203	KPT-08-IIIP/S-1	KILN: III period/West	Rim of a Crater
TRZ204	KPT-08-IIIP/S-2	KILN: III period/West	Closed rim common ware
TRZ205	KPT-08-IIIP/S-3	KILN: III period/West	Rim of a big bole
TRZ206	KPT-08-IIIP/S-4	KILN: III period/West	Open rim common ware
TRZ207	KPT-08-IIIP/S-5	KILN: III period/West	Open rim common ware
TRZ208	KPT-08-IIIP/S-6	KILN: III period/West	Small base
TRZ209	KPT-08-IP-1	Ciutadelle South-East/ 1st Period (II. B.d)	Open rim common ware
TRZ210	KPT-08-IP-2	Ciutadelle South-East/ 1st Period (II. B.d)	Open rim common ware
TRZ211	KPT-08-IP-3	Ciutadelle South-East/ 1st Period (II. B.d)	Base of a painted ware
TRZ212	KPT-08-IP-4	Ciutadelle South-East/ 1st Period (II. B.d)	Walls of a painted ware
TRZ213	KPT-08-IN-1	Ciutadelle North-East/ 1st Stratigraphic level upon the paviment	Base of a painted cup
TRZ214	KPT-08-IN-2	Ciutadelle North-East/ 1st Stratigraphic level upon the paviment	Base of a painted cup
TRZ215	KPT-08-IN-3	Ciutadelle North-East/ 1st Stratigraphic level upon the paviment	Base of a painted cup
TRZ216	KPT-08-IN-4	Ciutadelle North-East/ 1st Stratigraphic level upon the paviment	Base of a painted cup
TRZ217	KPT-08-IN-5	Ciutadelle North-East/ 1st Stratigraphic level upon the paviment	Base of a cup
TRZ218	KPT-08-IN-6	Ciutadelle North-East/ 1st Stratigraphic level upon the paviment	Walls and rim of a cooking ware
TRZ219	KPT-08-IIP-1	II PERIOD / III LEVEL	Open rim painted common ware
TRZ220	KPT-08-IIP-2	II PERIOD / III LEVEL	Open rim painted common ware
TRZ221	KPT-08-IIP-3	II PERIOD / III LEVEL	Open rim painted common ware
TRZ222	KPT-08-IIP-4	II PERIOD / III LEVEL	Open rim painted common ware (complete form)
TRZ223	KPT-08-IIP-5	II PERIOD / III LEVEL	Open rim painted common ware
TRZ224	KPT-08-IIP-6	II PERIOD / III LEVEL	Open rim painted common ware
TRZ225	KPT-08-IIP-7	II PERIOD / III LEVEL	Open rim painted common ware
TRZ226	KPT-08-IIP-8	II PERIOD / III LEVEL	Open rim painted common ware
TRZ227	KPT-08-IIP-9	II PERIOD / III LEVEL	Closed rim common ware
TRZ228	KPT-08-AC-1	BURIED CARBON LEVEL	Painted base
TRZ229	KPT-08-AC-2	BURIED CARBON LEVEL	Base of a cup
TRZ230	KPT-08-AC-3	BURIED CARBON LEVEL	Base of a jar
TRZ231	KPT-08-IN-1	Ciutadelle South-East/ 1st STRATIGRAPHIC LEVEL (Horizon)	Open rim painted common ware
TRZ232	KPT-08-IN-2	Ciutadelle South-East/ 1st STRATIGRAPHIC LEVEL (Horizon)	Handle of an open rim painted common ware
TRZ233	KPT-08-IN-3	Ciutadelle South-East/ 1st STRATIGRAPHIC LEVEL (Horizon)	Tap of a cooking ware
TRZ234	KPT-08-IN-1	Ciutadelle South-East/ 1st STRATIGRAPHIC LEVEL (Horizon)	Closed rim common ware
TRZ235	KPT-08-IN-2	Ciutadelle South-East/ 1st STRATIGRAPHIC LEVEL (Horizon)	Rim and handle of a cooking ware
TRZ236	KPT-08-IN-3	Ciutadelle South-East/ 1st STRATIGRAPHIC LEVEL (Horizon)	Base of a black common ware
TRZ237	KPT-08-IIIP-1	Ciutadelle South-East/ III PERIOD	Open rim common ware
TRZ238	KPT-08-IIIP-2	Ciutadelle South-East/ III PERIOD	Open rim common ware
TRZ239	KPT-08-IIIP-3	Ciutadelle South-East/ III PERIOD	Open rim common ware
TRZ240	KPT-08-IIIP-4	Ciutadelle South-East/ III PERIOD	Open rim common ware
TRZ241	KPT-08-IIIP-5	Ciutadelle South-East/ III PERIOD	Closed rim common ware
TRZ242	KPT-08-IIIP-6	Ciutadelle South-East/ III PERIOD	Closed rim common ware

Table 1: The analysed individuals

MATERIAL FROM ZAR TEPE			
Analytical code	**Number of inventory**	**Site**	**Type of ceramic**
TRZ243	ZT-08-01	Prospection - 1st century A.D.	Open rim, painted common ware
TRZ244	ZT-08-02	Prospection - 1st century A.D.	Open rim, common ware
TRZ245	ZT-08-03	Prospection - 1st century A.D.	Open rim, common ware
TRZ246	ZT-08-04	Prospection - 1st century A.D.	Closed rim, common ware
TRZ247	ZT-08-05	Prospection - 1st century A.D.	Open rim, common ware
TRZ248	ZT-08-06	Prospection - 1st century A.D.	Open rim, common ware - grey paste
TRZ249	ZT-08-07	Prospection - 1st century A.D.	Closed rim, common ware
TRZ250	ZT-08-08	Prospection - Kushan-Sassanian Period	Open rim, common ware (Tagine)
TRZ251	ZT-08-09	Prospection - Kushan-Sassanian Period	Open rim, common ware (Tagine)
TRZ252	ZT-08-10	Prospection - Kushan-Sassanian Period	Open rim, painted common ware (Tagine)
TRZ253	ZT-08-11	Prospection - Kushan-Sassanian Period	Open rim, painted common ware with stamped decoration
TRZ254	ZT-08-12	Prospection - Kushan-Sassanian Period	Open rim, common ware
TRZ255	ZT-08-13	Prospection - Kushan-Sassanian Period	Open rim, common ware
TRZ256	ZT-08-14	Prospection - Kushan-Sassanian Period	Closed rim, common ware
TRZ257	ZT-08-15	Prospection - Kushan-Sassanian Period	Closed rim, common ware
TRZ258	ZT-08-16	Prospection - Kushan-Sassanian Period	Closed rim, painted common ware
TRZ259	ZT-08-17	Prospection - Kushan-Sassanian Period	Closed rim, common ware
TRZ260	ZT-08-18	Prospection - Kushan-Sassanian Period	Closed rim, common ware
TRZ261	ZT-08-19	Prospection - Kushan-Sassanian Period	Closed rim, common ware
TRZ262	ZT-08-20	Prospection - Kushan-Sassanian Period	Closed rim, common ware
TRZ263	ZT-08-21	Prospection - Kushan-Sassanian Period	Closed rim, common ware
TRZ264	ZT-08-22	Prospection - Kushan-Sassanian Period	Closed rim, common ware
TRZ265	ZT-08-23	Prospection - Kushan-Sassanian Period	Closed rim, common ware
TRZ266	ZT-08-24	Prospection - Kushan-Sassanian Period	Closed rim, common ware
TRZ267	ZT-08-25	Prospection - Kushan-Sassanian Period	Closed rim, painted common ware
TRZ268	ZT-08-26	Prospection - Kushan-Sassanian Period	Closed rim, common ware
TRZ269	ZT-08-27	Prospection - Kushan-Sassanian Period	Closed rim, common ware
TRZ270	ZT-08-28	Prospection - Kushan-Sassanian Period	Closed rim, painted common ware
TRZ271	ZT-08-29	Prospection - Kushan-Sassanian Period	Closed rim, coarse ware
TRZ272	ZT-08-30	Prospection - Kushan-Sassanian Period	Open rim big bole coarse ware
TRZ273	ZT-08-31	Prospection - Kushan-Sassanian Period	Open rim big bole coarse ware
TRZ274	ZT-08-32	Prospection - Kushan-Sassanian Period	Open rim big bole coarse ware (overfired)
TRZ275	ZT-08-33	Prospection - Kushan-Sassanian Period	Open rim big bole coarse ware
TRZ276	ZT-08-34	Prospection - Kushan-Sassanian Period	Open rim bole coarse ware
TRZ277	ZT-08-35	Prospection - Kushan-Sassanian Period	Tap
TRZ278	ZT-08-36	Prospection - Kushan-Sassanian Period	Handle
TRZ279	ZT-08-37	Prospection - Kushan-Sassanian Period	Small angular base
TRZ280	ZT-08-38	Prospection - Kushan-Sassanian Period	Small angular base
TRZ281	ZT-08-39	Prospection - Kushan-Sassanian Period	Small angular base
TRZ282	ZT-08-40	Prospection - Kushan-Sassanian Period	Big angular base
TRZ283	ZT-08-41	Prospection - Kushan-Sassanian Period	Big angular base
TRZ284	ZT-08-42	Prospection - Kushan-Sassanian Period	Big angular base
TRZ285	ZT-08-43	Prospection - Kushan-Sassanian Period	Small plane base
TRZ286	ZT-08-44	Prospection - Kushan-Sassanian Period	Big plane base
TRZ287	ZT-08-45	Prospection - Kushan-Sassanian Period	Big plane base
TRZ288	ZT-08-46	Prospection - Kushan-Sassanian Period	Big plane base
TRZ289	ZT-08-47	Prospection - Kushan-Sassanian Period	Big plane base
TRZ290	ZT-08-48	Prospection - Kushan-Sassanian Period	Big plane base

Table 1: The analysed individuals

The archaeometrical study upon the total of 290 individuals has been carried out applying chemical and mineralogical techniques. The chemical composition has been determined by X-Ray Fluorescence (XRF), and the mineralogy has been studied using X-Ray Diffraction (XRD). We still need to complete these results with SEM and OM study.

The results first will be presented for each site separately then an integrated comparison will follow to be able to make some inferences upon pottery production and distribution in the broader territory.

At Table 1 we listed the location origin and the typology of the analysed ceramics. The analysed material includes painted wares covered with a red, brown or almost black slip (CER) non painted common wares (CC) some jars, plates and cooking wares.

The analytical programme and methodology

XRF was performed using a Phillips PW 2400 spectrometer with a Rh excitation source. A portion of specimens were dried at 100°C for 24 h. Major and minor elements were determined by preparing duplicate of glassy pills using 0.3 g of powdered specimen in an alkaline fusion with lithium tetraborate at 1/20 dilution. Trace elements and Na_2O were determined by powdered pills made from 5 g of specimen mixed with Elvacite agglutinating agent placed over boric acid in an aluminium capsule and pressed for 60 s at 200 kN. The quantification of the concentrations was obtained by using a calibration line performed with 60 International Geological Standards (Hein *et al.,* 2003). The identified elements are: identified comprised Fe_2O_3 (as total Fe), Al_2O_3, MnO, P_2O_5, TiO_2, MgO, CaO, Na_2O, K_2O, SiO_2, Ba, Rb, Mo, Th, Nb, Pb, Zr, Y, Sr, Sn, Ce, Co, Ga, V, Zn, W, Cu, Ni and Cr. The loss on ignition (LOI) was determined by firing 0.3 g of dried specimen at 950°C for 3 h.

XRD analyses were carried out by using the same specimens prepared for XRF analysis. Measurements were performed using a Siemens D-500 diffractometer working with the Cu $K\alpha$ radiation (λ=1.5406 Å), and graphite monochromator in the diffracted beam, at 1.2 kW (40 kV, 30 mA). Spectra were taken from 4 to 70°2Θ, at 1°2Θ/min (step size=0.05°2Θ; time=3 s). The evaluation of crystalline phases was carried out using the DIFFRACT/AT program by Siemens, which includes the Joint Committee of Powder Diffraction Standards (JCPDS) data bank.

Finally, Petrographic analysis was carried out upon selected individuals from Termez by thin-sections using an Olympus BX-41 polarising microscope working under magnification between 40X and 400X. Each ceramic specimen was impregnated with epoxy resin and mounted using Loctite UV glue and sectioned using a Struers Discoplan TS. The thin sections were finished by hand using a powder abrasive until reaching a thickness of 30 micrometers in which quartz presents a grey-white first order interference colour. The observations were carried out with Olympus BX41 microscope equipped with objectives of x4, x10, x20, 40 working between 40 and 400 magnifications. Photographs were taken using a digital camera Olympus DP-70 attached to the microscope controlled by specific computer software.

General Geological description of the studied area

Tchinguiz Tepe is located in Surkhan Darya valley, close to the Amu Darya River and near the confluence with Surkhan Darya River. This valley is integrated in Afghano-Tadjic depression, limited in the east by Pamir Mountains and in the south by Hindukush mountains. Amu Darya and Surkhan Darya rivers are the main collector of Afghano-Tadjic depression and the major Aral Sea tributaries. The basement is hercinic, formed by metamorphic and crystallitic rocks. Sediments from Mesozoic and Cenozoic are filling this basement. They are constituted by sandstones, claystones, limonite with salt levels and anhydrites. Surkhan Darya valley is enclosed by three mountains alienations. ***Tchinguiz Tepe*** is located in the inferior alineation, which is discontinuous and the nearest placed to Amu Darya River. Sandstones and calcareous rocks with shell fragments are the constituents of Lower Cretaceous. These rocks are also represented in Upper Cretaceous together with claystones, marls, limonite and gypsum. Sediments of marine origin are the main constituents of Paleogene and Neogene rocks. Lower levels are composed by calcareous, dolomites and gypsum whereas the upper levels contain also sandstones, claystones, marls and limonites. During Oligocene and Neogene the main sediments present an alluvial origin and they are constituted by sandstones, siltstones and clays (see chapter of Geomorphology in this same volume by Ana Sánchez del Corral).

chemical and petrographic results for Termez ceramics.

The normalised chemical composition of the analysed ceramic material from Termez can be seen in Table 2.

ID.	Fe2O3	Al2O3	TiO2	MgO	CaO	Na2O	K2O	SiO2	Ba	Rb	Th	Nb	Zr
TRZ001	5,67	15,20	0,62	4,25	10,97	2,15	3,39	57,59	0,0520	0,0128	0,0017	0,0016	0,0152
TRZ002	6,41	16,48	0,64	3,97	9,69	1,67	3,40	57,57	0,0586	0,0134	0,0015	0,0016	0,0153
TRZ003	5,91	15,65	0,65	4,23	10,56	1,69	3,53	57,60	0,0485	0,0129	0,0015	0,0017	0,0151
TRZ004	6,36	16,44	0,69	4,04	8,74	1,87	3,92	57,76	0,0539	0,0140	0,0017	0,0017	0,0157
TRZ005	6,30	16,20	0,70	4,03	10,66	1,54	3,61	56,80	0,0420	0,0128	0,0015	0,0016	0,0152
TRZ006	6,16	15,78	0,67	4,76	10,89	1,56	3,50	56,52	0,0474	0,0128	0,0016	0,0016	0,0160
TRZ008	6,11	16,08	0,69	3,43	8,16	1,78	3,89	59,71	0,0485	0,0126	0,0014	0,0015	0,0147
TRZ009	5,84	15,06	0,63	3,83	11,50	1,71	3,18	58,08	0,0528	0,0125	0,0017	0,0016	0,0161
TRZ010	5,89	15,83	0,62	4,04	10,67	1,48	3,42	57,89	0,0495	0,0130	0,0017	0,0016	0,0145
TRZ011	5,76	15,27	0,64	4,65	13,30	1,26	3,47	55,48	0,0483	0,0095	0,0015	0,0015	0,0140
TRZ012	6,29	16,03	0,65	3,85	11,21	1,33	3,37	57,06	0,0827	0,0128	0,0015	0,0017	0,0151
TRZ013	6,11	15,67	0,66	4,31	11,72	1,31	3,39	56,64	0,0607	0,0131	0,0015	0,0016	0,0161
TRZ014	5,82	15,48	0,62	3,95	13,26	1,38	3,45	55,88	0,0470	0,0128	0,0016	0,0016	0,0152
TRZ015	5,71	14,85	0,66	4,63	10,77	2,04	3,34	57,84	0,0510	0,0118	0,0015	0,0016	0,0168
TRZ016	6,10	15,49	0,67	4,29	11,96	2,10	3,46	55,75	0,0506	0,0106	0,0014	0,0016	0,0160
TRZ017	6,63	17,13	0,68	4,42	11,21	1,31	3,54	54,90	0,0536	0,0144	0,0018	0,0016	0,0150
TRZ018	5,92	15,83	0,67	3,57	8,40	1,98	3,54	59,92	0,0527	0,0128	0,0017	0,0017	0,0168
TRZ019	5,97	15,60	0,64	4,22	12,09	1,88	3,56	55,87	0,0497	0,0130	0,0016	0,0016	0,0146
TRZ020	6,08	15,66	0,70	3,85	10,63	2,07	2,71	58,12	0,0531	0,0106	0,0016	0,0017	0,0171
TRZ021	5,98	15,75	0,64	4,16	10,89	1,88	3,22	57,30	0,0503	0,0126	0,0014	0,0016	0,0155
TRZ022	6,01	15,82	0,64	4,03	11,95	1,55	3,57	56,26	0,0483	0,0130	0,0016	0,0016	0,0152
TRZ023	6,08	15,80	0,66	4,39	10,75	1,54	3,52	57,08	0,0502	0,0132	0,0017	0,0016	0,0151
TRZ024	5,92	15,59	0,64	4,20	12,14	1,52	3,44	56,39	0,0473	0,0127	0,0014	0,0016	0,0145
TRZ025	5,92	15,40	0,66	4,13	11,23	2,41	3,81	56,27	0,0495	0,0126	0,0016	0,0016	0,0150
TRZ026	6,07	15,81	0,65	4,30	12,48	1,55	3,23	55,75	0,0487	0,0120	0,0017	0,0016	0,0150
TRZ027	6,40	16,71	0,67	4,17	9,64	1,53	4,02	56,69	0,0504	0,0135	0,0015	0,0015	0,0144
TRZ028	6,29	15,82	0,70	4,01	11,06	2,29	2,33	57,35	0,0451	0,0086	0,0013	0,0016	0,0165
TRZ029	5,84	15,33	0,63	4,23	13,00	1,22	3,40	56,18	0,0477	0,0126	0,0014	0,0016	0,0147
TRZ030	5,97	15,40	0,67	4,36	12,66	1,66	2,98	56,14	0,0474	0,0115	0,0017	0,0016	0,0159
TRZ031	6,09	15,95	0,66	4,24	11,29	1,54	3,47	56,58	0,0480	0,0130	0,0016	0,0017	0,0153
TRZ032	5,90	15,76	0,62	4,12	11,79	1,60	3,38	56,66	0,0478	0,0130	0,0018	0,0016	0,0146
TRZ033	5,78	15,17	0,66	3,69	11,72	1,77	3,03	58,01	0,0492	0,0106	0,0015	0,0016	0,0158
TRZ034	6,23	16,03	0,69	3,94	11,36	1,44	3,45	56,67	0,0597	0,0124	0,0016	0,0017	0,0162
TRZ035	6,01	15,57	0,66	3,95	11,05	2,00	3,65	56,94	0,0552	0,0130	0,0016	0,0016	0,0150
TRZ036	6,20	16,24	0,67	3,92	9,33	1,60	3,96	57,92	0,0482	0,0135	0,0016	0,0016	0,0155
TRZ037	5,88	15,50	0,64	4,27	12,32	1,66	3,07	56,48	0,0517	0,0116	0,0015	0,0017	0,0151
TRZ038	5,83	15,17	0,69	3,64	11,93	1,39	3,22	57,95	0,0583	0,0118	0,0015	0,0016	0,0167
TRZ039	5,91	15,47	0,64	3,39	10,59	1,73	3,84	58,24	0,0566	0,0125	0,0015	0,0016	0,0160
TRZ040	5,95	15,55	0,65	4,47	11,52	1,40	3,10	57,18	0,0552	0,0115	0,0016	0,0017	0,0157
TRZ041	6,16	16,11	0,66	4,46	10,75	1,34	3,33	57,03	0,0488	0,0129	0,0015	0,0016	0,0154
TRZ042	5,49	14,71	0,61	3,43	11,29	1,82	3,44	59,05	0,0489	0,0118	0,0014	0,0015	0,0152
TRZ043	6,14	16,03	0,65	4,65	11,57	1,36	3,55	55,87	0,0472	0,0131	0,0016	0,0017	0,0146
TRZ044	5,65	15,41	0,63	3,60	10,10	1,39	3,24	59,80	0,0710	0,0124	0,0015	0,0016	0,0153
TRZ045	5,69	15,14	0,66	3,90	10,85	1,33	3,18	59,08	0,0610	0,0116	0,0015	0,0016	0,0162
TRZ046	5,75	14,99	0,66	4,27	11,32	1,47	3,04	58,33	0,0610	0,0110	0,0015	0,0016	0,0168
TRZ047	6,34	16,27	0,67	4,17	12,01	1,30	3,16	55,89	0,0698	0,0133	0,0017	0,0017	0,0153
TRZ048	6,10	15,86	0,67	3,66	10,16	1,26	3,41	58,71	0,0515	0,0124	0,0017	0,0016	0,0152
TRZ049	6,10	15,71	0,66	3,43	11,68	1,13	3,27	57,83	0,0791	0,0127	0,0016	0,0016	0,0154
TRZ050	5,51	14,71	0,65	3,57	9,88	1,12	3,24	61,10	0,0929	0,0111	0,0014	0,0016	0,0166
TRZ051	6,57	16,20	0,67	3,89	9,94	1,43	3,31	57,81	0,0671	0,0132	0,0013	0,0016	0,0147
TRZ052	6,27	16,18	0,66	4,04	10,03	1,34	3,33	57,98	0,0585	0,0121	0,0013	0,0015	0,0143
TRZ053	6,60	16,36	0,72	3,65	9,89	1,48	3,42	57,72	0,0595	0,0124	0,0014	0,0015	0,0157
TRZ054	5,81	15,59	0,67	4,42	9,37	1,27	3,21	59,51	0,0502	0,0110	0,0012	0,0014	0,0162
TRZ055	6,80	16,51	0,69	3,81	10,91	1,35	3,36	56,39	0,0660	0,0124	0,0017	0,0016	0,0146
TRZ056	6,32	15,89	0,69	3,47	10,46	1,57	3,16	58,27	0,0626	0,0115	0,0015	0,0015	0,0152

Table 2: Normalised chemical composition of the ceramics analysed from Termez

ID.	Y	Sr	Ce	Ga	V	Zn	Cu	Ni	Cr
TRZ001	0,0028	0,0398	0,0063	0,0022	0,0095	0,0107	0,0036	0,0049	0,0081
TRZ002	0,0028	0,0320	0,0063	0,0024	0,0105	0,0115	0,0037	0,0051	0,0079
TRZ003	0,0029	0,0387	0,0055	0,0023	0,0105	0,0114	0,0035	0,0050	0,0081
TRZ004	0,0030	0,0389	0,0072	0,0024	0,0111	0,0099	0,0037	0,0056	0,0084
TRZ005	0,0030	0,0337	0,0062	0,0022	0,0103	0,0107	0,0031	0,0048	0,0083
TRZ006	0,0029	0,0395	0,0059	0,0022	0,0103	0,0107	0,0035	0,0050	0,0082
TRZ008	0,0029	0,0276	0,0051	0,0021	0,0108	0,0081	0,0030	0,0049	0,0083
TRZ009	0,0028	0,0384	0,0052	0,0021	0,0093	0,0108	0,0037	0,0047	0,0078
TRZ010	0,0027	0,0326	0,0061	0,0022	0,0104	0,0107	0,0031	0,0050	0,0080
TRZ011	0,0028	0,0487	0,0042	0,0021	0,0100	0,0107	0,0035	0,0042	0,0072
TRZ012	0,0029	0,0445	0,0065	0,0024	0,0106	0,0108	0,0044	0,0056	0,0079
TRZ013	0,0029	0,0397	0,0072	0,0023	0,0103	0,0118	0,0038	0,0051	0,0079
TRZ014	0,0028	0,0383	0,0071	0,0022	0,0098	0,0111	0,0033	0,0052	0,0079
TRZ015	0,0030	0,0416	0,0070	0,0022	0,0109	0,0108	0,0032	0,0048	0,0080
TRZ016	0,0030	0,0412	0,0058	0,0022	0,0102	0,0102	0,0038	0,0055	0,0079
TRZ017	0,0030	0,0360	0,0071	0,0025	0,0113	0,0120	0,0042	0,0055	0,0081
TRZ018	0,0030	0,0338	0,0073	0,0022	0,0101	0,0100	0,0032	0,0049	0,0077
TRZ019	0,0029	0,0379	0,0044	0,0022	0,0107	0,0111	0,0033	0,0052	0,0078
TRZ020	0,0032	0,0330	0,0066	0,0023	0,0104	0,0113	0,0042	0,0049	0,0081
TRZ021	0,0029	0,0353	0,0053	0,0022	0,0102	0,0107	0,0040	0,0050	0,0078
TRZ022	0,0029	0,0379	0,0058	0,0021	0,0099	0,0109	0,0034	0,0051	0,0078
TRZ023	0,0029	0,0448	0,0066	0,0022	0,0107	0,0109	0,0034	0,0053	0,0083
TRZ024	0,0028	0,0390	0,0065	0,0021	0,0107	0,0111	0,0031	0,0054	0,0082
TRZ025	0,0030	0,0414	0,0073	0,0022	0,0098	0,0108	0,0031	0,0049	0,0078
TRZ026	0,0029	0,0396	0,0059	0,0022	0,0104	0,0113	0,0034	0,0053	0,0082
TRZ027	0,0030	0,0434	0,0044	0,0023	0,0122	0,0094	0,0028	0,0056	0,0086
TRZ028	0,0030	0,0339	0,0058	0,0023	0,0098	0,0099	0,0038	0,0051	0,0081
TRZ029	0,0029	0,0465	0,0049	0,0021	0,0099	0,0108	0,0036	0,0050	0,0078
TRZ030	0,0030	0,0367	0,0062	0,0022	0,0101	0,0107	0,0037	0,0052	0,0079
TRZ031	0,0029	0,0370	0,0073	0,0023	0,0107	0,0123	0,0034	0,0049	0,0080
TRZ032	0,0027	0,0342	0,0057	0,0022	0,0103	0,0114	0,0032	0,0051	0,0082
TRZ033	0,0029	0,0360	0,0065	0,0021	0,0097	0,0106	0,0033	0,0046	0,0081
TRZ034	0,0031	0,0414	0,0070	0,0023	0,0096	0,0114	0,0034	0,0051	0,0083
TRZ035	0,0029	0,0408	0,0066	0,0022	0,0108	0,0106	0,0030	0,0052	0,0079
TRZ036	0,0029	0,0392	0,0066	0,0022	0,0106	0,0106	0,0033	0,0053	0,0084
TRZ037	0,0028	0,0395	0,0074	0,0022	0,0103	0,0110	0,0036	0,0052	0,0086
TRZ038	0,0031	0,0418	0,0061	0,0021	0,0098	0,0107	0,0045	0,0048	0,0080
TRZ039	0,0030	0,0343	0,0076	0,0022	0,0104	0,0108	0,0032	0,0047	0,0079
TRZ040	0,0029	0,0419	0,0067	0,0022	0,0106	0,0111	0,0039	0,0051	0,0079
TRZ041	0,0027	0,0321	0,0041	0,0022	0,0097	0,0109	0,0034	0,0053	0,0088
TRZ042	0,0027	0,0363	0,0070	0,0021	0,0095	0,0095	0,0029	0,0044	0,0074
TRZ043	0,0029	0,0399	0,0069	0,0023	0,0097	0,0109	0,0037	0,0054	0,0088
TRZ044	0,0027	0,0393	0,0054	0,0022	0,0096	0,0101	0,0036	0,0045	0,0081
TRZ045	0,0028	0,0415	0,0056	0,0021	0,0100	0,0100	0,0041	0,0045	0,0080
TRZ046	0,0029	0,0428	0,0072	0,0021	0,0103	0,0104	0,0041	0,0049	0,0080
TRZ047	0,0028	0,0390	0,0057	0,0023	0,0111	0,0119	0,0043	0,0053	0,0079
TRZ048	0,0028	0,0361	0,0057	0,0022	0,0103	0,0097	0,0030	0,0050	0,0079
TRZ049	0,0029	0,0398	0,0042	0,0022	0,0108	0,0100	0,0041	0,0053	0,0074
TRZ050	0,0029	0,0490	0,0064	0,0020	0,0099	0,0097	0,0031	0,0044	0,0074
TRZ051	0,0026	0,0347	0,0052	0,0019	0,0107	0,0103	0,0034	0,0051	0,0076
TRZ052	0,0025	0,0330	0,0075	0,0018	0,0099	0,0104	0,0035	0,0047	0,0075
TRZ053	0,0027	0,0316	0,0065	0,0018	0,0101	0,0102	0,0037	0,0050	0,0074
TRZ054	0,0025	0,0352	0,0062	0,0016	0,0107	0,0092	0,0026	0,0040	0,0070
TRZ055	0,0027	0,0420	0,0073	0,0019	0,0110	0,0104	0,0035	0,0052	0,0077
TRZ056	0,0025	0,0306	0,0065	0,0018	0,0107	0,0091	0,0031	0,0050	0,0076

Table 2: Normalised chemical composition of the ceramics analysed from Termez

ID.	Fe_2O_3	Al_2O_3	TiO_2	MgO	CaO	Na_2O	K_2O	SiO_2	Ba	Rb	Th	Nb	Zr
TRZ057	6,66	16,41	0,72	3,65	9,76	1,41	3,46	57,77	0,0543	0,0130	0,0012	0,0015	0,0161
TRZ058	6,92	16,69	0,71	3,99	10,34	1,62	3,51	56,05	0,0610	0,0132	0,0014	0,0015	0,0159
TRZ059	6,84	16,48	0,70	3,74	11,63	1,60	3,78	55,06	0,0548	0,0132	0,0015	0,0016	0,0155
TRZ060	6,20	16,00	0,66	3,99	10,78	1,18	3,36	57,70	0,0437	0,0110	0,0011	0,0013	0,0132
TRZ063	6,76	16,35	0,70	3,92	11,57	2,30	1,93	56,31	0,0525	0,0073	0,0016	0,0015	0,0157
TRZ064	6,87	16,80	0,73	4,07	9,47	1,40	3,58	56,91	0,0578	0,0139	0,0014	0,0017	0,0165
TRZ065	6,61	16,15	0,72	3,77	10,15	1,45	3,41	57,56	0,0579	0,0132	0,0016	0,0016	0,0163
TRZ066	6,59	16,48	0,71	3,69	9,30	1,53	3,47	58,04	0,0598	0,0135	0,0016	0,0016	0,0164
TRZ067	6,07	15,55	0,66	3,46	11,91	1,30	3,19	57,69	0,0579	0,0136	0,0016	0,0016	0,0162
TRZ068	6,54	16,32	0,68	4,23	10,27	1,48	3,03	57,25	0,0767	0,0113	0,0015	0,0015	0,0153
TRZ069	5,91	15,05	0,65	4,15	13,29	1,50	2,90	56,36	0,0659	0,0118	0,0014	0,0016	0,0160
TRZ070	5,93	15,90	0,66	4,16	9,22	1,27	3,47	59,23	0,0661	0,0135	0,0013	0,0015	0,0159
TRZ071	5,70	14,76	0,63	3,86	11,97	1,21	3,13	58,54	0,0619	0,0123	0,0014	0,0015	0,0152
TRZ072	6,23	16,25	0,67	3,62	11,21	1,69	3,15	56,99	0,0693	0,0132	0,0015	0,0016	0,0165
TRZ073	6,26	15,86	0,67	3,46	11,33	1,44	3,42	57,38	0,0549	0,0130	0,0013	0,0015	0,0152
TRZ074	6,98	17,48	0,72	3,80	10,26	1,31	3,59	55,68	0,0614	0,0148	0,0015	0,0016	0,0157
TRZ075	6,65	16,78	0,69	4,46	10,49	1,32	3,51	55,95	0,0475	0,0135	0,0015	0,0015	0,0148
TRZ076	6,82	16,80	0,71	4,08	9,61	1,38	3,64	56,78	0,0575	0,0138	0,0016	0,0016	0,0156
TRZ077	6,49	16,11	0,66	3,95	11,64	2,33	2,40	56,26	0,0509	0,0081	0,0014	0,0015	0,0153
TRZ078	6,29	15,69	0,67	3,75	9,99	1,55	3,49	58,40	0,0537	0,0124	0,0014	0,0015	0,0161
TRZ079	6,66	16,59	0,71	4,06	10,70	2,00	2,87	56,26	0,0602	0,0107	0,0015	0,0016	0,0160
TRZ080	6,59	16,36	0,66	4,03	10,15	1,51	3,47	57,07	0,0547	0,0129	0,0014	0,0014	0,0143
TRZ081	6,49	16,49	0,66	3,91	11,02	1,37	3,28	56,60	0,0582	0,0144	0,0017	0,0015	0,0151
TRZ082	6,57	16,56	0,68	4,32	9,92	1,30	3,45	57,02	0,0582	0,0142	0,0016	0,0015	0,0155
TRZ083	6,35	15,86	0,66	4,01	11,74	1,77	2,84	56,60	0,0535	0,0116	0,0013	0,0015	0,0156
TRZ084	6,08	16,46	0,70	3,14	6,56	1,73	4,42	60,71	0,0572	0,0133	0,0011	0,0017	0,0165
TRZ085	5,39	14,97	0,57	3,14	9,67	1,52	3,44	61,13	0,0599	0,0127	0,0013	0,0014	0,0149
TRZ086	6,45	16,31	0,68	3,97	9,86	1,34	3,51	57,71	0,0516	0,0134	0,0013	0,0015	0,0155
TRZ087	6,42	16,15	0,68	3,56	10,92	1,46	3,42	57,20	0,0611	0,0136	0,0014	0,0015	0,0152
TRZ088	6,64	16,73	0,72	3,57	8,30	1,92	3,64	58,31	0,0609	0,0132	0,0014	0,0016	0,0156
TRZ089	5,86	15,26	0,66	3,31	9,34	1,58	3,35	60,47	0,0565	0,0120	0,0014	0,0015	0,0164
TRZ090	6,59	16,47	0,69	3,50	8,94	1,52	3,54	58,57	0,0692	0,0136	0,0015	0,0016	0,0159
TRZ091	6,21	16,04	0,64	3,86	10,51	1,46	3,09	58,03	0,0651	0,0132	0,0015	0,0015	0,0154
TRZ092	6,15	15,46	0,68	3,62	9,73	1,96	3,42	58,80	0,0655	0,0130	0,0015	0,0015	0,0157
TRZ093	7,03	17,21	0,70	3,69	8,87	1,39	3,88	57,06	0,0563	0,0140	0,0017	0,0015	0,0153
TRZ094	6,69	16,59	0,70	3,59	10,16	1,31	3,77	57,01	0,0559	0,0133	0,0014	0,0015	0,0155
TRZ095	6,24	16,35	0,69	3,45	9,61	1,59	3,57	58,34	0,0515	0,0126	0,0015	0,0015	0,0163
TRZ097	5,60	14,91	0,67	2,72	9,83	1,21	3,46	61,42	0,0527	0,0114	0,0013	0,0015	0,0157
TRZ098	6,36	15,92	0,65	3,35	10,38	0,96	3,50	58,71	0,0552	0,0115	0,0012	0,0014	0,0137
TRZ100	6,63	16,83	0,68	3,57	8,07	1,38	3,96	58,70	0,0576	0,0129	0,0014	0,0014	0,0158
TRZ101	5,92	15,19	0,69	3,19	9,29	1,25	3,61	60,70	0,0563	0,0117	0,0013	0,0016	0,0168
TRZ102	6,82	16,65	0,69	3,31	9,03	1,12	3,79	58,44	0,0463	0,0114	0,0013	0,0013	0,0136
TRZ103	6,90	16,16	0,67	3,54	10,61	1,23	3,68	57,02	0,0571	0,0135	0,0015	0,0015	0,0151
TRZ104	4,36	12,75	0,63	2,12	12,17	1,64	3,38	62,82	0,0287	0,0094	0,0012	0,0014	0,0208
TRZ105	5,93	15,44	0,69	2,99	9,87	1,36	3,47	60,08	0,0532	0,0119	0,0013	0,0015	0,0164
TRZ108	6,24	16,10	0,71	3,21	8,77	1,41	3,60	59,79	0,0575	0,0134	0,0015	0,0016	0,0177
TRZ109	6,01	15,30	0,63	3,79	12,65	1,87	2,58	56,99	0,0518	0,0093	0,0013	0,0014	0,0146
TRZ110	6,31	16,19	0,66	3,57	11,13	1,40	3,80	56,74	0,0559	0,0132	0,0014	0,0015	0,0147
TRZ112	5,94	15,57	0,62	3,57	11,97	1,36	3,70	57,08	0,0546	0,0128	0,0014	0,0015	0,0152
TRZ114	5,96	15,02	0,61	3,77	12,93	2,66	3,72	55,16	0,0487	0,0116	0,0014	0,0013	0,0132
TRZ115	6,64	16,61	0,70	3,49	11,90	1,40	3,83	55,24	0,0622	0,0138	0,0014	0,0016	0,0162
TRZ116	6,47	16,34	0,69	3,46	10,83	1,47	3,70	56,86	0,0584	0,0130	0,0015	0,0016	0,0169
TRZ117	6,37	16,52	0,68	3,30	8,39	1,45	3,62	59,51	0,0566	0,0130	0,0015	0,0015	0,0167
TRZ118	6,30	15,75	0,64	3,53	10,44	1,28	3,54	58,33	0,0527	0,0129	0,0013	0,0014	0,0146
TRZ119	6,74	16,82	0,69	3,70	11,18	1,48	3,29	55,92	0,0594	0,0123	0,0014	0,0015	0,0158

Table 2: Normalised chemical composition of the ceramics analysed from Termez

ID.	Y	Sr	Ce	Ga	V	Zn	Cu	Ni	Cr
TRZ057	0,0027	0,0322	0,0063	0,0018	0,0108	0,0097	0,0038	0,0052	0,0077
TRZ058	0,0027	0,0371	0,0060	0,0019	0,0105	0,0112	0,0040	0,0055	0,0078
TRZ059	0,0028	0,0396	0,0057	0,0019	0,0110	0,0107	0,0037	0,0052	0,0071
TRZ060	0,0023	0,0348	0,0053	0,0016	0,0086	0,0087	0,0027	0,0042	0,0061
TRZ063	0,0026	0,0314	0,0072	0,0019	0,0104	0,0110	0,0039	0,0054	0,0075
TRZ064	0,0028	0,0371	0,0069	0,0020	0,0109	0,0112	0,0040	0,0055	0,0078
TRZ065	0,0027	0,0355	0,0064	0,0019	0,0102	0,0104	0,0038	0,0052	0,0074
TRZ066	0,0027	0,0337	0,0063	0,0019	0,0104	0,0103	0,0037	0,0050	0,0074
TRZ067	0,0026	0,0274	0,0059	0,0018	0,0104	0,0098	0,0035	0,0050	0,0070
TRZ068	0,0026	0,0337	0,0059	0,0018	0,0106	0,0114	0,0047	0,0052	0,0076
TRZ069	0,0025	0,0372	0,0061	0,0018	0,0098	0,0094	0,0033	0,0050	0,0069
TRZ070	0,0026	0,0372	0,0057	0,0018	0,0097	0,0107	0,0040	0,0046	0,0074
TRZ071	0,0025	0,0408	0,0064	0,0017	0,0088	0,0105	0,0035	0,0046	0,0067
TRZ072	0,0026	0,0352	0,0063	0,0018	0,0105	0,0100	0,0033	0,0049	0,0070
TRZ073	0,0026	0,0443	0,0066	0,0018	0,0104	0,0102	0,0034	0,0048	0,0073
TRZ074	0,0027	0,0336	0,0079	0,0021	0,0117	0,0107	0,0040	0,0060	0,0082
TRZ075	0,0025	0,0347	0,0056	0,0019	0,0114	0,0106	0,0033	0,0052	0,0082
TRZ076	0,0027	0,0377	0,0069	0,0019	0,0106	0,0108	0,0040	0,0053	0,0079
TRZ077	0,0026	0,0312	0,0059	0,0019	0,0095	0,0110	0,0032	0,0053	0,0073
TRZ078	0,0026	0,0458	0,0052	0,0018	0,0096	0,0104	0,0037	0,0048	0,0069
TRZ079	0,0026	0,0349	0,0060	0,0020	0,0104	0,0105	0,0038	0,0051	0,0075
TRZ080	0,0024	0,0352	0,0064	0,0018	0,0101	0,0100	0,0041	0,0049	0,0073
TRZ081	0,0027	0,0314	0,0088	0,0020	0,0111	0,0105	0,0038	0,0051	0,0073
TRZ082	0,0027	0,0360	0,0061	0,0019	0,0102	0,0115	0,0039	0,0054	0,0078
TRZ083	0,0026	0,0312	0,0060	0,0018	0,0108	0,0098	0,0038	0,0052	0,0074
TRZ084	0,0024	0,0644	0,0069	0,0018	0,0113	0,0075	0,0025	0,0046	0,0079
TRZ085	0,0023	0,0367	0,0064	0,0017	0,0093	0,0089	0,0029	0,0042	0,0064
TRZ086	0,0026	0,0393	0,0057	0,0018	0,0103	0,0104	0,0035	0,0052	0,0075
TRZ087	0,0026	0,0380	0,0043	0,0019	0,0106	0,0100	0,0036	0,0054	0,0074
TRZ088	0,0024	0,0421	0,0032	0,0018	0,0096	0,0093	0,0035	0,0052	0,0078
TRZ089	0,0024	0,0415	0,0050	0,0016	0,0102	0,0096	0,0026	0,0045	0,0075
TRZ090	0,0028	0,0455	0,0055	0,0019	0,0110	0,0095	0,0032	0,0051	0,0081
TRZ091	0,0025	0,0328	0,0064	0,0018	0,0100	0,0103	0,0035	0,0049	0,0073
TRZ092	0,0026	0,0456	0,0051	0,0017	0,0088	0,0093	0,0036	0,0049	0,0074
TRZ093	0,0025	0,0353	0,0054	0,0020	0,0104	0,0102	0,0037	0,0050	0,0079
TRZ094	0,0026	0,0456	0,0076	0,0019	0,0101	0,0103	0,0039	0,0049	0,0075
TRZ095	0,0024	0,0299	0,0067	0,0017	0,0102	0,0090	0,0031	0,0046	0,0073
TRZ097	0,0024	0,0408	0,0058	0,0016	0,0107	0,0093	0,0026	0,0034	0,0068
TRZ098	0,0024	0,0372	0,0044	0,0016	0,0111	0,0099	0,0029	0,0043	0,0071
TRZ100	0,0024	0,0376	0,0070	0,0018	0,0118	0,0104	0,0027	0,0041	0,0077
TRZ101	0,0025	0,0325	0,0058	0,0017	0,0102	0,0100	0,0030	0,0042	0,0069
TRZ102	0,0023	0,0308	0,0050	0,0017	0,0114	0,0092	0,0030	0,0040	0,0076
TRZ103	0,0026	0,0492	0,0062	0,0018	0,0093	0,0101	0,0036	0,0048	0,0073
TRZ104	0,0027	0,0291	0,0059	0,0012	0,0118	0,0091	0,0020	0,0019	0,0069
TRZ105	0,0026	0,0433	0,0051	0,0017	0,0105	0,0101	0,0030	0,0042	0,0071
TRZ108	0,0027	0,0375	0,0084	0,0018	0,0100	0,0090	0,0033	0,0047	0,0074
TRZ109	0,0025	0,0484	0,0062	0,0018	0,0096	0,0105	0,0028	0,0047	0,0067
TRZ110	0,0025	0,0556	0,0063	0,0018	0,0106	0,0110	0,0031	0,0046	0,0073
TRZ112	0,0024	0,0630	0,0054	0,0018	0,0102	0,0134	0,0027	0,0046	0,0068
TRZ114	0,0022	0,0588	0,0050	0,0015	0,0092	0,0100	0,0030	0,0042	0,0064
TRZ115	0,0027	0,0538	0,0075	0,0020	0,0099	0,0106	0,0035	0,0049	0,0070
TRZ116	0,0025	0,0576	0,0077	0,0019	0,0088	0,0103	0,0035	0,0048	0,0071
TRZ117	0,0025	0,0324	0,0075	0,0018	0,0101	0,0099	0,0032	0,0049	0,0079
TRZ118	0,0025	0,0458	0,0071	0,0017	0,0103	0,0100	0,0025	0,0045	0,0071
TRZ119	0,0026	0,0437	0,0064	0,0020	0,0111	0,0109	0,0036	0,0052	0,0077

Table 2: Normalised chemical composition of the ceramics analysed from Termez

ID.	Fe2O3	Al2O3	TiO2	MgO	CaO	Na2O	K2O	SiO2	Ba	Rb	Th	Nb	Zr
TRZ120	6,47	16,66	0,74	3,49	8,92	1,59	3,69	58,26	0,0591	0,0143	0,0017	0,0018	0,0179
TRZ121	6,75	16,77	0,67	3,83	9,45	1,24	3,47	57,65	0,0566	0,0141	0,0016	0,0015	0,0156
TRZ123	5,89	15,18	0,63	3,90	12,01	1,15	3,24	57,82	0,0531	0,0131	0,0012	0,0016	0,0158
TRZ124	6,18	15,83	0,67	4,01	10,71	1,46	3,40	57,56	0,0574	0,0140	0,0016	0,0017	0,0162
TRZ126	6,67	16,78	0,68	3,79	10,58	1,60	3,75	55,97	0,0549	0,0133	0,0014	0,0015	0,0150
TRZ127	7,02	16,21	0,66	3,68	12,96	1,29	3,10	54,84	0,1250	0,0137	0,0015	0,0015	0,0144
TRZ128	6,60	17,22	0,68	4,19	11,03	1,37	3,50	55,22	0,0567	0,0148	0,0017	0,0017	0,0163
TRZ129	6,18	15,95	0,67	3,96	10,80	1,58	3,34	57,34	0,0552	0,0138	0,0015	0,0016	0,0164
TRZ130	6,26	15,81	0,67	3,48	11,03	1,48	3,21	57,88	0,0665	0,0140	0,0015	0,0016	0,0168
TRZ131	5,69	15,04	0,63	3,56	11,05	1,66	3,13	59,08	0,0531	0,0113	0,0013	0,0015	0,0160
TRZ132	6,34	15,95	0,70	3,69	10,65	1,44	3,21	57,83	0,0585	0,0124	0,0015	0,0016	0,0157
TRZ133	6,05	16,22	0,69	3,70	8,18	1,70	3,58	59,71	0,0545	0,0121	0,0015	0,0016	0,0162
TRZ134	5,63	15,35	0,61	3,17	9,54	1,84	3,19	60,51	0,0588	0,0118	0,0014	0,0015	0,0151
TRZ135	5,94	15,25	0,63	3,87	11,15	1,07	3,06	58,85	0,0525	0,0122	0,0014	0,0015	0,0148
TRZ136	6,28	16,25	0,65	4,47	10,63	1,32	3,28	56,93	0,0620	0,0130	0,0014	0,0016	0,0153
TRZ137	6,39	16,32	0,66	3,96	9,68	1,29	3,18	58,33	0,0545	0,0125	0,0014	0,0016	0,0150
TRZ138	6,40	16,48	0,70	3,71	9,97	1,60	3,66	57,29	0,0607	0,0142	0,0015	0,0016	0,0169
TRZ139	6,15	15,80	0,67	3,76	11,43	1,56	3,11	57,35	0,0549	0,0125	0,0014	0,0015	0,0158
TRZ140	6,21	15,50	0,67	3,67	11,84	1,99	2,90	57,04	0,0549	0,0119	0,0012	0,0015	0,0159
TRZ141	6,48	16,46	0,73	3,89	10,44	1,79	2,82	57,20	0,0562	0,0129	0,0014	0,0017	0,0179
TRZ142	5,69	14,56	0,63	3,88	12,07	2,76	2,68	57,57	0,0495	0,0117	0,0013	0,0014	0,0150
TRZ143	6,73	17,05	0,73	3,91	11,06	1,48	3,55	55,30	0,0554	0,0143	0,0014	0,0016	0,0165
TRZ144	6,82	16,62	0,69	3,89	10,18	1,78	3,38	56,46	0,0582	0,0133	0,0015	0,0015	0,0151
TRZ145	6,63	16,73	0,71	3,45	8,45	1,43	3,36	59,05	0,0645	0,0131	0,0022	0,0014	0,0164
TRZ146	6,25	15,74	0,69	3,25	10,02	1,10	3,22	59,54	0,0681	0,0122	0,0023	0,0014	0,0155
TRZ147	6,71	16,00	0,68	3,44	7,63	1,04	3,28	61,00	0,0772	0,0128	0,0022	0,0014	0,0151
TRZ148	6,34	16,11	0,69	3,20	8,11	1,16	3,30	60,88	0,0715	0,0129	0,0023	0,0015	0,0160
TRZ149	6,37	16,98	0,70	3,68	8,43	1,17	3,29	59,21	0,0566	0,0136	0,0021	0,0014	0,0150
TRZ150	6,51	16,22	0,72	3,15	7,65	1,02	3,17	61,36	0,0613	0,0121	0,0022	0,0015	0,0158
TRZ151	6,27	15,42	0,68	3,25	10,61	0,99	3,19	59,40	0,0651	0,0122	0,0020	0,0014	0,0161
TRZ152	5,74	16,39	0,68	2,29	8,28	1,50	3,35	61,56	0,0791	0,0132	0,0019	0,0013	0,0163
TRZ153	6,61	16,53	0,71	3,39	9,44	1,21	3,30	58,63	0,0665	0,0131	0,0020	0,0015	0,0154
TRZ154	6,45	16,10	0,70	3,50	10,44	1,25	3,21	58,16	0,0617	0,0130	0,0018	0,0014	0,0161
TRZ155	6,36	15,99	0,70	3,23	8,82	1,31	3,22	60,17	0,0624	0,0127	0,0017	0,0015	0,0173
TRZ156	5,69	15,46	0,69	2,63	8,88	0,93	3,35	62,20	0,0400	0,0120	0,0015	0,0013	0,0169
TRZ157	6,81	16,76	0,70	3,72	11,49	1,26	3,71	55,37	0,0556	0,0139	0,0018	0,0015	0,0141
TRZ158	6,17	16,25	0,67	3,99	9,71	1,42	3,37	58,26	0,0523	0,0131	0,0016	0,0014	0,0151
TRZ159	6,39	16,29	0,68	3,29	10,62	1,43	3,58	57,54	0,0582	0,0133	0,0018	0,0015	0,0145
TRZ160	6,55	16,28	0,72	3,31	9,47	1,68	3,78	58,04	0,0563	0,0134	0,0017	0,0016	0,0156
TRZ161	5,70	14,80	0,62	2,91	18,14	1,93	3,99	51,75	0,0398	0,0126	0,0015	0,0014	0,0142
TRZ162	5,62	16,60	0,75	2,12	2,73	1,50	3,71	66,82	0,0299	0,0132	0,0014	0,0014	0,0180
TRZ163	6,17	17,80	0,76	3,68	1,07	1,39	4,29	64,69	0,0420	0,0146	0,0014	0,0017	0,0184
TRZ164	6,18	15,74	0,69	3,29	10,73	1,40	3,29	58,52	0,0567	0,0129	0,0015	0,0016	0,0168
TRZ165	6,78	16,90	0,71	3,61	10,24	1,37	3,58	56,63	0,0573	0,0135	0,0015	0,0016	0,0156
TRZ166	6,26	15,88	0,66	3,50	10,56	1,22	3,67	58,08	0,0543	0,0134	0,0014	0,0015	0,0153
TRZ167	6,60	16,77	0,69	3,46	9,27	1,28	3,61	58,15	0,0592	0,0142	0,0014	0,0015	0,0151
TRZ168	6,55	16,48	0,72	3,25	8,46	1,40	3,90	59,06	0,0644	0,0144	0,0014	0,0016	0,0157
TRZ169	6,37	16,32	0,68	4,04	10,60	1,15	3,64	57,03	0,0518	0,0136	0,0014	0,0016	0,0149
TRZ170	6,14	17,26	0,73	3,68	1,30	1,62	4,33	64,77	0,0443	0,0152	0,0015	0,0017	0,0190
TRZ171	6,01	16,08	0,73	2,57	4,72	1,39	3,61	64,75	0,0315	0,0145	0,0013	0,0015	0,0189
TRZ172	6,28	16,79	0,73	2,70	6,04	2,38	3,61	61,29	0,0396	0,0159	0,0015	0,0017	0,0168
TRZ173	5,80	15,13	0,64	3,63	12,00	1,42	3,23	57,99	0,0520	0,0129	0,0015	0,0016	0,0155
TRZ174	6,63	16,61	0,69	3,41	10,61	1,17	3,58	57,13	0,0595	0,0144	0,0017	0,0017	0,0154
TRZ175	6,15	15,83	0,65	3,99	11,41	1,26	3,39	57,15	0,0527	0,0134	0,0019	0,0015	0,0146
TRZ176	6,54	16,59	0,69	3,80	8,24	1,38	3,90	58,68	0,0555	0,0139	0,0019	0,0015	0,0156

Table 2: Normalised chemical composition of the ceramics analysed from Termez

ID.	Y	Sr	Ce	Ga	V	Zn	Cu	Ni	Cr
TRZ120	0,0027	0,0273	0,0055	0,0019	0,0098	0,0094	0,0036	0,0055	0,0078
TRZ121	0,0026	0,0340	0,0072	0,0021	0,0103	0,0113	0,0037	0,0051	0,0074
TRZ123	0,0026	0,0470	0,0051	0,0018	0,0102	0,0108	0,0031	0,0050	0,0069
TRZ124	0,0027	0,0313	0,0058	0,0020	0,0108	0,0116	0,0038	0,0055	0,0079
TRZ126	0,0026	0,0350	0,0057	0,0018	0,0111	0,0107	0,0043	0,0049	0,0075
TRZ127	0,0026	0,0393	0,0073	0,0019	0,0113	0,0112	0,0044	0,0059	0,0076
TRZ128	0,0028	0,0417	0,0074	0,0020	0,0121	0,0119	0,0038	0,0056	0,0083
TRZ129	0,0027	0,0415	0,0072	0,0019	0,0103	0,0118	0,0034	0,0051	0,0072
TRZ130	0,0028	0,0378	0,0069	0,0020	0,0103	0,0118	0,0039	0,0056	0,0074
TRZ131	0,0026	0,0380	0,0083	0,0016	0,0092	0,0098	0,0031	0,0044	0,0069
TRZ132	0,0025	0,0362	0,0072	0,0018	0,0103	0,0102	0,0035	0,0048	0,0074
TRZ133	0,0027	0,0402	0,0059	0,0017	0,0107	0,0100	0,0024	0,0045	0,0076
TRZ134	0,0025	0,0404	0,0072	0,0018	0,0086	0,0090	0,0037	0,0044	0,0067
TRZ135	0,0024	0,0457	0,0060	0,0016	0,0107	0,0104	0,0036	0,0048	0,0071
TRZ136	0,0026	0,0428	0,0078	0,0018	0,0107	0,0112	0,0038	0,0051	0,0075
TRZ137	0,0025	0,0527	0,0073	0,0018	0,0113	0,0117	0,0036	0,0052	0,0080
TRZ138	0,0027	0,0378	0,0066	0,0019	0,0114	0,0109	0,0034	0,0054	0,0098
TRZ139	0,0027	0,0359	0,0065	0,0017	0,0101	0,0102	0,0033	0,0050	0,0070
TRZ140	0,0027	0,0389	0,0049	0,0017	0,0106	0,0094	0,0045	0,0049	0,0073
TRZ141	0,0029	0,0389	0,0055	0,0020	0,0099	0,0112	0,0038	0,0052	0,0073
TRZ142	0,0025	0,0421	0,0054	0,0016	0,0089	0,0094	0,0034	0,0045	0,0067
TRZ143	0,0028	0,0390	0,0081	0,0019	0,0120	0,0109	0,0033	0,0053	0,0080
TRZ144	0,0026	0,0346	0,0074	0,0020	0,0108	0,0103	0,0037	0,0054	0,0076
TRZ145	0,0024	0,0359	0,0051	0,0020	0,0103	0,0110	0,0043	0,0054	0,0084
TRZ146	0,0023	0,0367	0,0051	0,0019	0,0097	0,0098	0,0045	0,0056	0,0077
TRZ147	0,0023	0,0462	0,0070	0,0019	0,0116	0,0103	0,0049	0,0057	0,0090
TRZ148	0,0022	0,0439	0,0070	0,0019	0,0114	0,0101	0,0043	0,0056	0,0087
TRZ149	0,0024	0,0378	0,0079	0,0020	0,0118	0,0107	0,0030	0,0056	0,0087
TRZ150	0,0023	0,0437	0,0064	0,0018	0,0113	0,0096	0,0038	0,0051	0,0092
TRZ151	0,0024	0,0491	0,0056	0,0018	0,0104	0,0104	0,0043	0,0049	0,0078
TRZ152	0,0023	0,0511	0,0062	0,0019	0,0116	0,0089	0,0042	0,0040	0,0087
TRZ153	0,0023	0,0379	0,0062	0,0019	0,0094	0,0084	0,0039	0,0059	0,0086
TRZ154	0,0025	0,0353	0,0070	0,0018	0,0089	0,0099	0,0047	0,0057	0,0085
TRZ155	0,0025	0,0422	0,0054	0,0017	0,0099	0,0092	0,0052	0,0050	0,0082
TRZ156	0,0025	0,0393	0,0076	0,0015	0,0115	0,0108	0,0054	0,0033	0,0071
TRZ157	0,0025	0,0378	0,0077	0,0020	0,0114	0,0111	0,0031	0,0057	0,0082
TRZ158	0,0025	0,0373	0,0074	0,0018	0,0104	0,0114	0,0035	0,0055	0,0082
TRZ159	0,0025	0,0377	0,0070	0,0019	0,0104	0,0100	0,0033	0,0053	0,0079
TRZ160	0,0027	0,0402	0,0062	0,0018	0,0110	0,0098	0,0033	0,0054	0,0081
TRZ161	0,0023	0,0472	0,0047	0,0018	0,0105	0,0103	0,0032	0,0039	0,0062
TRZ162	0,0025	0,0392	0,0066	0,0018	0,0130	0,0100	0,0020	0,0026	0,0087
TRZ163	0,0031	0,0135	0,0076	0,0019	0,0126	0,0122	0,0033	0,0050	0,0098
TRZ164	0,0028	0,0399	0,0059	0,0018	0,0091	0,0102	0,0036	0,0050	0,0077
TRZ165	0,0027	0,0322	0,0067	0,0019	0,0109	0,0119	0,0036	0,0058	0,0083
TRZ166	0,0027	0,0362	0,0056	0,0018	0,0110	0,0110	0,0030	0,0048	0,0077
TRZ167	0,0027	0,0306	0,0059	0,0019	0,0111	0,0101	0,0036	0,0058	0,0088
TRZ168	0,0026	0,0311	0,0066	0,0018	0,0106	0,0088	0,0036	0,0058	0,0085
TRZ169	0,0026	0,0412	0,0076	0,0019	0,0106	0,0108	0,0032	0,0053	0,0079
TRZ170	0,0032	0,0157	0,0081	0,0018	0,0116	0,0121	0,0033	0,0049	0,0093
TRZ171	0,0026	0,0303	0,0052	0,0018	0,0125	0,0090	0,0022	0,0029	0,0104
TRZ172	0,0028	0,0381	0,0064	0,0019	0,0235	0,0111	0,0018	0,0044	0,0243
TRZ173	0,0025	0,0431	0,0067	0,0017	0,0093	0,0110	0,0033	0,0053	0,0083
TRZ174	0,0028	0,0346	0,0070	0,0020	0,0112	0,0119	0,0036	0,0058	0,0083
TRZ175	0,0025	0,0437	0,0061	0,0020	0,0104	0,0122	0,0037	0,0054	0,0081
TRZ176	0,0027	0,0350	0,0067	0,0020	0,0104	0,0117	0,0035	0,0057	0,0085

Table 2: Normalised chemical composition of the ceramics analysed from Termez

ID.	Fe2O3	Al2O3	TiO2	MgO	CaO	Na2O	K2O	SiO2	Ba	Rb	Th	Nb	Zr
TRZ177	6,41	15,90	0,70	3,68	10,13	1,35	3,41	58,24	0,0647	0,0130	0,0016	0,0015	0,0158
TRZ178	6,21	15,81	0,67	3,39	9,65	1,38	3,54	59,16	0,0717	0,0129	0,0014	0,0014	0,0148
TRZ179	6,45	16,13	0,69	3,55	10,55	1,31	3,66	57,48	0,0537	0,0132	0,0017	0,0015	0,0151
TRZ180	6,20	15,81	0,65	4,18	12,23	1,10	3,08	56,59	0,0529	0,0131	0,0016	0,0015	0,0148
TRZ181	6,22	15,95	0,66	4,27	11,00	1,19	3,41	57,14	0,0496	0,0131	0,0018	0,0015	0,0146
TRZ182	5,89	16,49	0,73	3,56	5,88	1,62	3,47	62,16	0,0461	0,0153	0,0013	0,0017	0,0174
TRZ183	5,66	14,92	0,60	3,15	10,19	1,92	2,80	60,59	0,0605	0,0100	0,0014	0,0013	0,0139
TRZ184	6,04	15,35	0,65	3,29	12,62	1,05	3,36	57,44	0,0690	0,0129	0,0014	0,0015	0,0146
TRZ185	6,49	16,49	0,67	4,08	10,60	1,23	3,35	56,91	0,0485	0,0134	0,0015	0,0015	0,0153
TRZ186	6,45	16,21	0,66	4,27	10,79	1,37	3,56	56,51	0,0488	0,0135	0,0016	0,0016	0,0152
TRZ187	6,30	17,31	0,76	3,27	6,82	0,67	3,68	60,98	0,0551	0,0162	0,0014	0,0017	0,0176
TRZ188	6,36	16,07	0,67	3,50	10,49	1,47	3,36	57,92	0,0531	0,0129	0,0014	0,0015	0,0153
TRZ189	5,41	13,16	0,57	2,82	24,41	1,95	3,20	48,31	0,0417	0,0116	0,0014	0,0014	0,0137
TRZ190	6,22	16,12	0,65	4,15	10,58	1,41	3,35	57,35	0,0508	0,0135	0,0015	0,0015	0,0147
TRZ191	6,12	15,45	0,64	4,01	14,49	1,30	3,66	54,17	0,0504	0,0130	0,0013	0,0016	0,0138
TRZ192	5,92	15,26	0,65	3,72	12,31	1,50	3,27	57,19	0,0526	0,0120	0,0013	0,0016	0,0157
TRZ193	6,20	16,12	0,70	3,69	9,97	1,45	3,24	58,46	0,0506	0,0129	0,0014	0,0016	0,0159
TRZ194	6,40	16,22	0,66	3,92	12,03	1,47	3,09	56,04	0,0513	0,0130	0,0014	0,0015	0,0149
TRZ195	6,12	16,08	0,66	3,43	9,16	1,42	3,29	59,69	0,0478	0,0130	0,0014	0,0015	0,0145
TRZ196	6,34	16,02	0,66	4,17	11,37	1,17	3,50	56,59	0,0511	0,0130	0,0013	0,0016	0,0143
TRZ197	6,13	15,70	0,70	3,50	11,58	1,42	3,13	57,66	0,0560	0,0120	0,0014	0,0015	0,0159
TRZ198	5,90	15,72	0,62	4,23	11,65	1,26	3,28	57,17	0,0499	0,0131	0,0014	0,0015	0,0138
TRZ199	6,53	16,24	0,69	3,40	11,51	1,23	3,38	56,84	0,0578	0,0136	0,0014	0,0016	0,0156
TRZ200	6,23	15,82	0,67	3,62	9,99	1,43	3,16	58,89	0,0718	0,0125	0,0013	0,0016	0,0159
TRZ201	6,61	16,49	0,68	3,44	9,39	1,44	3,54	58,23	0,0665	0,0136	0,0016	0,0016	0,0150
TRZ202	6,07	15,78	0,65	3,44	12,77	1,49	3,29	56,34	0,0526	0,0131	0,0016	0,0015	0,0143

ID.	Y	Sr	Ce	Ga	V	Zn	Cu	Ni	Cr
TRZ177	0,0026	0,0355	0,0071	0,0019	0,0102	0,0118	0,0042	0,0056	0,0083
TRZ178	0,0025	0,0408	0,0057	0,0018	0,0105	0,0111	0,0034	0,0051	0,0076
TRZ179	0,0026	0,0408	0,0062	0,0019	0,0105	0,0115	0,0035	0,0051	0,0072
TRZ180	0,0025	0,0301	0,0068	0,0018	0,0101	0,0095	0,0035	0,0054	0,0097
TRZ181	0,0026	0,0421	0,0061	0,0019	0,0103	0,0118	0,0034	0,0055	0,0078
TRZ182	0,0024	0,0338	0,0078	0,0019	0,0207	0,0115	0,0020	0,0044	0,0245
TRZ183	0,0023	0,0367	0,0062	0,0017	0,0098	0,0091	0,0032	0,0046	0,0080
TRZ184	0,0025	0,0415	0,0063	0,0017	0,0104	0,0105	0,0033	0,0050	0,0076
TRZ185	0,0026	0,0381	0,0051	0,0020	0,0107	0,0113	0,0035	0,0058	0,0083
TRZ186	0,0026	0,0431	0,0077	0,0019	0,0106	0,0119	0,0028	0,0057	0,0083
TRZ187	0,0026	0,0372	0,0082	0,0019	0,0218	0,0121	0,0022	0,0047	0,0189
TRZ188	0,0026	0,0345	0,0065	0,0018	0,0096	0,0105	0,0031	0,0051	0,0096
TRZ189	0,0023	0,0581	0,0059	0,0016	0,0095	0,0104	0,0025	0,0042	0,0060
TRZ190	0,0026	0,0408	0,0059	0,0019	0,0108	0,0114	0,0034	0,0055	0,0082
TRZ191	0,0023	0,0501	0,0054	0,0018	0,0101	0,0108	0,0034	0,0051	0,0075
TRZ192	0,0026	0,0422	0,0068	0,0018	0,0098	0,0107	0,0032	0,0048	0,0074
TRZ193	0,0027	0,0428	0,0063	0,0018	0,0101	0,0107	0,0034	0,0052	0,0079
TRZ194	0,0027	0,0336	0,0068	0,0018	0,0102	0,0112	0,0033	0,0054	0,0082
TRZ195	0,0025	0,0320	0,0050	0,0017	0,0100	0,0098	0,0031	0,0047	0,0080
TRZ196	0,0025	0,0455	0,0058	0,0018	0,0109	0,0110	0,0035	0,0053	0,0083
TRZ197	0,0026	0,0464	0,0064	0,0016	0,0093	0,0097	0,0034	0,0046	0,0071
TRZ198	0,0024	0,0403	0,0064	0,0017	0,0110	0,0108	0,0034	0,0052	0,0081
TRZ199	0,0026	0,0411	0,0062	0,0018	0,0103	0,0096	0,0038	0,0054	0,0077
TRZ200	0,0025	0,0358	0,0051	0,0017	0,0097	0,0101	0,0034	0,0053	0,0085
TRZ201	0,0027	0,0377	0,0066	0,0019	0,0107	0,0105	0,0035	0,0056	0,0081
TRZ202	0,0024	0,0427	0,0069	0,0017	0,0105	0,0096	0,0033	0,0050	0,0073

Table 2: Normalised chemical composition of the ceramics analysed from Termez

At first site, there is one important general observation can be made on the data set. The Na_2O concentrations are clearly high in all the individuals. According to previous results (Martínez *et al.*, 2008) the generally high concentrations in this element can be explained by the presence of NaCl crystals in the ceramic paste. The presence of these crystals, most likely, can be the result of post-depositional alteration and/or contamination due to the high concentrations of NaCl in the specific geographical area where the ceramics were discovered. In the deserts the high salt concentrations are ordinary and that can be the reason for this specific alteration and/or contamination process. Additionally, the formation of a zeolithe called analcyme ($Na_2AlSi_2O_6 \times H_2O$) in the higher fired ceramics could be confirmed in this study and it can be also consequence of the NaCl contamination presence in the ceramic paste.

One of the most important steps in a chemical analysis, as it aims to compare the composition of the individuals analysed, is to calculate somehow the variability in the data set. One of the common ways to do that is to calculate the Compositional Variation Matrix (CVM) (Buxeda and Kilikoglou, 2003). This matrix includes all the necessary information to identify the variability in the data set, like the total variation and the variability that each element is introducing in the data set. Beside the above mentioned, it also indicates the relation between all the pair of elements. The CVM calculated for our data set can be seen in Table 3. It has been calculated without considering the following elements: Mo, Sn, Co, W, MnO P_2O_5 and Pb. The first two elements have been left out in the cause of analytical imprecision, as both of them are under their regression limits in ceramics. MnO is an element with analytical accuracy problems. Co and W have been left out from the statistical treatment because of the possibility that can be contaminated due to the sample preparation process and, the last two above mentioned elements (P_2O_5 and Pb) because they are elements very susceptible to suffer post-depositional contaminations, therefore they can introduce a false high variability in the data set.

The total variation (vt) in this data set according to the CVM is 0.3541 which generally indicates a polygenetic data (the presence of more than one production in the data set) but also the similar geochemical character (the raw materials possibly come from areas with similar geological character) for all the analysed material. At the first site the variability introduced by all the elements is relatively low. In Table 3 we pointed out by yellow the elements which introduce more than the 50% of the variability in this data set which are CaO, Na_2O, Sr, Ba, Ce, Cu and Cr. From these elements in the case of Na_2O and Ba the high variability is due to post-depositional contaminations. The first one is almost altered in the whole data set as above explained, because of the presence of NaCl (salt) and at specific cases (TRZ028, TRZ030, TRZ037, TRZ056, TRZ059, TRZ063, TRZ071, TRZ077, TRZ079, TRZ083, TRZ119, TRZ141, TRZ183 and TRZ200) because of the presence of analcime ($Na_2AlSi_2O_6 \times H_2O$), which affects in these specific individuals also the K_2O and Rb concentrations (Picon, 1976; Segebade and Lutz, 1980; Lemoin *et al.*, 1981; Scmitt, 1989; Buxeda and Cau, 1997; Buxeda and Gurt, 1998; Buxeda, 1999b; Buxeda *et al.*, 2001; Buxeda *et al.*, 2002; Schwedt *et al.*, 2006). On the other hand, Ba seems to be altered in specific individuals: TRZ050, TRZ049, TRZ044, TRZ012 and TRZ127. To avoid that the chemical differences introduced by the above mentioned alterations and/or contaminations dominate the statistical treatment of the data set we ignored Na_2O, K_2O, Rb and Ba in the rest of the statistical treatment.

In the new CVM the vt is equal to 0.2890 and he most variable elements in this new CVM are maintained (CaO, Sr, Ce, Cu and Cr). Looking at the chemical data (Table 2) the high variability introduced by CaO and Sr which are chemically associated elements is owed to the fact that even though the most of the analysed individuals are calcareous (approximately between 8-12% CaO) there are two chemical loners TRZ163 and TRZ170 which are no calcareous and one individual (TRZ189) which is much more calcareous than the rest its CaO concentration is approximately 20%. Finally, there are seven individuals (TRZ084, TRZ104, TRZ171, TRZ172, TRZ182, TRZ187 and TRZ189) which are border calcareous.

El.	Fe2O3	Al2O3	TiO2	MgO	CaO	Na2O	K2O	SiO2	Ba	Rb	Th
Fe2O3	0,0000	0,0013	0,0027	0,0167	0,0935	0,0468	0,0121	0,0063	0,0241	0,0099	0,0149
Al2O3	0,0013	0,0000	0,0013	0,0169	0,1002	0,0438	0,0090	0,0029	0,0273	0,0079	0,0144
TiO2	0,0027	0,0013	0,0000	0,0215	0,1047	0,0440	0,0101	0,0026	0,0293	0,0098	0,0156
MgO	0,0167	0,0169	0,0215	0,0000	0,0823	0,0506	0,0306	0,0228	0,0412	0,0282	0,0301
CaO	0,0935	0,1002	0,1047	0,0823	0,0000	0,1163	0,1179	0,1033	0,0982	0,1164	0,1027
Na2O	0,0468	0,0438	0,0440	0,0506	0,1163	0,0000	0,0566	0,0422	0,0820	0,0624	0,0601
K2O	0,0121	0,0090	0,0101	0,0306	0,1179	0,0566	0,0000	0,0104	0,0426	0,0066	0,0252
SiO2	0,0063	0,0029	0,0026	0,0228	0,1033	0,0422	0,0104	0,0000	0,0301	0,0116	0,0166
Ba	0,0241	0,0273	0,0293	0,0412	0,0982	0,0820	0,0426	0,0301	0,0000	0,0347	0,0318
Rb	0,0099	0,0079	0,0098	0,0282	0,1164	0,0624	0,0066	0,0116	0,0347	0,0000	0,0205
Th	0,0149	0,0144	0,0156	0,0301	0,1027	0,0601	0,0252	0,0166	0,0318	0,0205	0,0000
Nb	0,0061	0,0039	0,0043	0,0145	0,0942	0,0383	0,0120	0,0049	0,0294	0,0104	0,0182
Zr	0,0092	0,0057	0,0032	0,0266	0,1094	0,0410	0,0137	0,0029	0,0344	0,0136	0,0199
Y	0,0104	0,0075	0,0075	0,0146	0,0965	0,0368	0,0149	0,0079	0,0373	0,0158	0,0210
Sr	0,0393	0,0396	0,0411	0,0509	0,0631	0,0748	0,0432	0,0383	0,0504	0,0471	0,0491
Ce	0,0259	0,0232	0,0241	0,0402	0,1264	0,0674	0,0330	0,0247	0,0493	0,0291	0,0338
Ga	0,0134	0,0114	0,0140	0,0133	0,0954	0,0436	0,0207	0,0153	0,0368	0,0195	0,0173
V	0,0157	0,0117	0,0111	0,0370	0,1280	0,0595	0,0179	0,0127	0,0483	0,0150	0,0285
Zn	0,0092	0,0076	0,0098	0,0142	0,0931	0,0494	0,0171	0,0104	0,0365	0,0140	0,0180
Cu	0,0237	0,0269	0,0287	0,0308	0,0950	0,0746	0,0458	0,0317	0,0268	0,0386	0,0252
Ni	0,0109	0,0141	0,0183	0,0139	0,0920	0,0596	0,0292	0,0232	0,0237	0,0204	0,0187
Cr	0,0265	0,0217	0,0207	0,0446	0,1496	0,0682	0,0299	0,0224	0,0597	0,0225	0,0340
t.i	0,4186	0,3981	0,4243	0,6417	2,1782	1,2179	0,5983	0,4432	0,8740	0,5542	0,6156
vt/t.i	0,8458	0,8895	0,8345	0,5518	0,1626	0,2907	0,5918	0,7988	0,4051	0,6389	0,5752
r v,t	0,9945	0,9947	0,9884	0,9340	0,1054	0,9302	0,9783	0,9837	0,8921	0,9782	0,9818

El.	Nb	Zr	Y	Sr	Ce	Ga	V	Zn	Cu	Ni	Cr
Fe2O3	0,0061	0,0092	0,0104	0,0393	0,0259	0,0134	0,0157	0,0092	0,0237	0,0109	0,0265
Al2O3	0,0039	0,0057	0,0075	0,0396	0,0232	0,0114	0,0117	0,0076	0,0269	0,0141	0,0217
TiO2	0,0043	0,0032	0,0075	0,0411	0,0241	0,0140	0,0111	0,0098	0,0287	0,0183	0,0207
MgO	0,0145	0,0266	0,0146	0,0509	0,0402	0,0133	0,0370	0,0142	0,0308	0,0139	0,0446
CaO	0,0942	0,1094	0,0965	0,0631	0,1264	0,0954	0,1280	0,0931	0,0950	0,0920	0,1496
Na2O	0,0383	0,0410	0,0368	0,0748	0,0674	0,0436	0,0595	0,0494	0,0746	0,0596	0,0682
K2O	0,0120	0,0137	0,0149	0,0432	0,0330	0,0207	0,0179	0,0171	0,0458	0,0292	0,0299
SiO2	0,0049	0,0029	0,0079	0,0383	0,0247	0,0153	0,0127	0,0104	0,0317	0,0232	0,0224
Ba	0,0294	0,0344	0,0373	0,0504	0,0493	0,0368	0,0483	0,0365	0,0268	0,0237	0,0597
Rb	0,0104	0,0136	0,0158	0,0471	0,0291	0,0195	0,0150	0,0140	0,0386	0,0204	0,0225
Th	0,0182	0,0199	0,0210	0,0491	0,0338	0,0173	0,0285	0,0180	0,0252	0,0187	0,0340
Nb	0,0000	0,0050	0,0031	0,0407	0,0243	0,0083	0,0143	0,0072	0,0297	0,0149	0,0219
Zr	0,0050	0,0000	0,0069	0,0442	0,0243	0,0169	0,0140	0,0118	0,0331	0,0273	0,0235
Y	0,0031	0,0069	0,0000	0,0461	0,0274	0,0059	0,0187	0,0084	0,0306	0,0201	0,0273
Sr	0,0407	0,0442	0,0461	0,0000	0,0634	0,0482	0,0534	0,0412	0,0604	0,0525	0,0696
Ce	0,0243	0,0243	0,0274	0,0634	0,0000	0,0335	0,0309	0,0253	0,0511	0,0371	0,0398
Ga	0,0083	0,0169	0,0059	0,0482	0,0335	0,0000	0,0243	0,0117	0,0294	0,0158	0,0287
V	0,0143	0,0140	0,0187	0,0534	0,0309	0,0243	0,0000	0,0166	0,0558	0,0350	0,0087
Zn	0,0072	0,0118	0,0084	0,0412	0,0253	0,0117	0,0166	0,0000	0,0303	0,0174	0,0263
Cu	0,0297	0,0331	0,0306	0,0604	0,0511	0,0294	0,0558	0,0303	0,0000	0,0220	0,0664
Ni	0,0149	0,0273	0,0201	0,0525	0,0371	0,0158	0,0350	0,0174	0,0220	0,0000	0,0388
Cr	0,0219	0,0235	0,0273	0,0696	0,0398	0,0287	0,0087	0,0263	0,0664	0,0388	0,0000
t.i	0,4055	0,4868	0,4647	1,0566	0,8340	0,5233	0,6571	0,4752	0,8565	0,6049	0,8507
vt/t.i	0,8731	0,7274	0,7620	0,3351	0,4245	0,6766	0,5389	0,7451	0,4134	0,5854	0,4162
r v,t	0,9917	0,9761	0,9799	0,6984	0,9907	0,9799	0,9404	0,9931	0,8638	0,9347	0,9576
vt	0,3541										

Table 3: Compositional Variation Matrix (CVM) calculated upon the 202 individuals sampled at Termez and upon the subcomposition: Fe_2O_3, Al_2O_3, TiO_2, MgO, CaO, Na_2O, K_2O, SiO_2, Ba, Rb, Th, Nb, Zr, Y, Sr, Ce, Ga, V, Zn, Cu, Ni, Cr

To continue the statistical treatment the chemical data were transformed into logratios following the consideration of Aitchison (1986) and Buxeda (1999) on compositional data, according to the following equation:

$$\mathbf{x} \in S^{d} \rightarrow \mathbf{y} = \log(\frac{\mathbf{x}_{-D}}{\mathrm{x}_{D}}) \in R^{d}$$

where S^d is a d-dimensional simplex (d=D-1) and $\mathbf{x}_{-D}=(x_1,...,x_d)$. The logratio transformation was performed upon the subcomposition: Fe_2O_3 TiO_2, MgO, CaO, SiO_2, Rb, Zr, Y, Sr, Ce, Ga, V, Nb, Zn, Cu, Ni and Cr where Al_2O_3 was used as divisor, as according to the second CVM it was the element less contributing to the chemical variability (Buxeda and Kilikoglou 2003), of the 202 analysed individuals. The chemical results are summarized in the dendrogram of Figure 2, resulting from the cluster analysis performed upon the previous subcomposition, using the Square Euclidean distance and the centroid algorithm, performed by S-plus2000 (MathSoft, 1999). In this dendrogram there are 12 (TRZ163, TRZ170, TRZ172, TRZ182, TRZ187, TRZ162, TRZ171, TRZ104, TRZ084, TRZ161, TRZ189 and TRZ088) individuals located in the left side in a marginal position all of them present important chemical differences from the rest of the analysed individuals, therefore they are clearly represent chemical outliers. However, between these outliers two different chemical groups can be recognised. The first composed by two opened rim cooking ware TRZ163 (TZ08-RC-4-1) and TRZ170 (TZ08-RC-5-7) have a very similar chemical composition. The cooking ware TRZ163 comes from the stratigraphical unit 4 from RC grid of ***Tchinguiz Tepe*** whereas TRZ170 belongs to the stratigraphical unit 5 from RC grid. Both are very low calcareous, have significantly higher composition in K_2O, Ce and Zn and slightly higher MgO content. Together they represent one single production (called $\mathbf{TRZ_{(A)}}$ in the dendrogram). These chemical differences are important enough to indicate that this production stands out chemically from the rest of the analysed individuals but only a petrographical study can confirm the *in situ* or foreign character of the raw materials. The mean chemical composition and the standard deviation of each element of this production are given in Table 4, and in Figure 3 we present the typology of this production.

From a petrographic point of view, the opened rim cooking wares TRZ163 and TRZ170 of $TRZ_{(A)}$ are very similar and both are characteristics of a medium-fine fabric named $TRZ_{(A)}$ (Table 5). Groundmass is more homogeneous in TRZ163 than in TRZ170 because of the streaks of calcareous clay displayed on the matrix. Nodules of micritic calcite are more frequents in TRZ170. The colour under PPL is reddish-brown and the optical activity is low. The inclusions are moderately sorted, open-spaced and they present a bimodal grain-size distribution (Figure 4). The coarse fraction (500µm of maximum long axis dimension) contains monocrystalline and polycrystalline quartz, plagioclase, amphiboles and mica-muscovite detached from granitic rocks and other isolated minerals as epidote and opaques. Predominant rocks are quartz-mica schist with few chert and sandstones. The fine fraction is mainly composed by quartz and mica-muscovite. Few voids are present, consisting of rare elongate macrovughs, orientated in a parallel axis to the vessel margins. They are partially filled by secondary micritic calcite.

Another clear chemical group is $\mathbf{TRZ_{(B)}}$ (Figure 5) which contains three cooking wares: Two of them (TRZ172=TZ08-RC-5-9, TRZ182=TZ08-RC-21-6) coming from RC grid (stratigraphical units 5 and 21 respectively) and the other (TRZ187=TZ08-RF-11-6) coming from the stratigraphical unit 11 from RF grid, where a kiln of ***Tchinguiz Tepe*** is located. This group is border calcareous with significant differences in Ce, Cu and Cr from the rest of the analysed material. Specifically, the very high Cr concentration that characterise them regarding to the rest of the ceramic material is an indication of the possible foreign character of this production. However, this hypothesis is being crosschecked by the petrographical study at the moment.

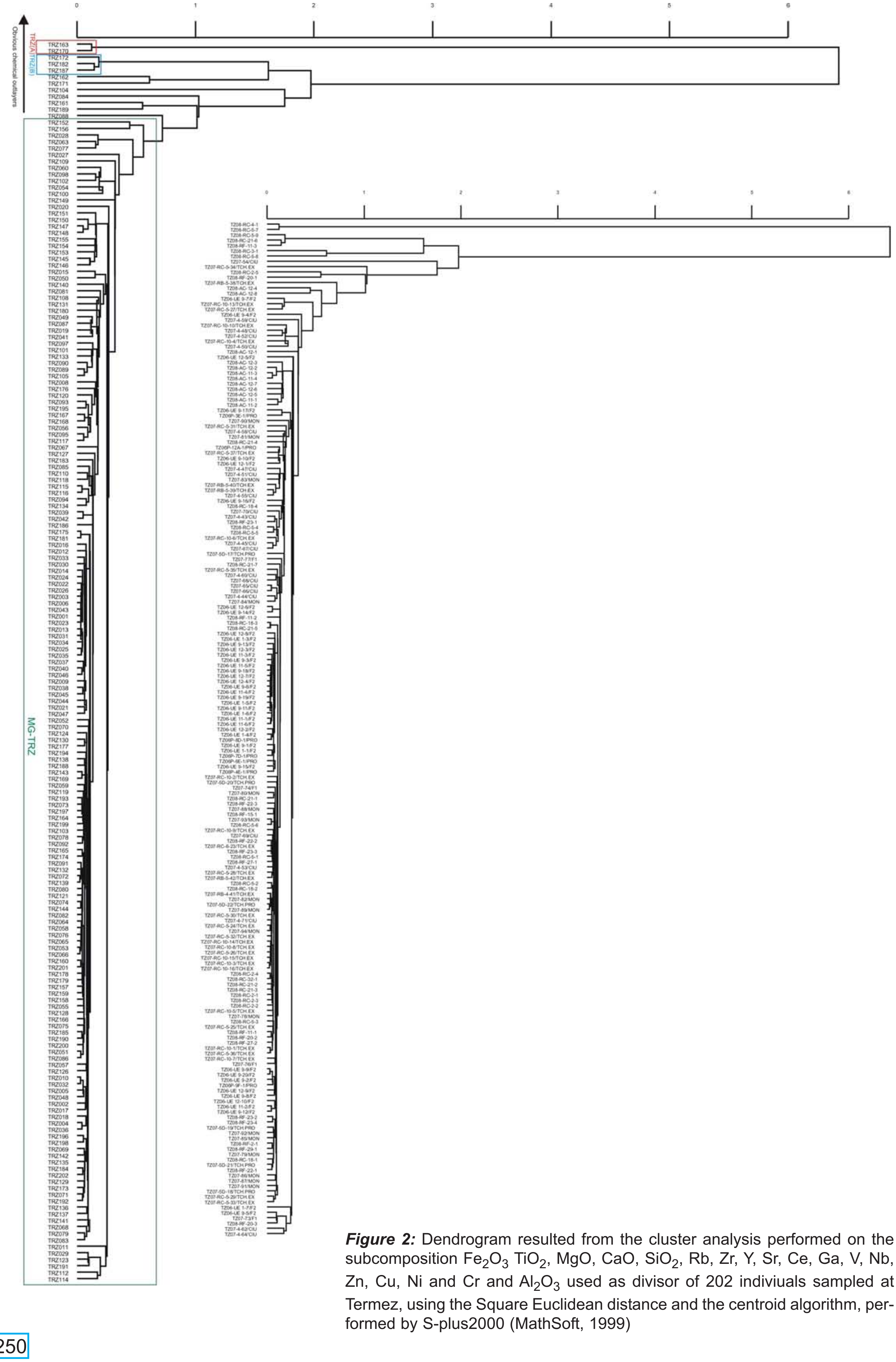

Figure 2: Dendrogram resulted from the cluster analysis performed on the subcomposition Fe_2O_3 TiO_2, MgO, CaO, SiO_2, Rb, Zr, Y, Sr, Ce, Ga, V, Nb, Zn, Cu, Ni and Cr and Al_2O_3 used as divisor of 202 indiviuals sampled at Termez, using the Square Euclidean distance and the centroid algorithm, performed by S-plus2000 (MathSoft, 1999)

TRZ(A) n=2		
EL.	**MEAN**	**St Desv**
Fe2O3%	6,03	0,00
Al2O3%	17,17	0,32
TiO2%	0,73	0,01
MgO%	3,60	0,01
CaO%	1,17	0,16
Na2O%	1,48	0,16
K2O%	4,22	0,04
SiO2%	63,38	0,26
Ba ppm	422,50	17,68
Rb ppm	146,00	4,24
Th ppm	14,50	0,71
Nb ppm	17,00	0,00
Zr ppm	183,00	4,24
Y ppm	30,50	0,71
Sr ppm	143,00	15,56
Ce ppm	76,50	3,54
Ga ppm	18,50	0,71
V ppm	118,50	6,36
Zn ppm	119,00	0,00
Cu ppm	32,00	0,00
Ni ppm	48,50	0,71
Cr ppm	93,50	3,54

Table 4: The mean chemical composition and the standard deviation of each element of $TRZ_{(A)}$

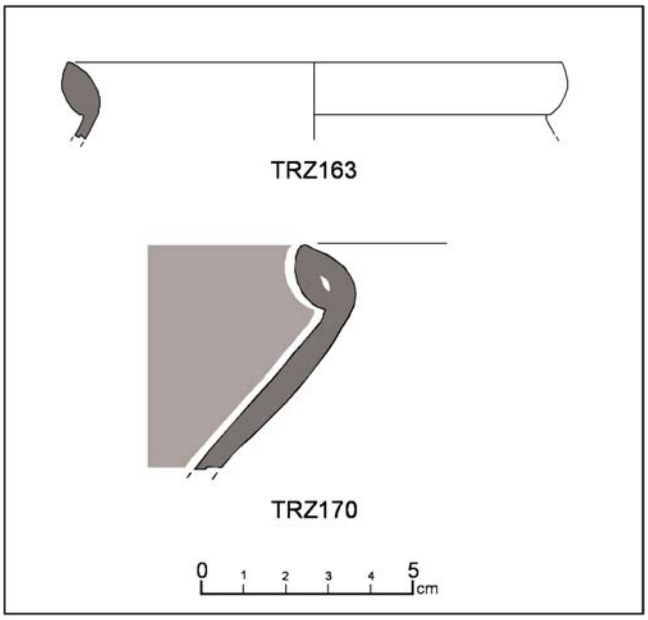

Figure 3: Typology of the group $TRZ_{(A)}$

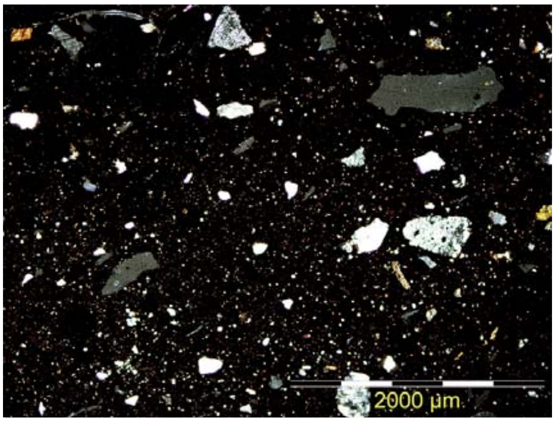

TRZ 163 40 X

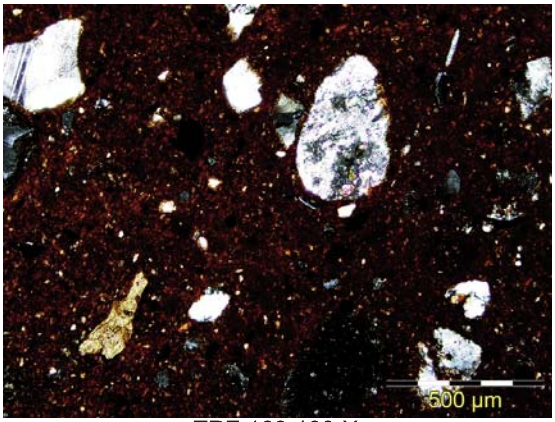

TRZ 163 100 X

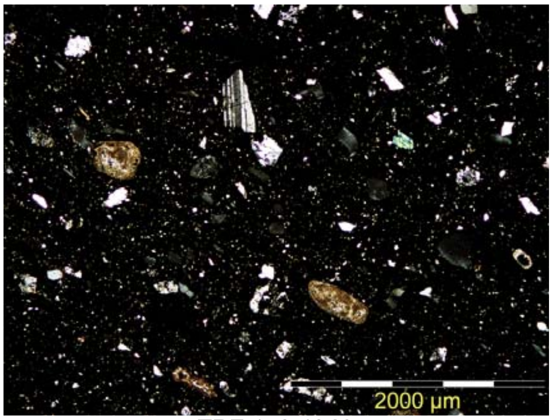

TRZ 170 40 X

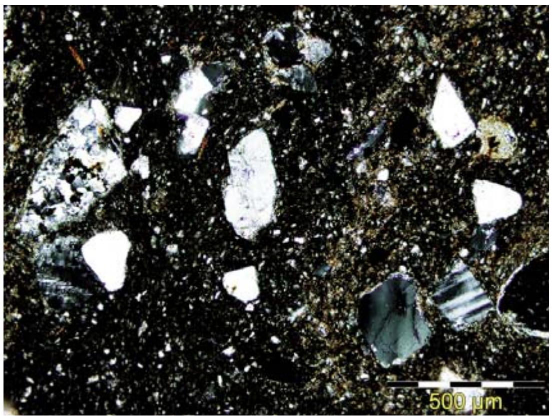

TRZ 170 100 X

Figure 4: A microphotograph by crossed polars of the samples TRZ163 and TRZ170 belonging to fabric $TRZ_{(A)}$

FABRIC NAME	SAMPLE	TYPOLOGY	FABRIC TYPE	COLOUR IN PPL	INCLUSIONS	VOIDS
TRZ$_{(A)\text{ - RC}}$	TRZ163, 170	Cooking ware	Medium-Fine	reddish-brown	Few, eq, sr, Φ < 500 µm Predominant: granitic rocks and crystals (qtz, pg, kfs, amph, ill) Frequents: quartz-mica schist Few: sandstone, chert, epid, opaque	Few meso-vesicles, macro-vesicles
TRZ$_{(B)\text{ – RC/RF}}$	TRZ172	Cooking ware	Coarse	reddish-brown	Frequents, el, sr, Φ < 3 mm Predominant c. fr.: shell fragments Few c. fr.: chert, opaques, mica muscovite Predominant f. fr.: qtz and mica muscovite	Macrovughs and channels
	TRZ182	Cooking ware	Coarse	orange- brown	Frequents, el, sr, Φ < 3 mm Predominant: siltstone, claystones, Frequents: quartz-mica schist, Few: quartz plagioclase, amph, ill, opaques Rares: shell fragments	Few mesovughs, macrovughs
	TRZ187	Cooking ware	Coarse	orange- brown	Frequents, el, sr, Φ < 3 mm Predominant c. fr.: shell fragments, microfossils, siltstone, claystones Predominant f. fr.: qtz and mica muscovite	Frequent macrovughs, channels
TRZ$_{(c)\text{ – RC}}$ similar to TRZ$_{(A)}$	TRZ084	Painted common ware	Medium-coarse	orange-brown	Few, eq, sr, Φ < 1 mm Predominant: granitic rocks and crystals (qtz, pg, kfs, amph, ill) Frequents: quartz-mica schist Rare: sandstone, chert, epid, opaque	Very rare micro-vesicles
TRZ$_{(D)\text{ - RC}}$	TRZ162	Cooking ware	Coarse	reddish-brown	Frequents, el, sr, Φ < 3 mm Predominant: sandstone, claystones, fossils Frequents: micritic calcite, opaques Few: chert qtz, ill Predominant f. fr.: qtz, mica muscov., opaque	Frequents macrovughs, channels
	TRZ171	Cooking ware	Coarse	orange-brown	Frequents, el-eq, sr, Φ < 3 mm Predominant: sandstone, claystones, shell fragments, microfossils Frequents: micritic calcite, opaques Few: chert qtz, ill Predominant f. fr.: qtz; few: mica muscovite	Few mesovughs
TRZ$_{(E)\text{ – RC, RF,}}$ Citadel	TRZ104	Cooking ware	Coarse	yellowish-brown	Frequents, el, sr, Φ < 3 mm Predominant: sedimentary rock with shell fragments, claystone, siltstone Frequent:, qtz, ill	Frequents mesovughs, meso-vesicles
	TRZ161	Cooking ware	Coarse	yellowish-brown	Frequents, el, sr, Φ < 3 mm Predominant: sedimentary rock with shell fragments, claystone, siltstone Frequent: qtz, ill Few: Quartz-mica schist	Frequents mesovughs and channels
	TRZ189	Cooking ware	Coarse	yellowish-brown	Frequents, el, sr, Φ < 3 mm Predominant: sedimentary rock with shell fragments, claystone, siltstone Few: Quartz-mica schist, sandstone	Frequents mesovughs and channels
KT-K2	TRZ006, 25, 33, 36	Common ware	Medium-Fine	reddish-brown	Few, eq, sr, Φ 600 µm Predominant: qrtz, quartz-mica schist Frequent: pg, kfs, amph, ill, epid Few: chert, sandstone, shell and fossil fragments Evidence of clay mixing	Few micro-vesicles

Table 5: Typological and petrographic characteristics of the identified productions

FABRIC NAME	SAMPLE	TYPOLOGY	FABRIC TYPE	COLOUR IN PPL	INCLUSIONS	VOIDS
KT-K2 loners	TRZ020	Common ware	Medium-Fine	yellowish-brown	Few, eq, sr, Φ < 500 µm Predominant: granitic rocks and crystals (qtz, pg, kfs, amph, ill) Frequent: chert Few: quartz-mica squist	Few micro-vesicles
	TRZ041	Common ware	Medium-Fine	reddish-brown	Frequents, eq, sr, Φ < 800 µm Predominant: qtz, ill Frequent: quartz-mica schist, chert, , sandstone Few: pg, amph	Few micro-vesicles
TRZ1$_{(A)}$ Monst, K1, RC	TRZ065, 76, 126, 132, 133, 138, 143	Common ware and painted common ware	Medium-Fine	yellowish-brown	Few, eq-el, sr-sa, Φ < 600 µm Predominant: granitic rocks and crystals (qtz, pg, kfs, amph, ill), qtz-mica schist Few: chert, micritic calcite	Few micro-vesicles
TRZ1$_{(B)}$ - RC	TRZ085	Cooking ware	Medium-coarse	orange-brown	Few, eq, el, sr, Φ < 2 mm Predominant: qtz, shell fragments Frequent: qtz-mica schist, pg, amph, epid Few: granitic rocks, opaques, ill, micritic calc.	Frequent mesovughs
TRZ1$_{(C)}$ - RC	TRZ183	Cooking ware	Medium-coarse	yellowish-brown	Few, eq, sr, Φ < 800 µm Predominant: qtz, ill, qtz-mica schist, pg, Frequent: sandstone, amph, opaques Few: chert	Frequent micro channels
TRZ1$_{(D)}$ - RF	TRZ188	Cooking ware	Medium-Fine	yellowish-brown	Few, eq, sr, Φ < 500 µm Predominant: granitic rocks and crystals (qtz, pg, kfs), Frequent: qtz-mica schist Few: amph, ill, opaques	Few mesovughs
KT-K1 loners	TRZ123	Painted common ware	Medium-Fine	reddish-brown	Few, eq, sr, Φ < 600 µm Predominant: qtz, ill Frequent: qtz-mica schist, pg Few: chert, amph, epid, opaques	Very few mesovughs, microvughs
	TRZ127	Common ware	Fine	yellowish-orange	Very few, eq, sr, , Φ < 400 µm Predominant: qtz, pg, ill, opaques Evidence of clay mixing	Very few mesovughs, microvughs
KT Monastery loner	TRZ142	Common ware	Medium-Fine	reddish-brown	Few, eq, sr, Φ < 650 µm Predominant: qtz, ill Frequent: qtz-mica schist, pg Few: amph, opaques	Very few mesovughs
Tch T loners - Prospc	TRZ067	Common ware	Medium-coarse	dark green	Frequent, eq, sr, Φ < 700 µm Predominant: qtz Few: sandstone, pg	Frequent Meso-vesicles
	TRZ068	Common ware	Medium-Fine	yellowish-orange	Few, eq, sr, Φ < 500 µm Predominant: qtz Frequent: ill, pg, opaques, Few: microfossils, qtz-mica squist, amph.	Very few mesovughs
AC loner	TRZ156	Cooking ware	Coarse	orange-brown	Frequent, el, sr, Φ < 4 mm Predominant: shell fragments, sandstones, siltstones, opaques Rare: qtz, ill	Frequent mesochannels, mesovughs
RC loner	TRZ060	Common ware	Medium-Fine	reddish-brown	Few, eq, sr, Φ < 500 µm Predominant: qtz, ill Frequent: pg, qtz-mica squist, granitic rock Few: amph, chert, micritic calcite	Few mesovughs

Table 5: Typological and petrographic characteristics of the identified productions

FABRIC NAME	SAMPLE	TYPOLOGY	FABRIC TYPE	COLOUR IN PPL	INCLUSIONS	VOIDS
Citadell loners	TRZ098	Common ware	Medium-Fine	yellowish-brown	Few, eq, sr, Φ < 500 µm Predominant: qtz, microfossils, micritic calcite, ill Frequent: pg, qtz-mica squist, granitic rock Evidence of clay mixing	Few mesovughs
	TRZ112	Common ware	Medium-Fine	reddish-brown	Frequent, eq, sr, Φ < 500 µm Predominant: granitic rocks and crystals (qtz, pg, kfs, amph, ill), qtz-mica schist Frequent: microfossils, micritic calcite Few: epid, opaques	Few mesovughs
	TRZ114	Common ware	Medium-Fine	orange-brown	Few, eq, sr, Φ < 500 µm Predominant: granitic rocks and crystals (qtz, pg, kfs, amph, ill), qtz-mica schist Frequent: microfossils, micritic calcite Few: epid, opaques	Frequent mesovughs
$KPT_{(A)}$	TRZ233	Cooking ware	Medium-coarse	reddish-brown/orange	Frequent, eq-el, sa, Φ < 700 µm Predominant: qtz, pg, qtz-mica schist, ill Frequent: mica schist, sandstones, kfs, amph Few: opaques, chert	Few meso-vesicles, mesovughs
KPT Loner	TRZ235	Cooking ware	Medium-coarse	orange-brown/ yellowish	Frequent, eq-el, sa, Φ < 500 µm Predominant: qtz, pg, qtz-mica schist, mica schist, ill, opaque Frequent: kfs, amph Few: shell fragments, microfossils	Few meso-vesicles, mesovughs
ZT	TRZ272	Cooking ware	Coarse	reddish-brown	Frequent, eq, sr, Φ < 1.5 mm Predominant: granitic rocks and crystals (qtz, pg, kfs, amph, ill), Frequent: sandstone, micritic calc. Few: quartzite, qtz-mica schist	Few mesovughs, macrovughs, meso-vesicles

Table 5: Typological and petrographic characteristics of the identified productions

The mean chemical composition and the standard deviation of each element of this production are given in Table 6 and in Figure 5 we present the typology of this production.

In thin section, these three cooking wares present various similarities between them and they are very different to the previous two cooking wares from $\mathbf{TRZ_{(A)}}$. The main characteristic of this coarse fabric ($\mathbf{TRZ_{(B)}}$) is the presence of shell fragments (Table 5). However, several differences point at the existence of various sub-fabrics. Shell fragments measure almost 3mm long axis dimension (Figure 6) and are the predominant inclusions in TRZ172 together with few chert, opaques and mica-muscovite. Quartz fragments are presents only in the fine fraction. The predominant inclusions in the sub-fabric represented by the cooking ware TRZ182 are sedimentarious rocks as sandstones and siltstones. The coarse fraction of TRZ182 also contains shell macrofossils, quartz-mica schist (300µm) and fragments of quartz, plagioclase (200µm), amphiboles (110µm), epidote (150µm), opaques (400µm) and mica-muscovite (130µm). Finally, TRZ187 is characterised by the presence of sandstones and siltstones rock fragments as dominant inclusions together with shell fragments and mica-muscovite. There are also frequent microfossils, some of which have been decomposed during the firing process becoming micritic calcite (Cau *et al.*, 2002). Macrovughs are more frequents in TRZ182 as the consequence of decomposition of calcite from shell fragments due to the high firing temperature.

TRZ(B) n=3		
EL.	MEAN	St.Desv
Fe2O3%	5,88	0,09
Al2O3%	16,10	0,27
TiO2%	0,71	0,02
MgO%	3,04	0,48
CaO%	5,96	0,41
Na2O%	1,49	0,81
K2O%	3,42	0,04
SiO2%	58,72	1,89
Ba ppm	448	74
Rb ppm	151	2
Th ppm	13	1
Nb ppm	16	1
Zr ppm	165	6
Y ppm	25	1
Sr ppm	347	14
Ce ppm	71	10
Ga ppm	18	1
V ppm	210	10
Zn ppm	111	5
Cu ppm	19	2
Ni ppm	43	2
Cr ppm	216	33

Table 6: The mean chemical composition and the standard deviation of each element of TRZ(B)

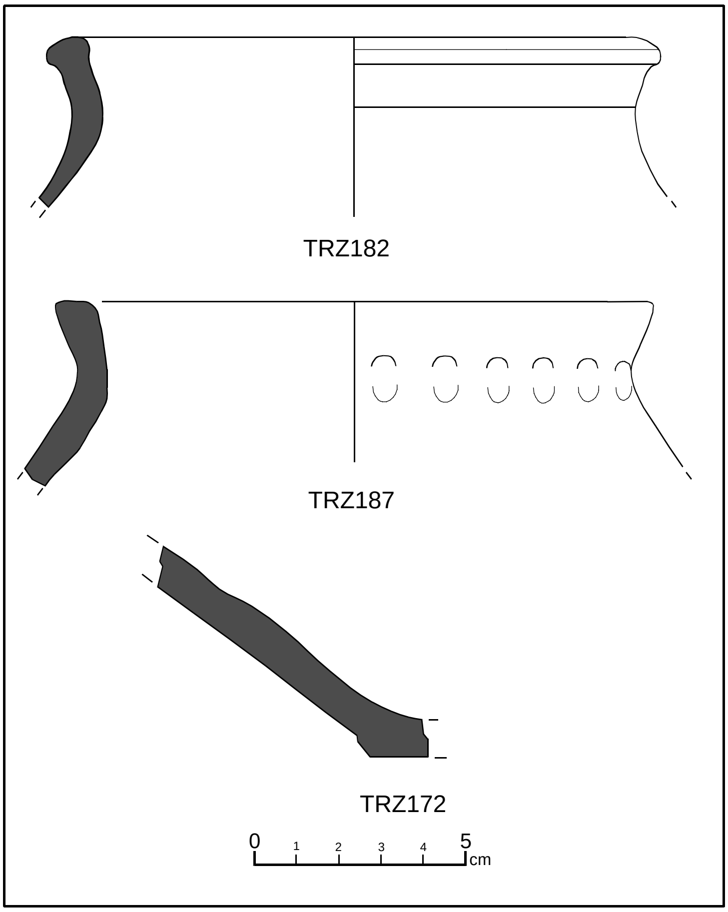

Figure 5: Typology of the group TRZ(B)

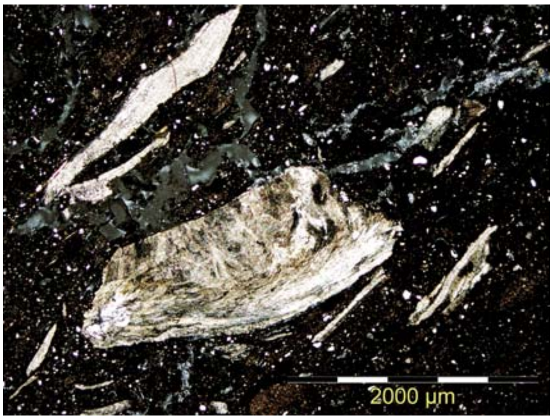

TRZ 172 40 X

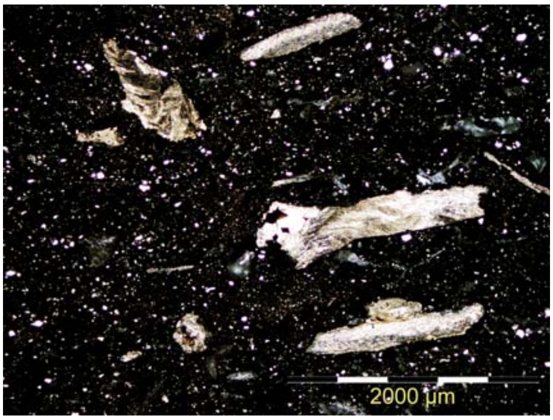

TRZ 172 40 X

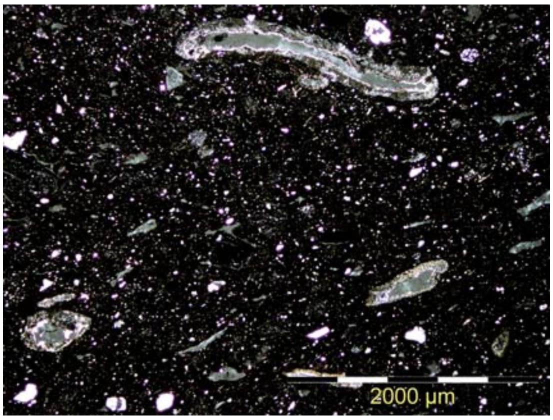

TRZ 182 40 X

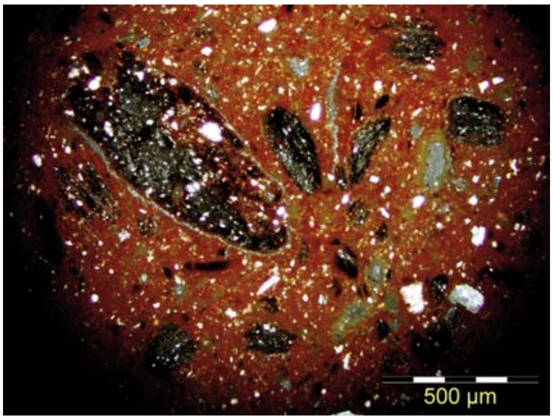

TRZ 182 100 X

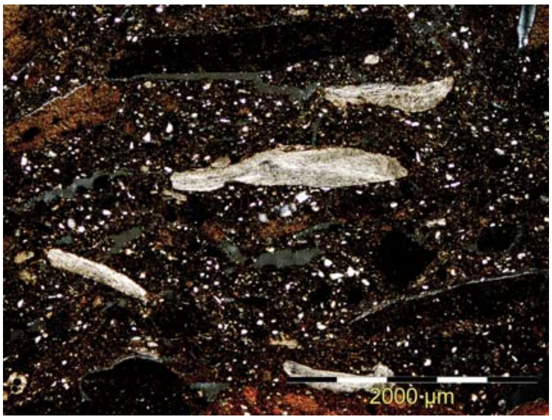

TRZ 187 40 X

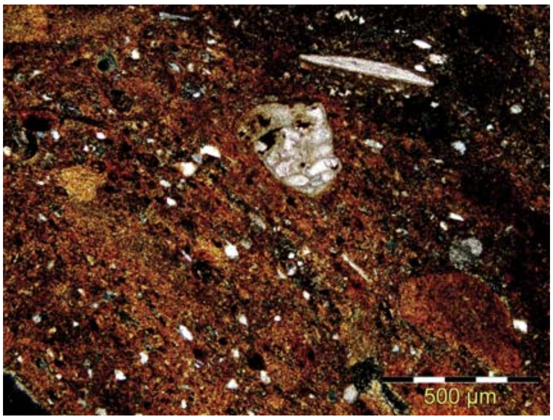

TRZ 187 100 X

Figure 6: A microphotograph by crossed polars of the samples TRZ172, TRZ182 and TRZ187 belonging to fabric $TRZ_{(B)}$

The rest of the chemical outliers (TRZ162=TZ08RC-3-1, TRZ171=TZ08-RC-5-8, TRZ104=TZ07-54, TRZ189=TZ08-RF-20-1, TRZ084=TZ07-RC-5-34, TRZ161=TZ08-RC-2-5 and TRZ088=TZ07-RB-5-38) correspond to chemical loners. Most of them are cooking wares except the individuals TRZ189, TRZ084 and TRZ088. Each one of them presents a slightly different chemical composition. Despite this, TRZ162 and TRZ171 (Figure 7) have similar chemical composition and TRZ104 seems to be chemically related to TRZ189 (Figure 8). Finally, the rest of these chemical outliers (TRZ084, TRZ161 and TRZ088) are much more similar to the rest of the analysed ceramics (Figure 9) but also present certain differences between themselves.

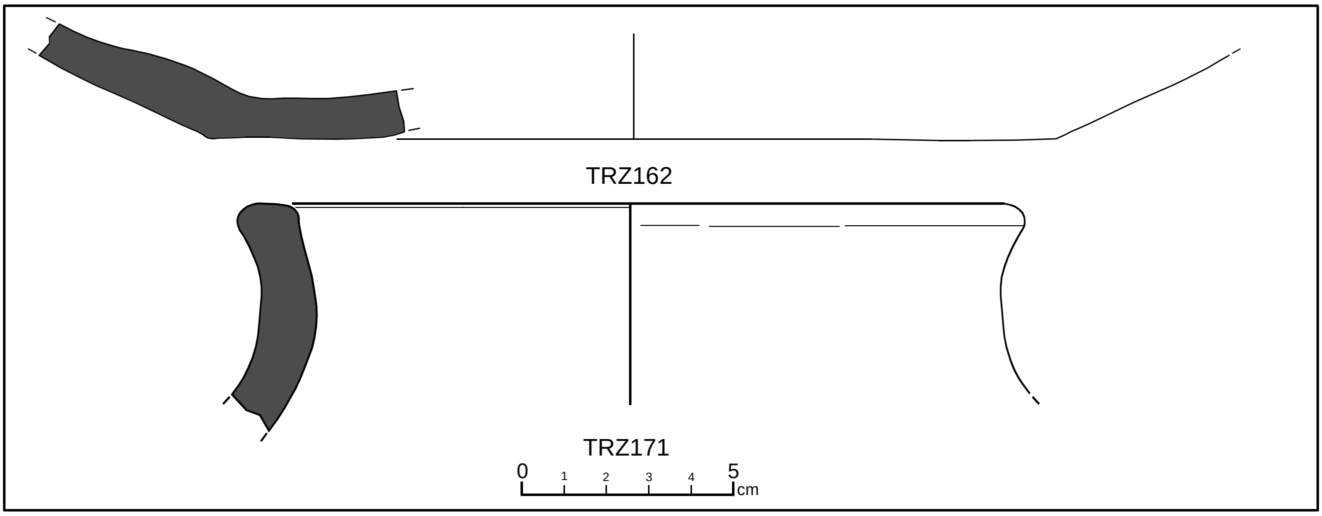

Figure 7: Typology of TRZ162 and TRZ171

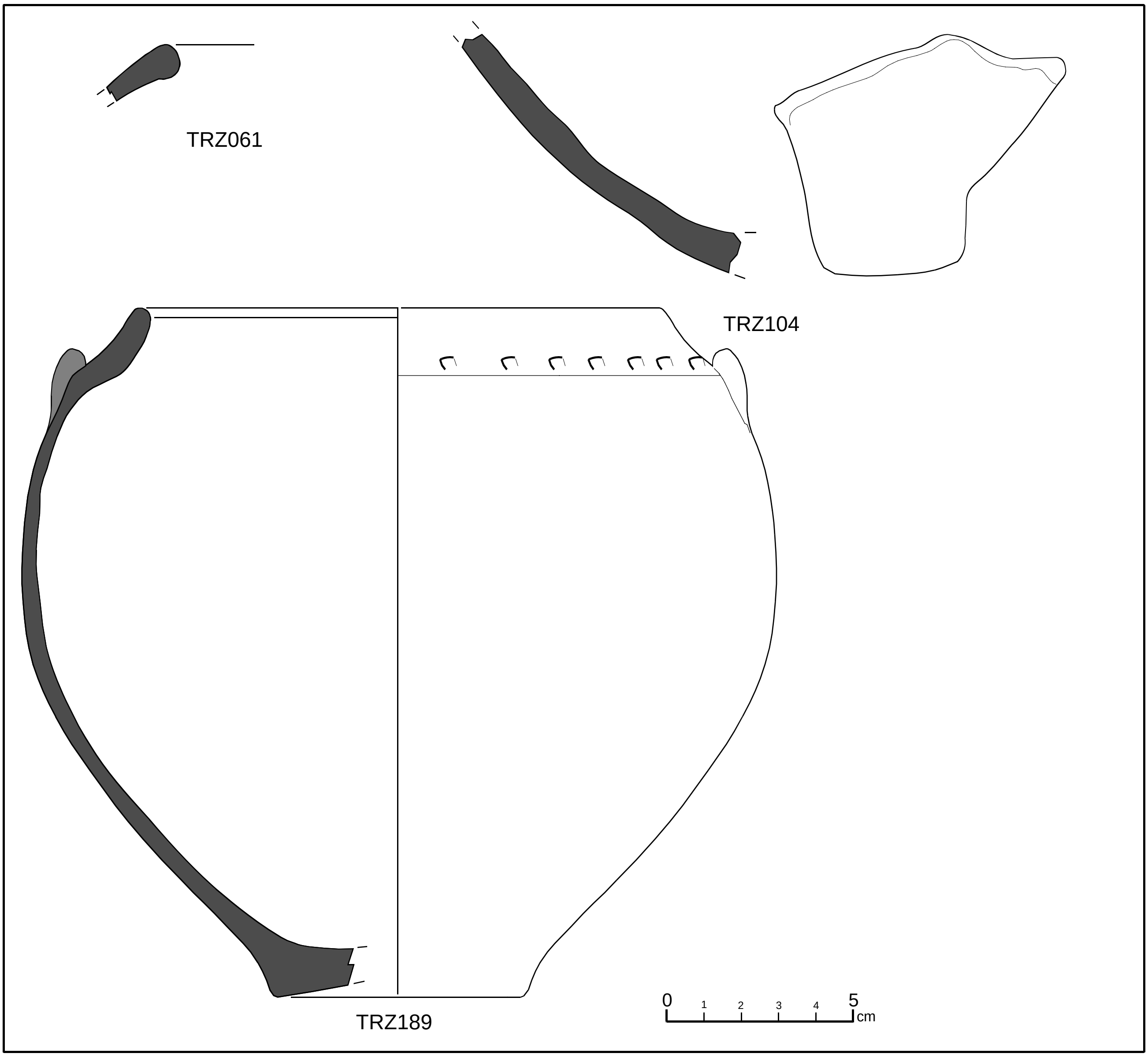

Figure 8: Typology of TRZ104, TRZ061 and TRZ189

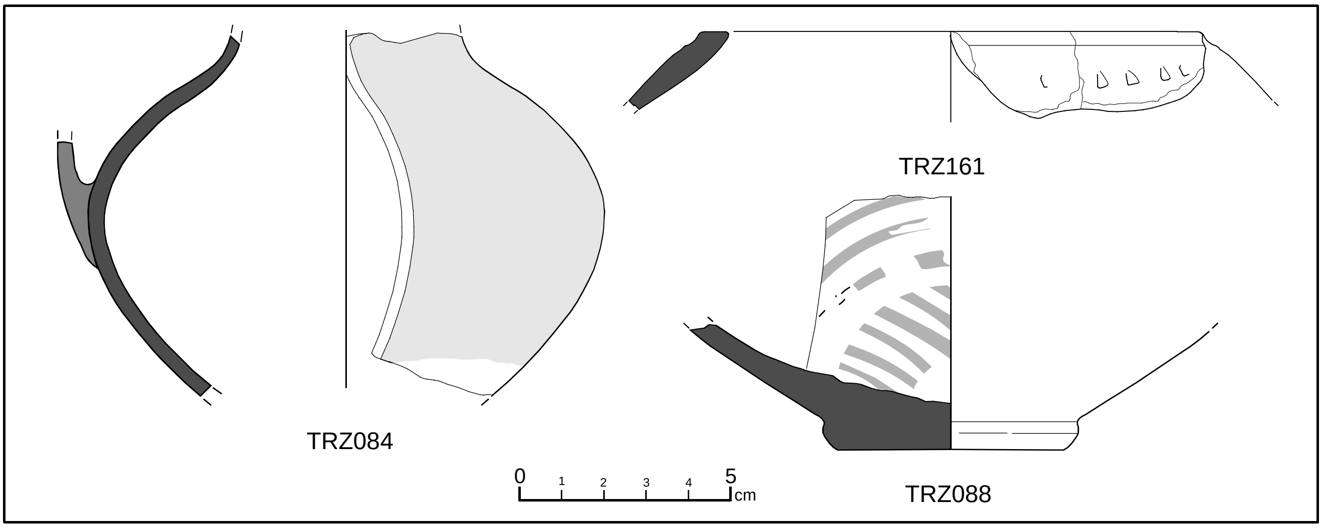

Figure 9: Typology of TRZ084, TRZ161 and TRZ088

Thin section analysis point at three petrographic fabrics between these chemical outliers (Table 5). Only TRZ084, from RC grid, corresponds to a common painted ware whereas the other individuals are cooking wares and it represents the medium coarse **TRZ**$_{(C)}$ fabric. The groundmass of this common ware is homogeneous, yellowish-brown under PPL and the optical activity of the groundmass is medium-low. The coarse fraction of the inclusions is well-sorted and open-spaced, presenting a bimodal grain-size distribution (Figure 10). Petrographic composition is similar to **TRZ**$_{(A)}$ fabric but TRZ084 contains more inclusions in the fine fraction and the inclusions of the coarse fraction is bigger sized. Quartz-mica

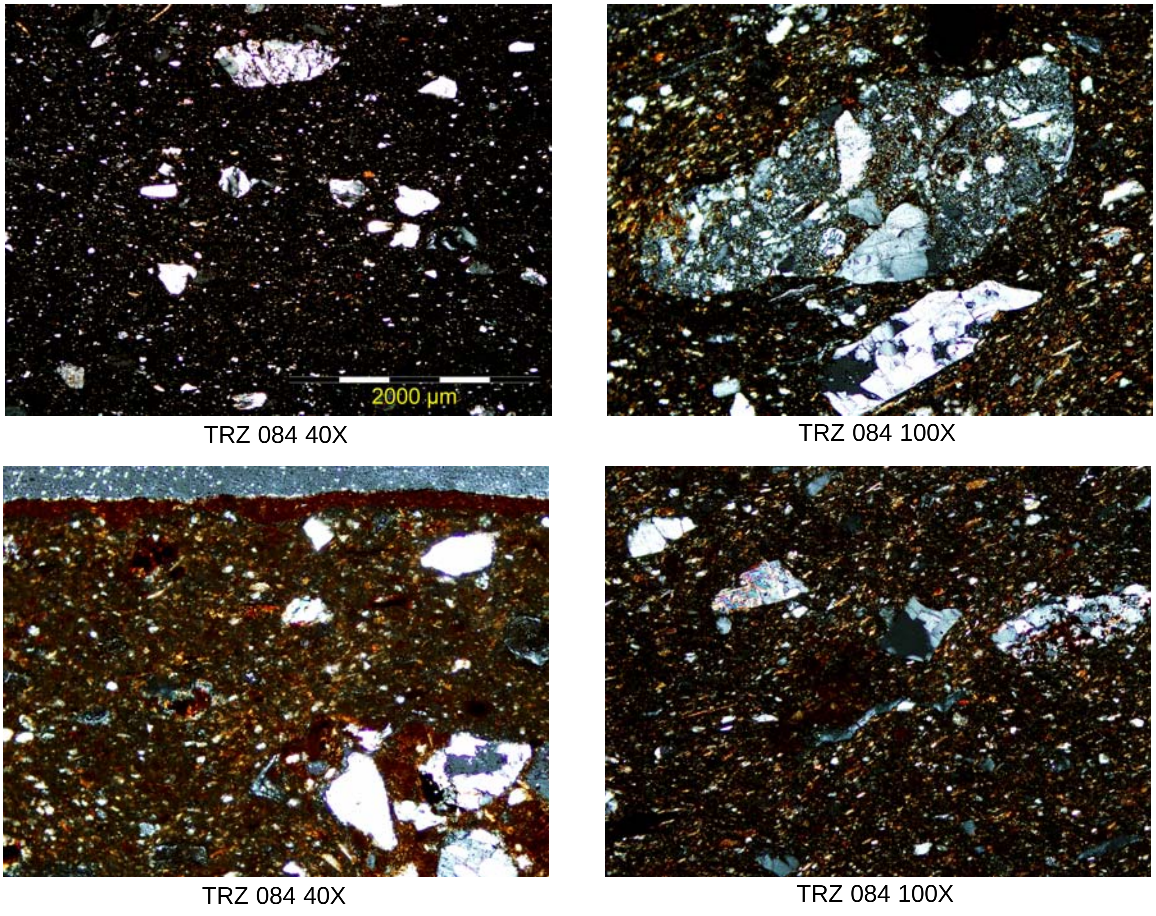

Figure 10: A microphotograph by crossed polars of the sample TRZ084 corresponding to a chemical loner bellowing to TRZ$_{(C)}$ fabric

schist fragments (500µm) are predominant together with other non-plastics fragments of quartz, plagioclase, amphibole, epidote, biotite (600µm) and mica-muscovite (200µm). Rare quartzite and quartzarenite of almost 1mm long axis dimension are comprised in the coarse fraction. Voids are rare, predominantly mesovughs.

Another coarse fabric (**TRZ$_{(D)}$**) is formed by TRZ162 and TRZ171 cooking wares coming from RC grid of the ***Tchinguiz Tepe*** (Table 5). However, differences in composition between both ceramics leads to divided in two sub-fabrics (Figure 11). The groundmass of TRZ162 is homogeneous, reddish brown under PPL with low optical activity. Sedimentary inclusions are predominant, formed by quartzarenite of 3mm of maximum length, siltstones (1mm) and few cherts (1mm). Isolated fragments of quartz, plagioclase, amphiboles, epidotes, opaques and mica-muscovite are frequents. Some microfossils have been identified and calcareous fossils (probably shell fragments) have been altered to secondary micritic calcite due to high firing temperatures (Cau *et al.*, 2002). The sub-fabric represented by the individual TRZ171 is also characterised by the presence of sandstones and frequent nodules of secondary micritic calcite derived from calcareous shell fragments. Nevertheless, no cherts, plagioclases, amphiboles nor epidotes are present. Frequent voids in both subfabrics can be observed, corresponding mainly to macro-vughs and meso-vughs, sometimes partially or totally filled with secondary calcite, created by a non total decomposition of calcareous shells or due to the re-precipitation of carbonate inclusions (Cau *et al*., 2002).

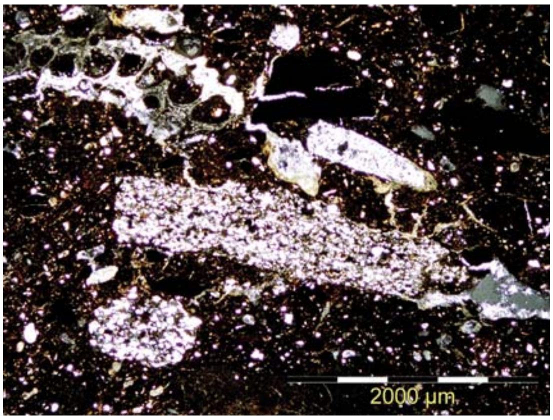

TRZ 162 40 X

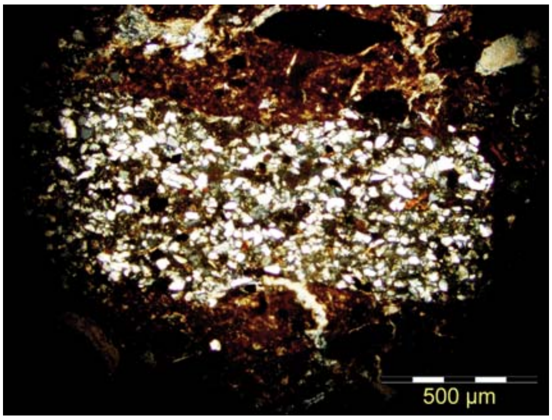

TRZ 162 100 X

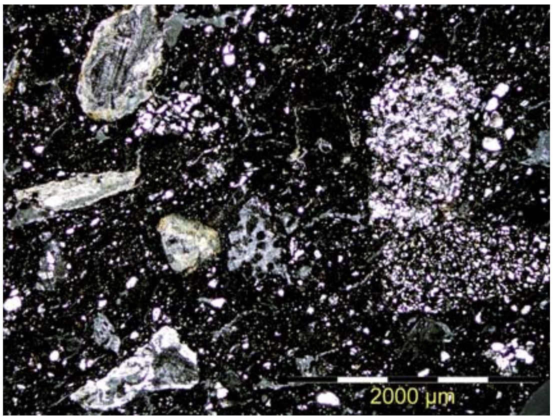

TRZ 171 40 X

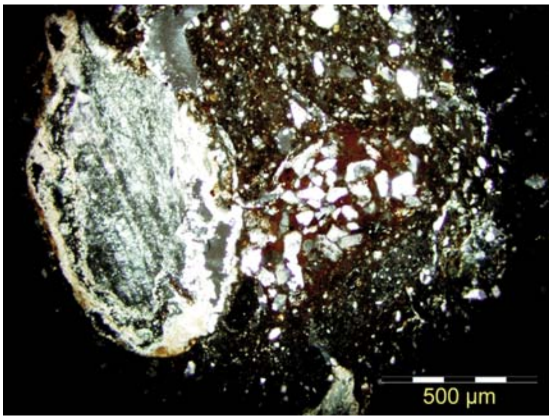

TRZ 171 100 X

Figure 11: A microphotograph by crossed polars of the samples TRZ162 and TRZ171 corresponding to similar chemical loners bellowing to TRZ$_{(D)}$ fabric

A fifth coarse fabric (**TRZ$_{(E)}$**) is formed by three cooking wares presenting several similarities on the petrographical composition: TRZ161 from RC grid, TRZ189 from RF grid and TRZ104 from the ***Citadel*** of ***Tchinguiz Tepe*** (Table 5). This fabric corresponds to a coarse fabric with common non-plastic inclusions in a reddish carbonated and ferric micromass (Figure 12). The coarse fraction (lower than 3 mm long axis dimension) contains shell macrofossils, up to 1.5 mm long axis dimension and calcareous sedimentary rock fragments (fine-grained sandstone). Some of these rocks have become in a silicate rock altogether with spathic calcite crystals forming the sedimentary rocks. These thin sections include some crystals of ferric carbonate and frequent nodules of micrite calcite. Finally, some volcanic-glass fragments appear as accessory minerals. Quartz-mica schist (600μm), quartz and plagioclase crystals and mica-muscovite is common. Fine fraction is represented by calcareous and quartz grains dislodged from the sedimentary rocks. To this fabric can be attributed the cooking ware TRZ061 analysed only by thin section analysis (Martínez *et al.*, 2008). Voids are common, corresponding to mesovughs, sometimes partially filled with secondary calcite (Cau *et al.*, 2002) and orientated following the vessel margins.

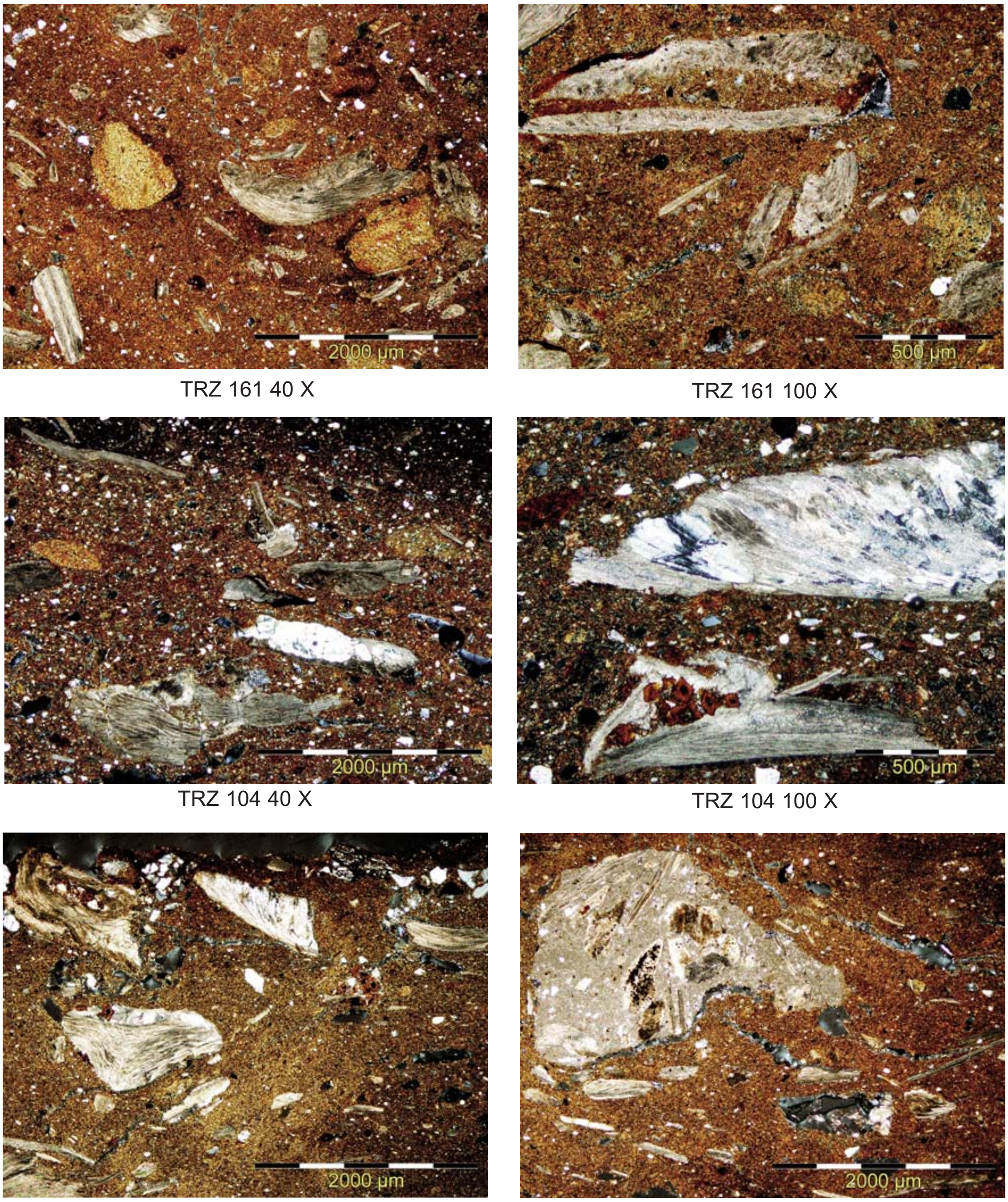

TRZ 161 40 X | TRZ 161 100 X

TRZ 104 40 X | TRZ 104 100 X

TRZ 189 40 X | TRZ 189 40 X

Figure 12: A microphotograph by crossed polars of the samples TRZ161, TRZ104 and TRZ189 corresponding to similars chemical loners bellowing to TRZ$_{(E)}$ fabric

Repeating the above mentioned statistical routine upon the subcomposition Fe_2O_3, Al_2O_3 TiO_2, MgO, CaO, SiO_2, Rb, Zr, Y, Sr, Ce, Ga, V, Nb, Zn, Cu, Ni and Cr leaving out the above mentioned chemical outliers (TRZ163, TRZ170, TRZ172, TRZ182, TRZ187, TRZ162, TRZ171, TRZ104, TRZ084, TRZ161, TRZ189 and TRZ088) the vt of the new CVM is much more lower, in fact, is equal to: 0.1505. A total variation of this range indicates a very homogeneous data set. In mathematical terms, it would correspond to a monogenetic data set (Buxeda and Kilikoglou, 2003) representing probably one single production. On the other hand, this total variation, in geochemical terms regarding to the restricted geological variation at the desert area where Termez is located, can point towards the same geochemical origin of the raw materials. It is very probable that the raw materials used for the fabrication of these individuals coming from the same o very similar clay deposit because of the limited clay deposits in the area. The limitation in the access to adequate clay sources probably leaded to a log lasting local/regional ceramic tradition, where the exploded raw material recourses are the same, even though there are differences in the production processes, chronology or typology.

To visualize the results of the last statistical treatment, we present a new dendrogram in Figure 13 resulting from the cluster analysis performed on the above mentioned subcomposition, leaving out also the 12 chemical outliers, using the Square Euclidean distance and the centroid algorithm, done by S-plus2000 (MathSoft, 1999). Keeping in mind the very low total variation, two different wider groups **AC** and **TRZ**-**F2**, joint at relatively small ultra-metrical distance, can be distinguished at Figure 13. One of the groups **AC** contains all the individuals sampled at the Antique Quarters except tree TRZ149 (TZ08-AC-12-1) TRZ152 (TZ08-AC-12-4) and TRZ156 (TZ08-AC-12-8) which stands at a marginal position respect to this group. Regarding this group (**AC**) small differences in the trace elements can be observed compared with TRZ-F2. It has slightly lower Nb, Zr, Y, Ce and Ga concentrations and rather higher V, Ni Th and Cr content indicating that this group must correspond to a single Paste Compositional Reference Unit (PCRU). However, this hypothesis are going to be explored in much more detail following.

At Figure's 13 dendrogram inside the wider group **TRZ**-**F2** the separation a small sub-groups F2, which contains the majority of the individuals of ***Kara Tepe's Kiln Nº 2*** and the group TRZ, which basically contains individuals from the stratigraphical units of the new kiln site RF of ***Tchinguiz Tepe*** and also numerous individuals from the different archaeological sites sampled at ***Termez*** (RC-Tchinguiz Tepe; Monateries, Ciutadelle, etc.,) including materials with possible chronological differences and clear typological differences. According to previous study (Tsantini *et. al* 2006) the reference group of **Kara Tepe's Kiln Nº 2** includes almost all the individuals sampled at this site beside TRZ008, TRZ020, TRZ027, TRZ028, TRZ041, TRZ049 and TRZ050. All the above mentioned individuals are located outside of the rectangle called **TRZ-F2(B)** in Figure 13. However, as **F2** and **TRZ** share some of the individuals identified in previous studies within the Reference Group of ***Kara Tepe's Kiln Nº 2***, both of this sub-groups must reflect a common geological origin or common clay source for the raw materials (the same uncertainty zone) and might represent the same local ceramic production with two slightly different sub-productions, from which one is basically associated to the kiln of ***Kara Tepe*** and the other is associated to the Kiln of ***Tchinguiz Tepe***. The distance between these two settlements is only 1km. By looking at the chemical data it can be confirmed that F2 only differs by slightly higher MgO, Ga and Zn content from TRZ.

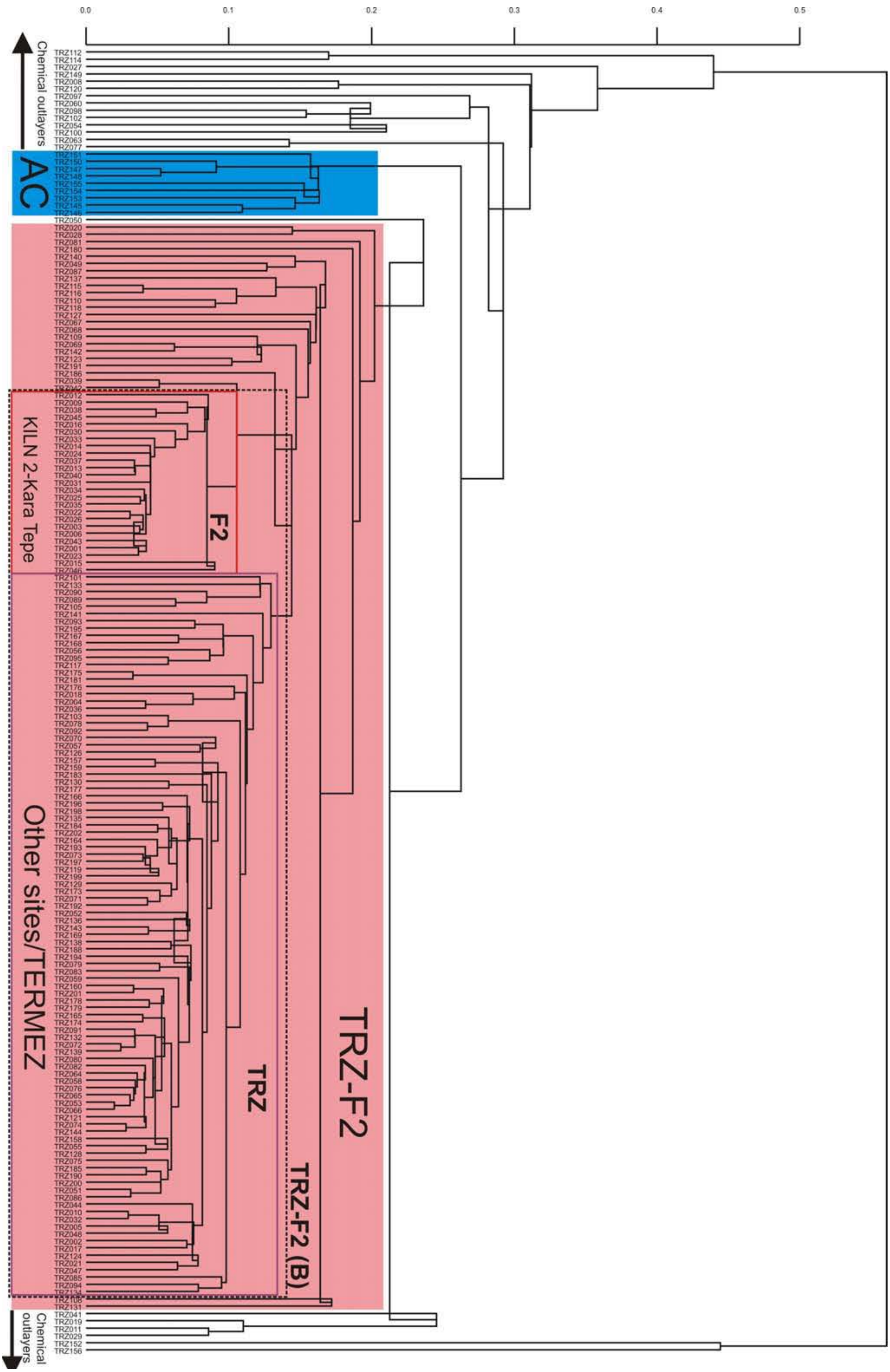

Figure 13: Dendrogram resulted from the cluster analysis performed on the subcomposition Fe_2O_3 TiO_2, MgO, CaO, SiO_2, Rb, Zr, Y, Sr, Ce, Ga, V, Nb, Zn, Cu, Ni and Cr and Al_2O_3 used as divisor of the 190 individuals of Termez using the Square Euclidean distance and the centroid algorithm, performed by S-plus2000 (MathSoft, 1999)

To crosscheck the above hypothesis, taking as a reference production the RG (Reference Group) of ***Kiln Nº 2 of Kara Tepe*** , we calculated the Mahalanobis distances of the 190 individuals (all individuals present in the dendrogram of Figure13) regarding to the centroid of this GR. For the calculation of this distances we used the following subcomposition: Fe_2O_3, Al_2O_3 TiO_2, MgO, CaO, SiO_2, Rb, Zr, Y, Sr, Ce, Ga, V, Nb, Zn, Cu, Ni and Cr and we calculated the Mahalanobis distances according to the following equation:

$$D^2 = (\mathbf{y} - \mu)' \Sigma^{-1} (\mathbf{y} - \mu)$$

where y vector defined on the logratio transformed data (with all the individuals), μ is the vector of the means of the logratios of the group (only individuals belong to the group) and Σ^{-1} is the reverse of the variance-covariance matrix calculated on the logratio transformed data. The significance of these distances can be calculated via the equation of Hotelling (Davis, 1986):

$$T^2 = \frac{n_a n_b}{n_a + n_b} D^2$$

where n_a corresponds to the number of the individuals in *y* and n_b to number of individuals considered as a part of the group. T2 then can be transformed to F by the equation:

$$F = \left(\frac{n_a + n_b - s - 1}{(n_a + n_b - 2)s} \right) T^2$$

from where the probabilities of the different individuals belonging or not to the group can be calculated.

In Table 7 Mahalanobis distances and probabilities calculated upon the specific subcomposition can be seen. In this table we indicated with a grey background the individuals which could belong to the GR of ***Kara Tepe's Kiln Nº 2***. The individuals highlighted in green (TRZ002, TRZ004, TRZ005, TRZ010, TRZ017, TRZ021 and TRZ036) are the ones which according to the Square Euclidian Distance (Figure 13) belong to **TRZ** instead of **F2**. Despite this and, according to the Mahalanobis Distance, they form part of the same production with significantly high probability. Crosschecking these results with the raw chemical composition we can say that the chemical similarities of TRZ002, TRZ004, TRZ005, TRZ010, TRZ017, TRZ021 and TRZ036 regarding to the rest of the individuals in **F2** are elevated enough to consider them as part of the same chemical group. Therefore this extended F2 group would correspond to the ***Reference Group of the Kiln Nº2 of Kara Tepe*** which has been already identified in previous studies (Tsantini *et al.*, 2007). This hypothesis can be confirmed by the petrographic results also which will be explained following. On the other hand, both the Square Euclidian Distances and the Mahalanobis Distances indicate that the individuals (TRZ008, TRZ020, TRZ027, TRZ041, TRZ049 and TRZ050) which have been already identified in previous studies (Tsantini *et al*, 2007; Mertínez *et al.*, 2007) as chemical outliers of this RG can not be classified into this group and probably represent slightly different variants of this production (Figure 14). Finally, the extended group F2 by the individuals TRZ002, TRZ004, TRZ005, TRZ010, TRZ017, TRZ021 and TRZ036 corresponds to ***Kara Tepe's Kiln Nº 2 RG***. The mean chemical composition and the standard deviation of each element of this group are given in Table 8.

ID	MAHALANOBIS	PROBABILITIES
TRZ035	9,16	0,995
TRZ010	9,39	0,995
TRZ026	10,01	0,992
TRZ033	10,25	0,991
TRZ045	11,11	0,987
TRZ032	12,15	0,979
TRZ040	12,45	0,976
TRZ022	12,70	0,974
TRZ029	12,88	0,972
TRZ001	13,01	0,971
TRZ031	13,23	0,968
TRZ046	13,90	0,960
TRZ048	15,08	0,943
TRZ006	15,82	0,931
TRZ037	15,89	0,930
TRZ003	16,01	0,928
TRZ019	16,30	0,922
TRZ004	16,50	0,918
TRZ023	16,56	0,917
TRZ021	17,02	0,908
TRZ036	17,19	0,904
TRZ014	17,22	0,904
TRZ030	17,71	0,893
TRZ025	17,86	0,890
TRZ016	18,72	0,869
TRZ024	19,17	0,858
TRZ002	19,20	0,858
TRZ044	20,09	0,834
TRZ005	20,13	0,833
TRZ034	20,68	0,818
TRZ012	20,73	0,817
TRZ013	20,99	0,809
TRZ047	21,34	0,800
TRZ039	21,95	0,782
TRZ038	21,99	0,781
TRZ009	22,35	0,770
TRZ042	22,64	0,761
TRZ015	22,80	0,757
TRZ043	23,01	0,750
TRZ017	25,92	0,660
TRZ018	26,06	0,655
TRZ011	30,83	0,510
TRZ049	35,65	0,382
TRZ050	41,76	0,255
TRZ020	46,18	0,188
TRZ028	46,49	0,184
TRZ041	54,45	0,104
TRZ008	76,53	0,022
TRZ124	127,37	0,001
TRZ192	127,39	0,001
TRZ166	128,55	0,001
TRZ185	131,31	0,001
TRZ087	138,71	0,000
TRZ164	140,84	0,000
TRZ190	141,59	0,000
TRZ167	141,67	0,000
TRZ067	145,73	0,000
TRZ083	147,66	0,000
TRZ194	148,85	0,000
TRZ091	149,39	0,000
TRZ174	149,75	0,000
TRZ130	150,27	0,000
TRZ123	150,67	0,000
TRZ140	155,03	0,000
TRZ195	162,04	0,000
TRZ079	167,73	0,000
TRZ105	168,99	0,000
TRZ027	169,46	0,000
TRZ069	170,90	0,000
TRZ129	171,31	0,000
TRZ077	171,99	0,000
TRZ193	174,19	0,000
TRZ139	177,04	0,000
TRZ169	177,72	0,000
TRZ159	178,55	0,000
TRZ086	179,67	0,000
TRZ200	179,74	0,000
TRZ184	181,33	0,000
TRZ075	181,69	0,000
TRZ051	183,38	0,000
TRZ074	184,27	0,000
TRZ175	184,50	0,000
TRZ073	185,23	0,000
TRZ082	185,84	0,000
TRZ142	186,05	0,000
TRZ186	186,30	0,000
TRZ056	186,58	0,000
TRZ066	188,45	0,000
TRZ196	189,93	0,000
TRZ141	193,82	0,000

ID	MAHALANOBIS	PROBABILITIES
TRZ085	196,04	0,000
TRZ198	195,53	0,000
TRZ081	198,70	0,000
TRZ089	198,60	0,000
TRZ165	198,05	0,000
TRZ173	198,29	0,000
TRZ119	200,47	0,000
TRZ057	201,15	0,000
TRZ072	201,48	0,000
TRZ108	202,15	0,000
TRZ064	203,68	0,000
TRZ181	205,09	0,000
TRZ059	205,54	0,000
TRZ160	205,94	0,000
TRZ097	207,54	0,000
TRZ133	209,02	0,000
TRZ202	210,20	0,000
TRZ058	214,52	0,000
TRZ144	214,48	0,000
TRZ183	213,15	0,000
TRZ199	212,99	0,000
TRZ201	213,64	0,000
TRZ188	215,83	0,000
TRZ065	217,66	0,000
TRZ121	217,01	0,000
TRZ138	218,46	0,000
TRZ143	218,65	0,000
TRZ092	221,34	0,000
TRZ128	222,17	0,000
TRZ157	223,25	0,000
TRZ078	225,12	0,000
TRZ101	225,77	0,000
TRZ063	229,51	0,000
TRZ090	229,70	0,000
TRZ094	229,82	0,000
TRZ134	227,90	0,000
TRZ071	232,59	0,000
TRZ131	234,29	0,000
TRZ180	231,68	0,000
TRZ070	239,15	0,000
TRZ093	238,19	0,000
TRZ168	236,18	0,000
TRZ176	238,35	0,000
TRZ117	245,27	0,000
TRZ132	244,03	0,000
TRZ052	250,15	0,000
TRZ053	247,41	0,000
TRZ076	254,01	0,000
TRZ135	252,28	0,000
TRZ136	248,12	0,000
TRZ191	255,56	0,000
TRZ054	262,84	0,000
TRZ055	259,50	0,000
TRZ095	269,36	0,000
TRZ110	269,45	0,000
TRZ179	258,73	0,000
TRZ197	267,32	0,000
TRZ080	302,56	0,000
TRZ098	286,64	0,000
TRZ109	293,51	0,000
TRZ115	297,32	0,000
TRZ126	271,55	0,000
TRZ137	295,09	0,000
TRZ145	300,77	0,000
TRZ149*	278,89	0,000
TRZ158	297,68	0,000
TRZ178	279,89	0,000
TRZ060	960,36	0,000
TRZ068	315,81	0,000
TRZ100	331,89	0,000
TRZ102	447,99	0,000
TRZ103	409,36	0,000
TRZ112	443,10	0,000
TRZ114	403,32	0,000
TRZ116	407,35	0,000
TRZ118	343,59	0,000
TRZ120	325,96	0,000
TRZ127	372,66	0,000
TRZ146	478,89	0,000
TRZ147	660,73	0,000
TRZ148	437,03	0,000
TRZ150	423,74	0,000
TRZ151	341,95	0,000
TRZ152*	545,37	0,000
TRZ153	359,41	0,000
TRZ154	414,36	0,000
TRZ155	327,57	0,000
TRZ156	542,60	0,000
TRZ177	315,52	0,000

Table 7: Mahalanobis ditances and probabilities calculated regarding the Reference Group of Kara Tepe's Kiln Nº 2 (F2) upon the subcomposition: Fe_2O_3 , Al_2O_3, TiO_2, MgO, CaO, SiO_2, Rb, Zr, Y, Sr, Ce, Ga, V, Nb, Zn, Cu, Ni and Cr of 190 individuals

Kara Tepe's RG (33)		
Elements	Mean	Stan. Desv.
Fe_2O_3%	5,98	0,24
Al_2O_3%	15,62	0,48
MnO%	0,1	0,01
P_2O_5%	0,27	0,07
TiO_2%	0,65	0,02
MgO%	4,05	0,34
CaO%	11,07	1,12
Na_2O%	1,6	0,3
K_2O%	3,38	0,3
SiO_2%	57,09	1,28
Ba ppm	538	99
Rb ppm	123	11
Th ppm	15	1
Nb ppm	16	1
Pb ppm	19	6
Zr ppm	154	7
Y ppm	29	1
Sr ppm	386	43
Ce ppm	61	9
Ga ppm	22	1
V ppm	103	5
Zn ppm	107	7
Cu ppm	35	4
Ni ppm	50	3
Cr ppm	80	3

Table 8: The mean chemical composition and the standard deviation of each element of Kara Tepe's RG

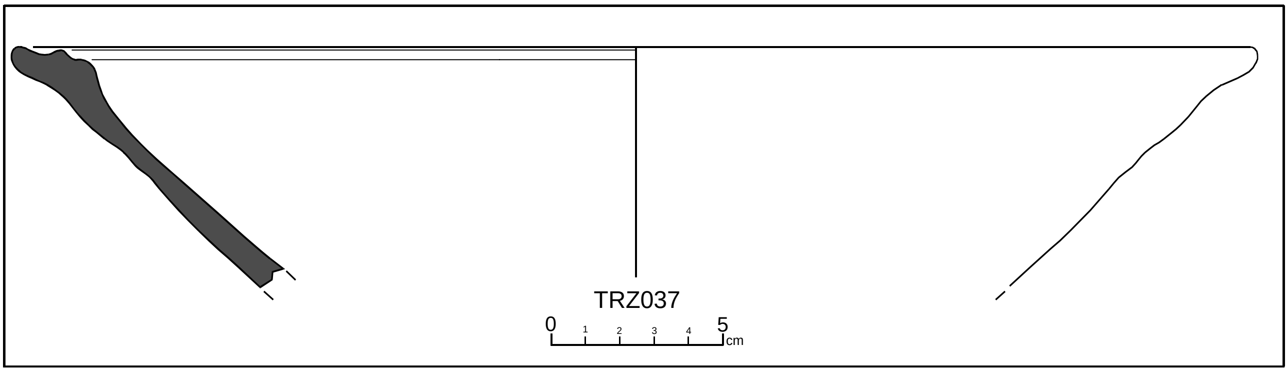

Figure 14: Typology of the extended group F2 of Kara Tepe

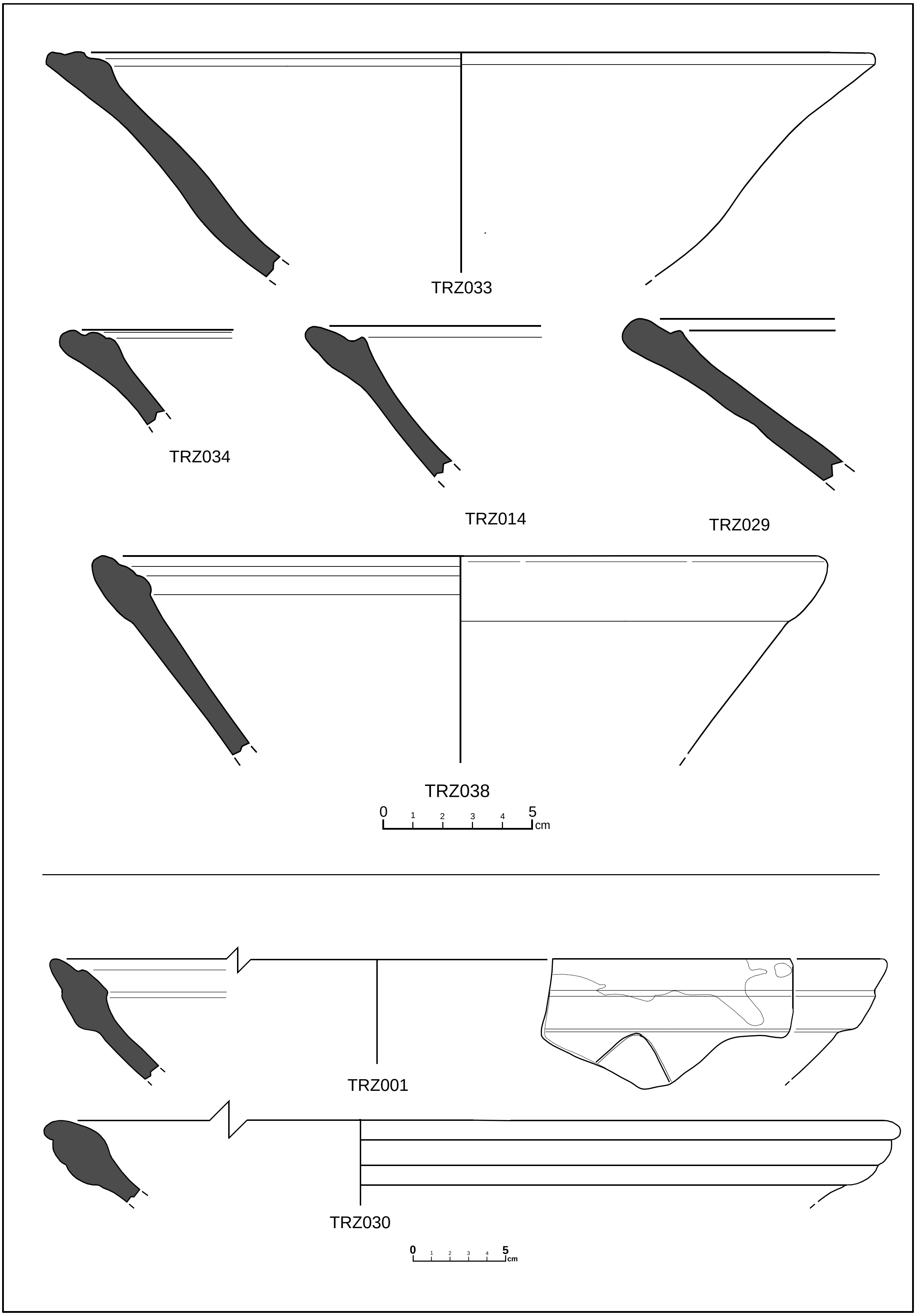

Figure 14: Typology of the extended group F2 of Kara Tepe

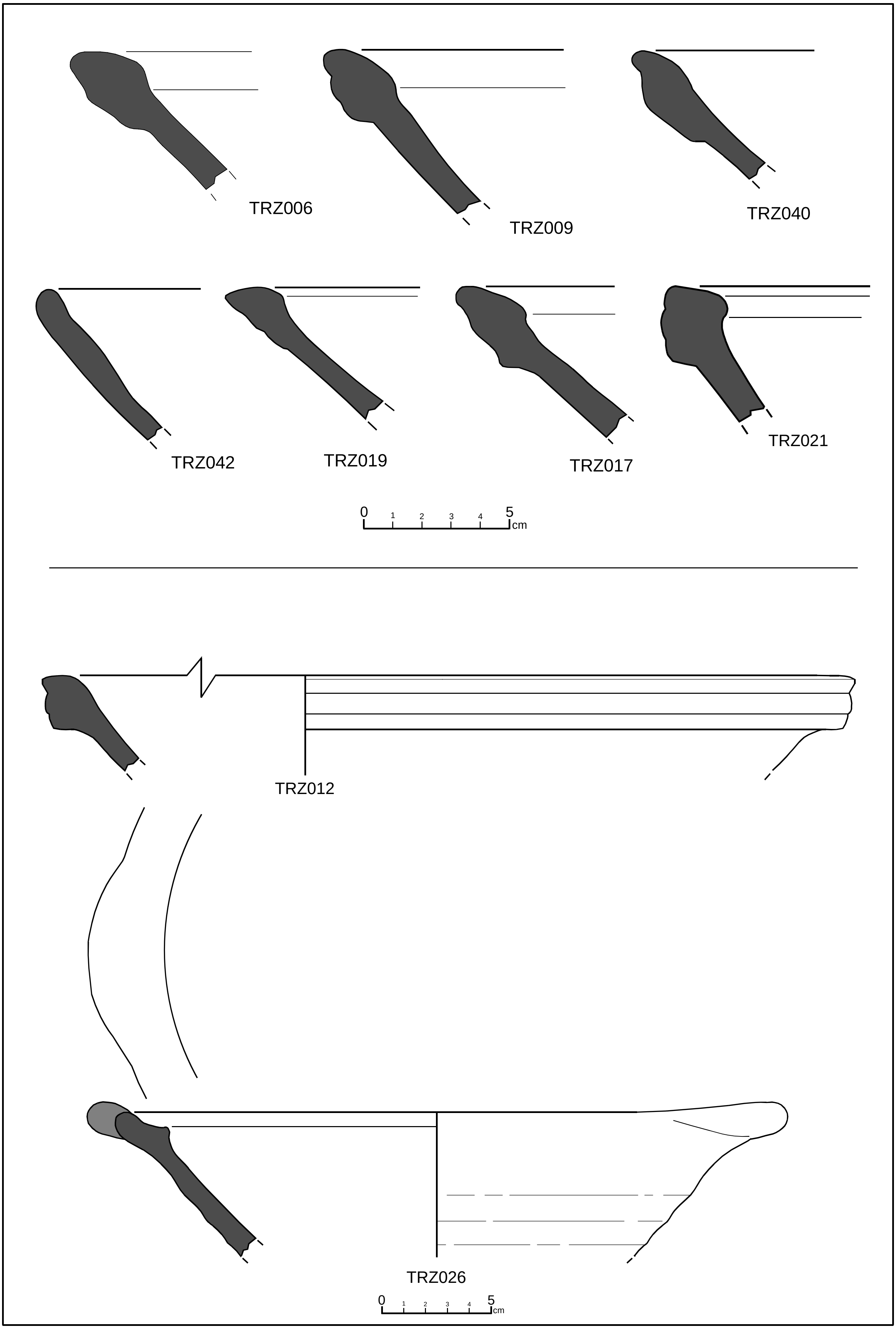

Figure 14: Typology of the extended group F2 of Kara Tepe

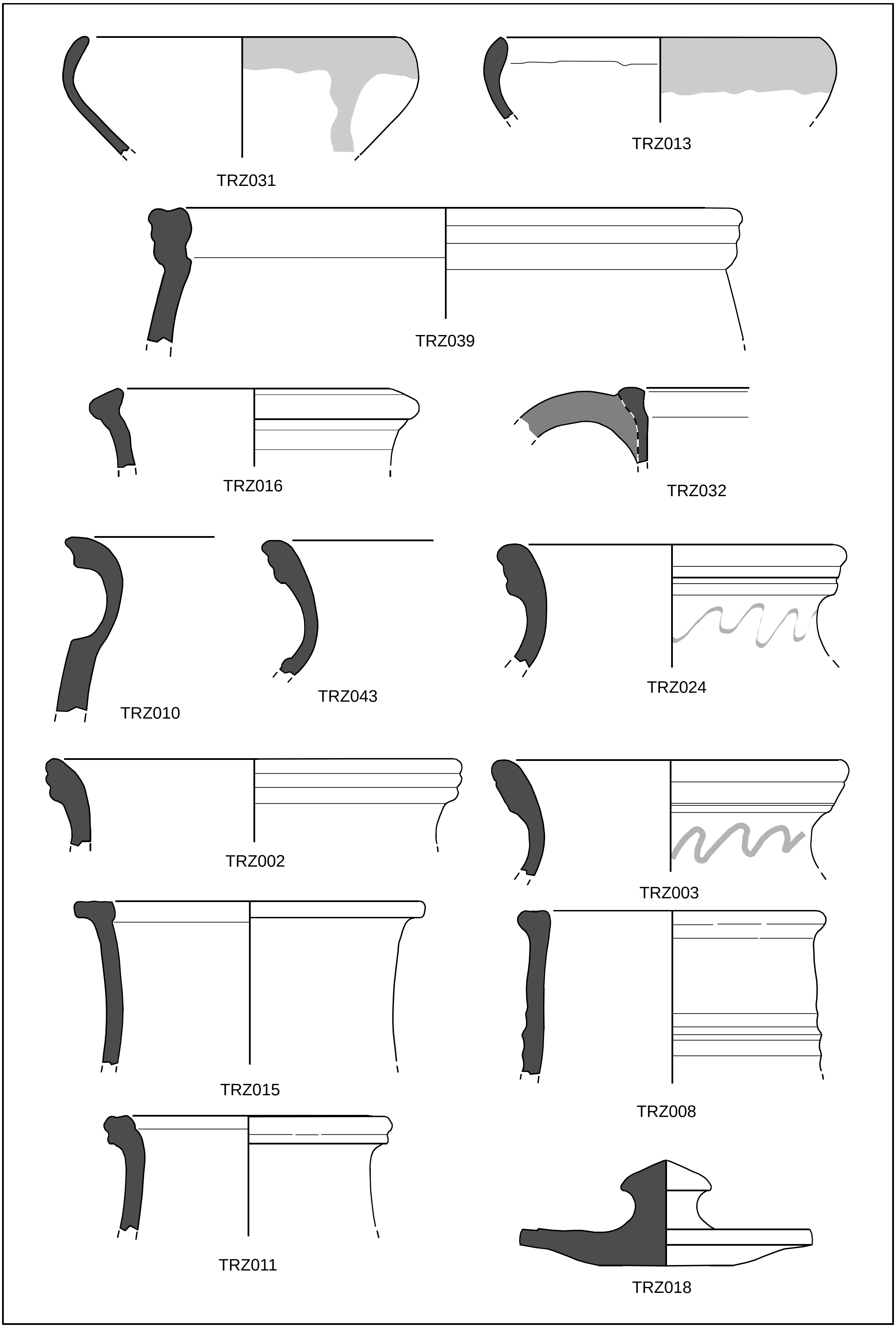

Figure 14: Typology of the extended group F2 of Kara Tepe

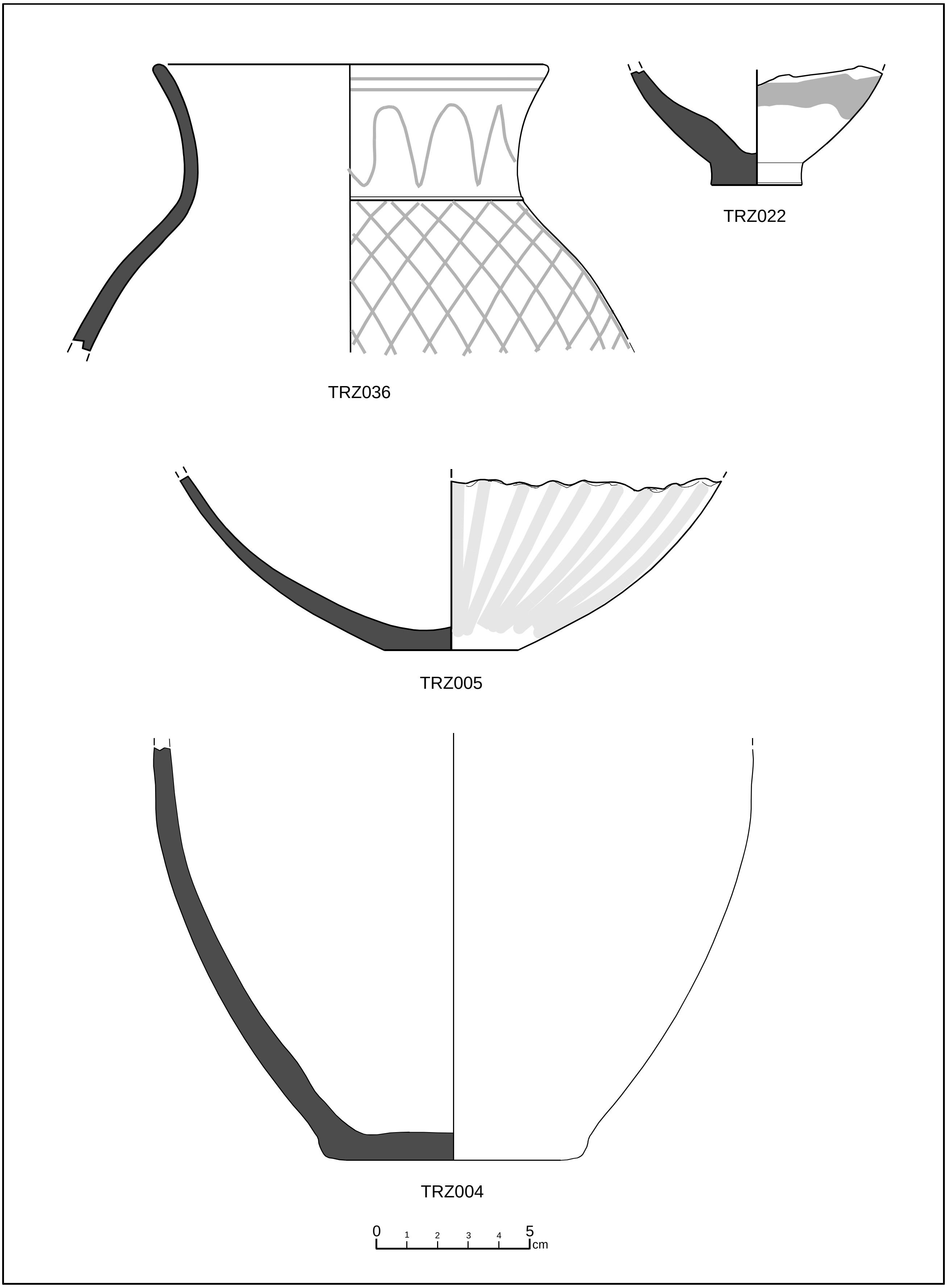

Figure 14: Typology of the extended group F2 of Kara Tepe

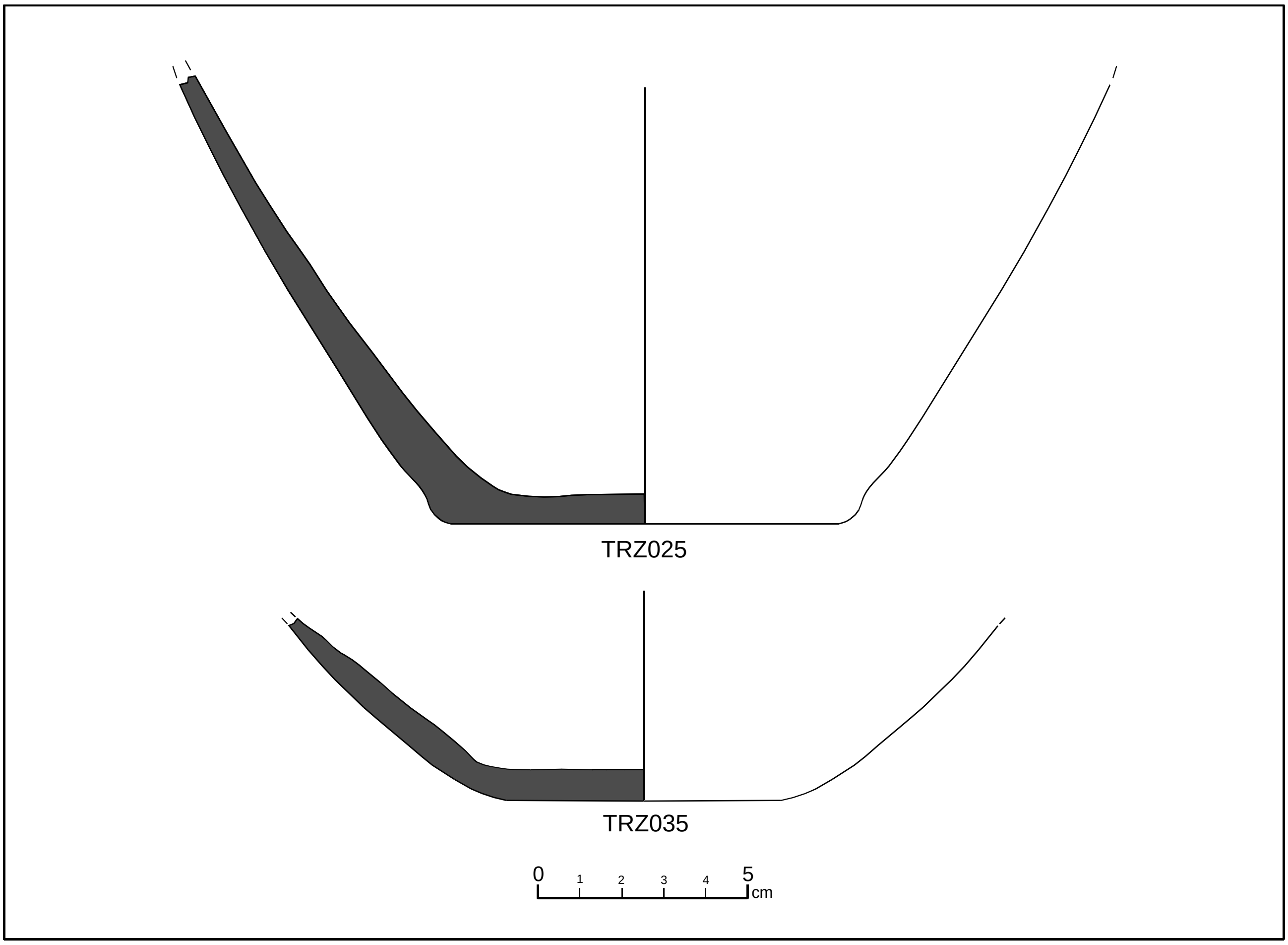

Figure 14: Typology of the extended group F2 of Kara Tepe

From the stratigraphical levels of the Kiln 2 of Kara Tepe, 6 individuals have been examined by thin section (Table 5). The petrographical analysis reveals that all of them had a similar petrographical composition. However, two individuals (TRZ020 and TRZ041) are very different to the other ceramics from Kiln 2 and both are considered chemical and petrographical loners and they will be described later. The rest of the ceramics (common wares TRZ006, TRZ025, TRZ033 and TRZ036) can be grouped in a mean petrographical group, ***KT-K2*** fabric, according to the similarity in composition, frequency and size of non plastic inclusions (Figure15). The groundmass is homogeneous, reddish-brown under PPL. The inclusions are rare, open-spaced and reflect a bimodal grain-size distribution. The grains are moderately to well-sorted, prevalently monocrystalline and polycrystalline subangular quartz (300µm), plagioclase, amphiboles (200µm) and epidote (250µm). Bigs crystalls of biotite (900µm of maximum length) and mica-muscovite (800µm) are dominants. Fragments of metamorphic rocks as quartz-mica schist (300 to 700µm) are frequents and sedimentary rocks as sandstones (800µm) and cherts (700µm) are rares. There are also frequent microfossils, some of which have decomposed during the firing process or have become nodules of secondary micritic calcite (Cau *et al.*, 2002). In the case of TRZ033, fragments of shells are still present. Voids are rares and they are present as mesovughs.

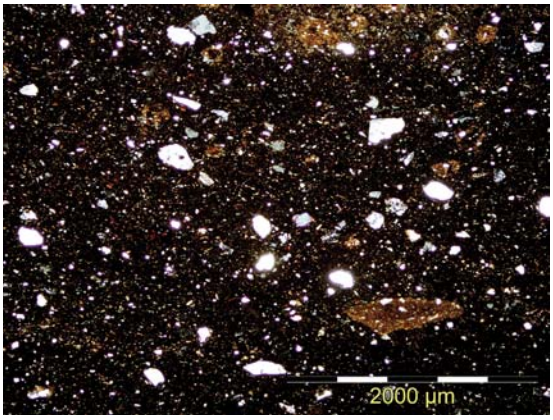

TRZ 006 40 X

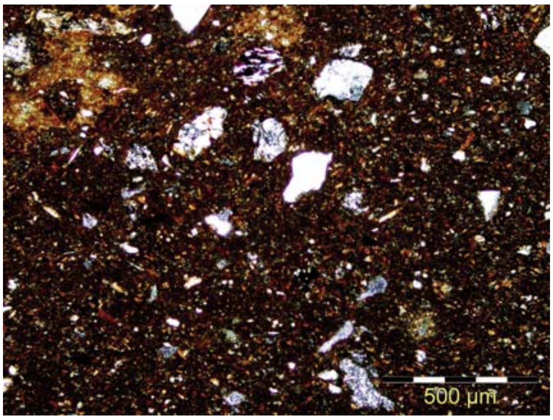

TRZ 006 006 X

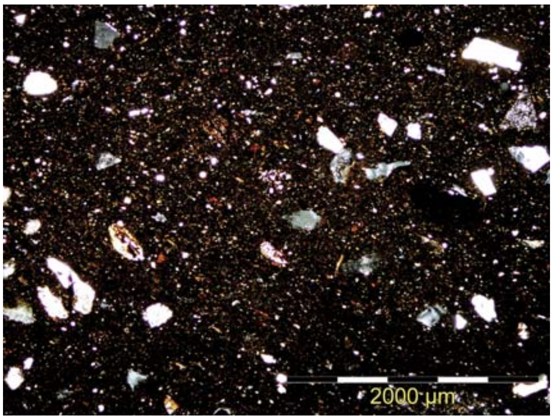

TRZ 025 40 X

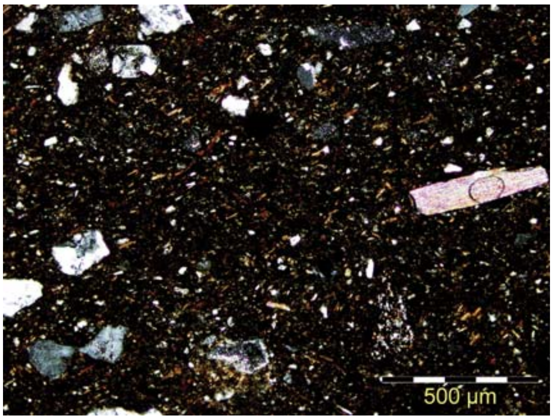

TRZ 025 100 X

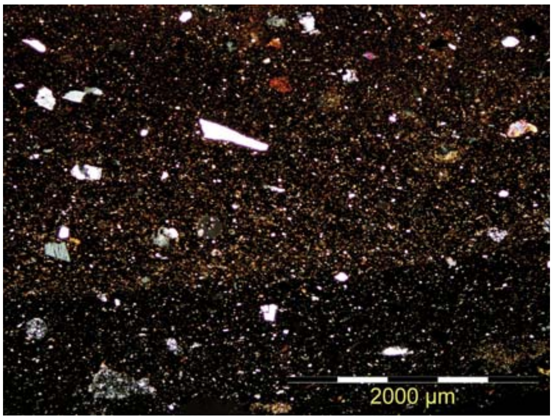

TRZ 033 40 X

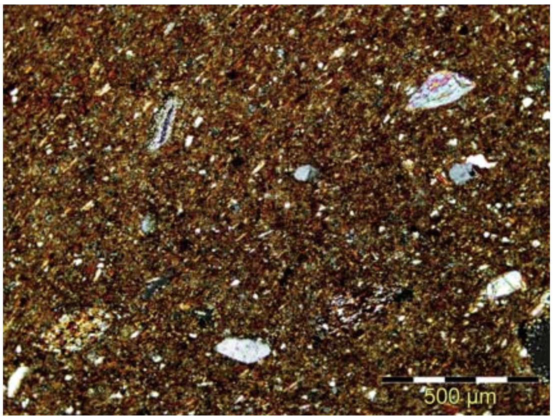

TRZ 033 100 X

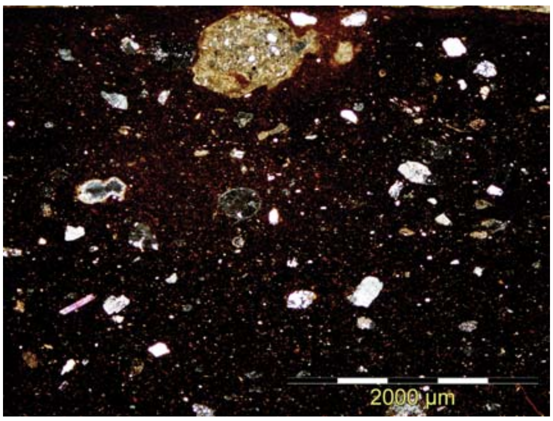

TRZ 036 40 X

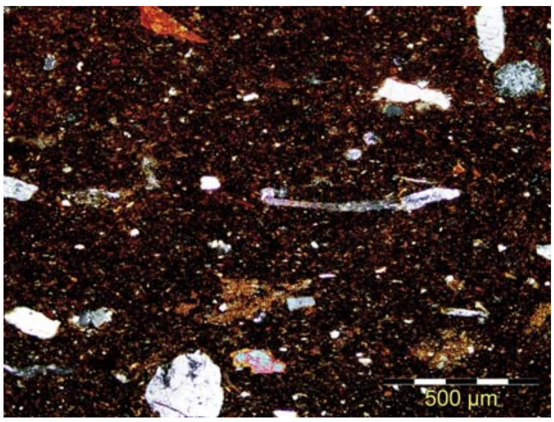

TRZ 036 100 X

Figure 15: A microphotograph by crossed polars of the samples TRZ006, TRZ025, TRZ033 and TRZ036 belonging to KT-K2 fabric from Kara Tepe site

Concerning the outliers from ***Kiln 2 of Kara Tepe*** (Table 5), the common ware TRZ020 presents a similar petrographic composition than the fabric of ***Kara Tepe's K2***: quartz, quartz-mica schist, chert, sandstone, plagioclase, amphiboles, epidote, opaques biotite (900µm) and mica-muscovite (800µm). However, the matrix of TRZ020 is more calcareous (Figure 16). Nevertheless, the common ware TRZ041 presents several differences in typology and petrographic composition to the other ceramics coming from ***Kiln 2 of Kara Tepe***. The walls are wider and non-plastic inclusions are more abundant but they don't present more than 700µm long axis dimension. The groundmass is homogeneous, reddish-brown under PPL, rich in ferric minerals. Isolated fragments of quartz, plagioclase, k-feldspar, amphibole and epidote are dominant together with big biotites and mica-muscovite. Few quartz-mica schist and chert are also present (Figure 16).

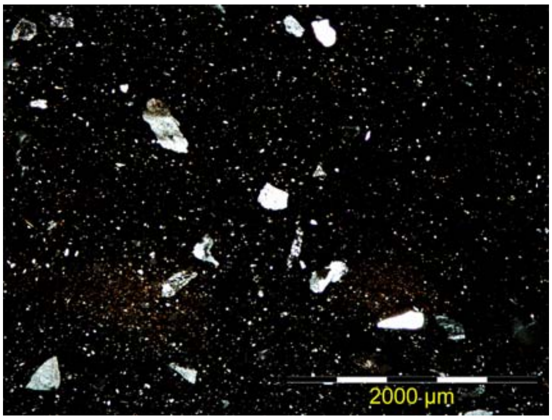

TRZ 020 40 X

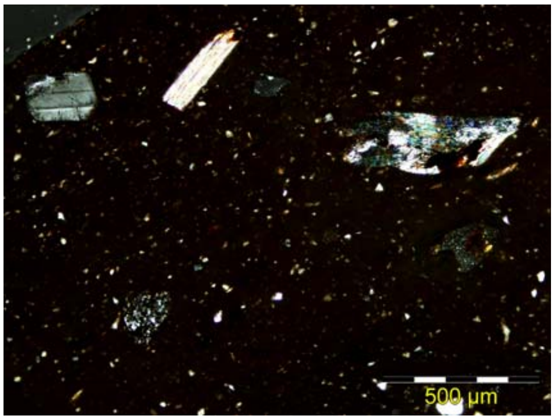

TRZ 020 100 X

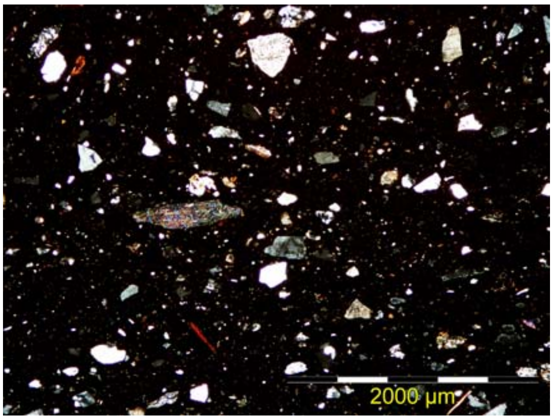

TRZ 041 40 X

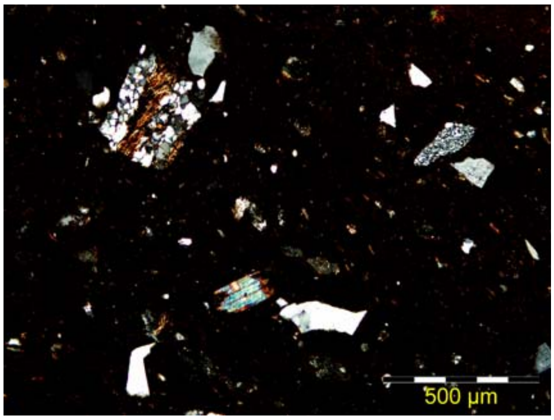

TRZ 041 100 X

Figure 16: A microphotograph by crossed polars of the outliers TRZ020 and TRZ041 from Kara Tepe's K2

99 individuals belong to the chemical group **TRZ** (Figure 13) apart from TRZ002, TRZ004, TRZ005, TRZ010, TRZ017, TRZ021 and TRZ036 that already have been classified within ***Kara Tepe's Kiln N2 Reference Group***. Crosschecking these results with the raw chemical composition it is obvious that **TRZ** and **F2** present slight differences mainly in trace elements thus **F2** and **TRZ** must represent two slightly different productions probably sharing the same clay source or the same uncertainty zone. As the majority of the individuals sampled at the kiln founded in RF grid of ***Tchinguiz Tepe*** and coming from the stratigraphical units of RC grid belong to this group, **TRZ** might be associated with high probability to the ceramic production of the kiln RF of ***Tchinguiz Tepe***. The mean chemical composition and the standard deviation of each element of **TRZ** are given in Table 9 and in Figure 17 we present its typology.

TRZ (n=99)		
EL	Mean	St.dev
Fe2O3%	6,11	0,36
Al2O3%	15,55	0,59
TiO2%	0,65	0,03
MgO%	3,60	0,32
CaO%	9,98	0,92
Na2O%	1,40	0,18
K2O%	3,29	0,22
SiO2%	55,53	1,58
Ba ppm	553	61
Rb ppm	126	8
Th ppm	14	1
Nb ppm	15	1
Zr ppm	149	7
Y ppm	25	1
Sr ppm	363	41
Ce ppm	61	7
Ga ppm	18	2
V ppm	100	6
Zn ppm	101	8
Cu ppm	34	4
Ni ppm	49	4
Cr ppm	75	5

Table 9: Mean chemical composition and the standard deviation of each element of TRZ

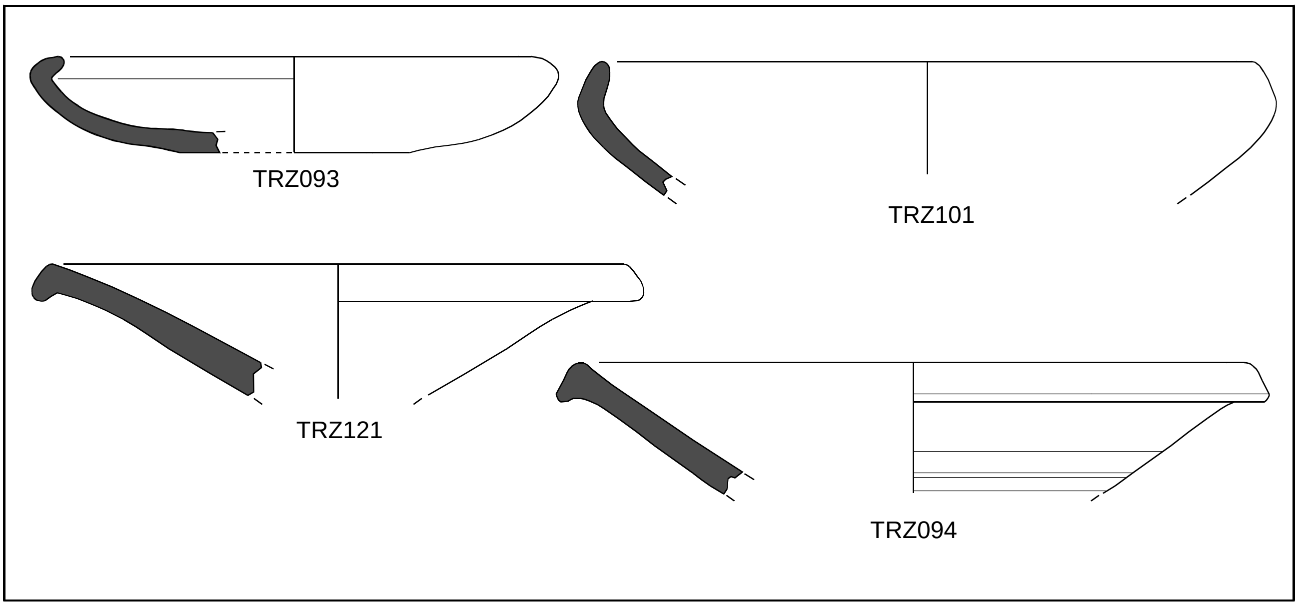

Figure 17: Typology of the group TRZ

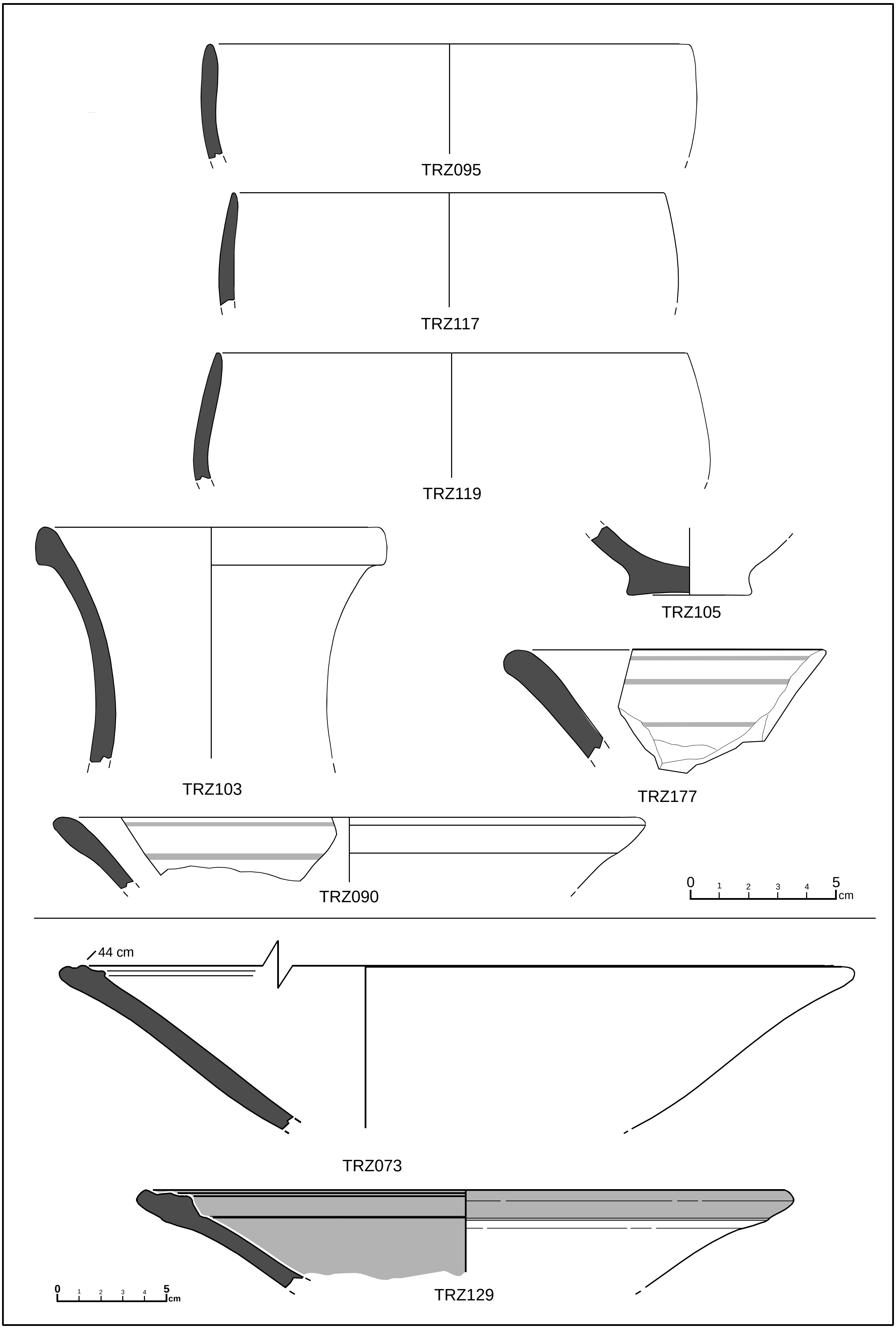

Figure 17: Typology of the group TRZ

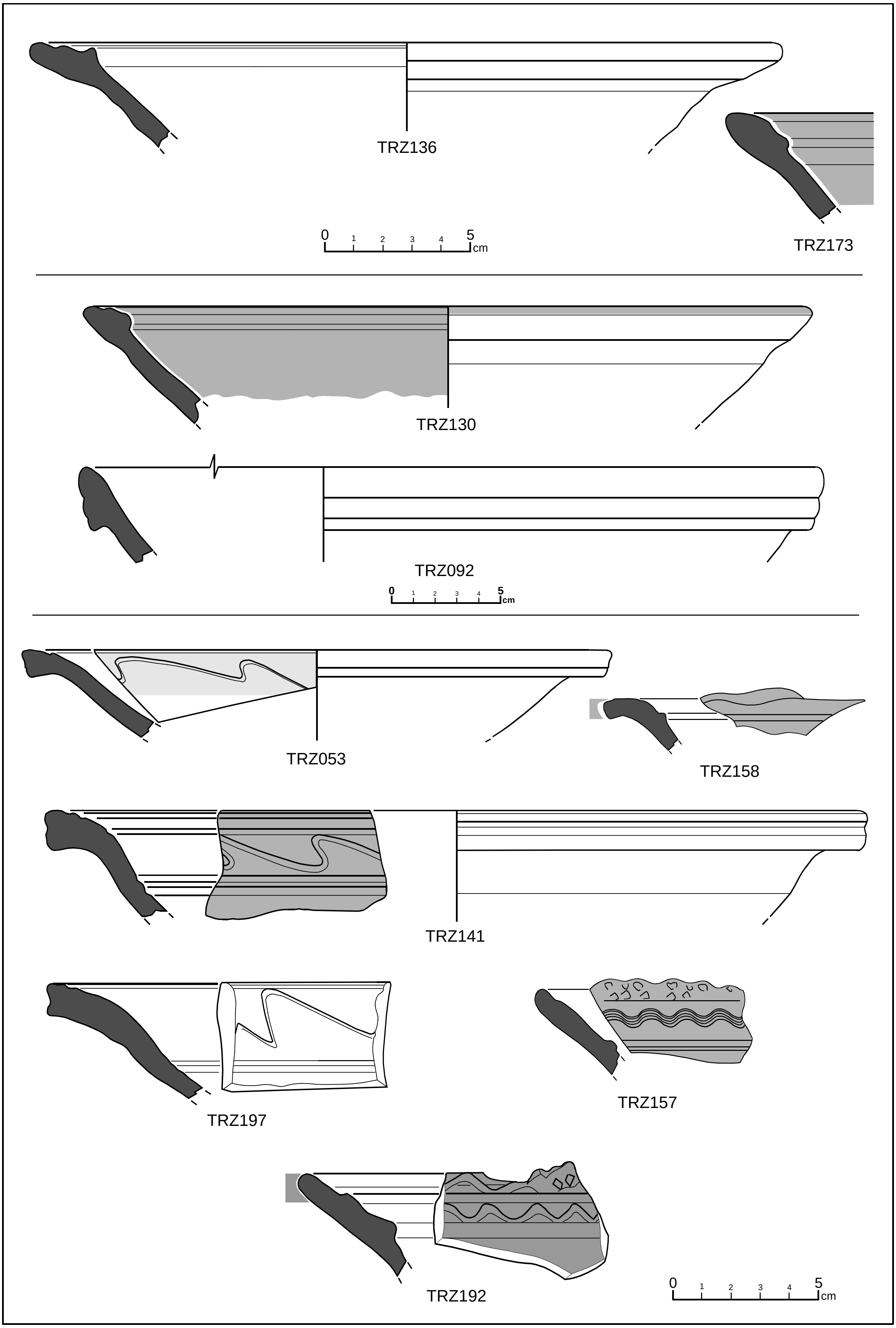

Figure 17: Typology of the group TRZ

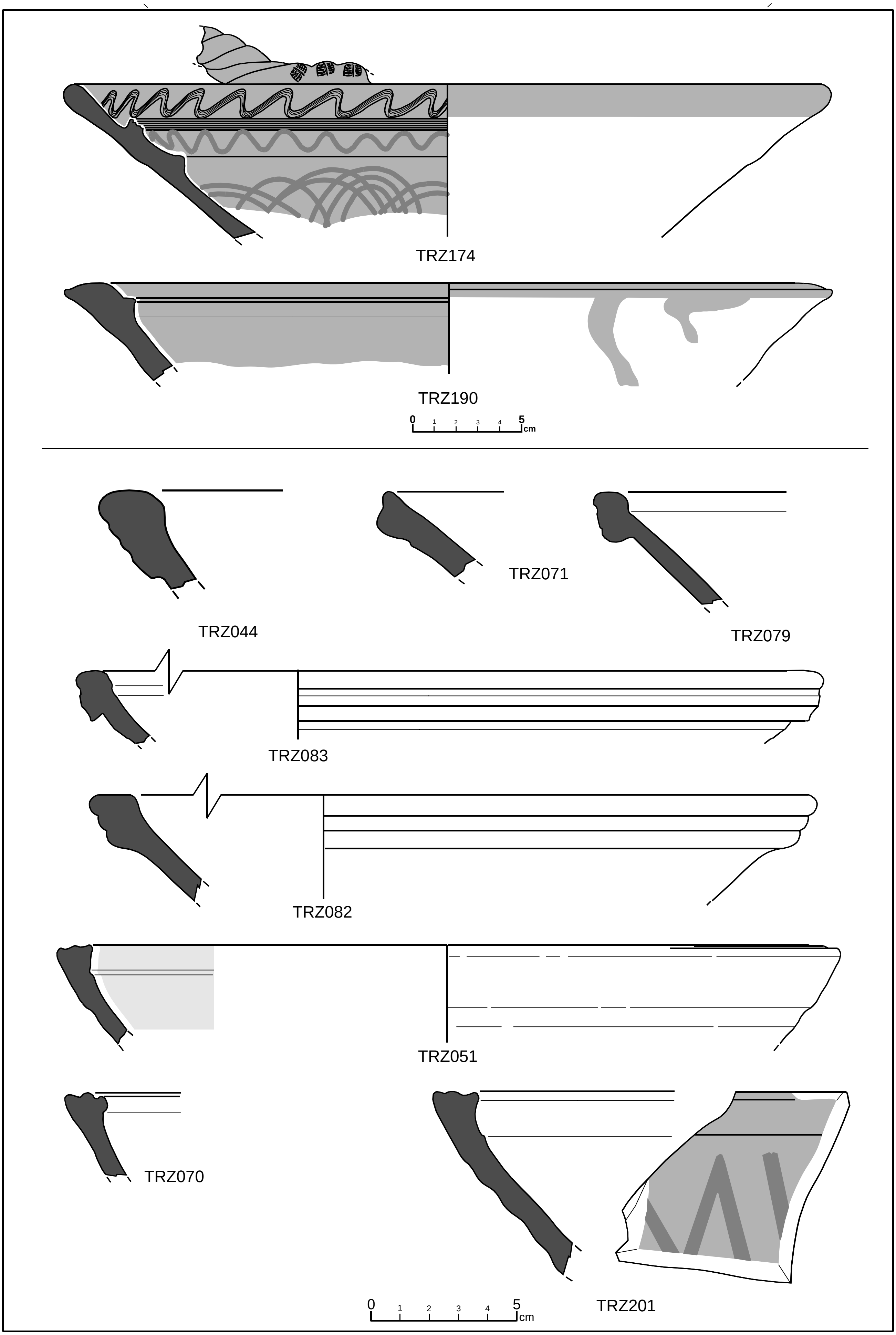

Figure 17: Typology of the group TRZ

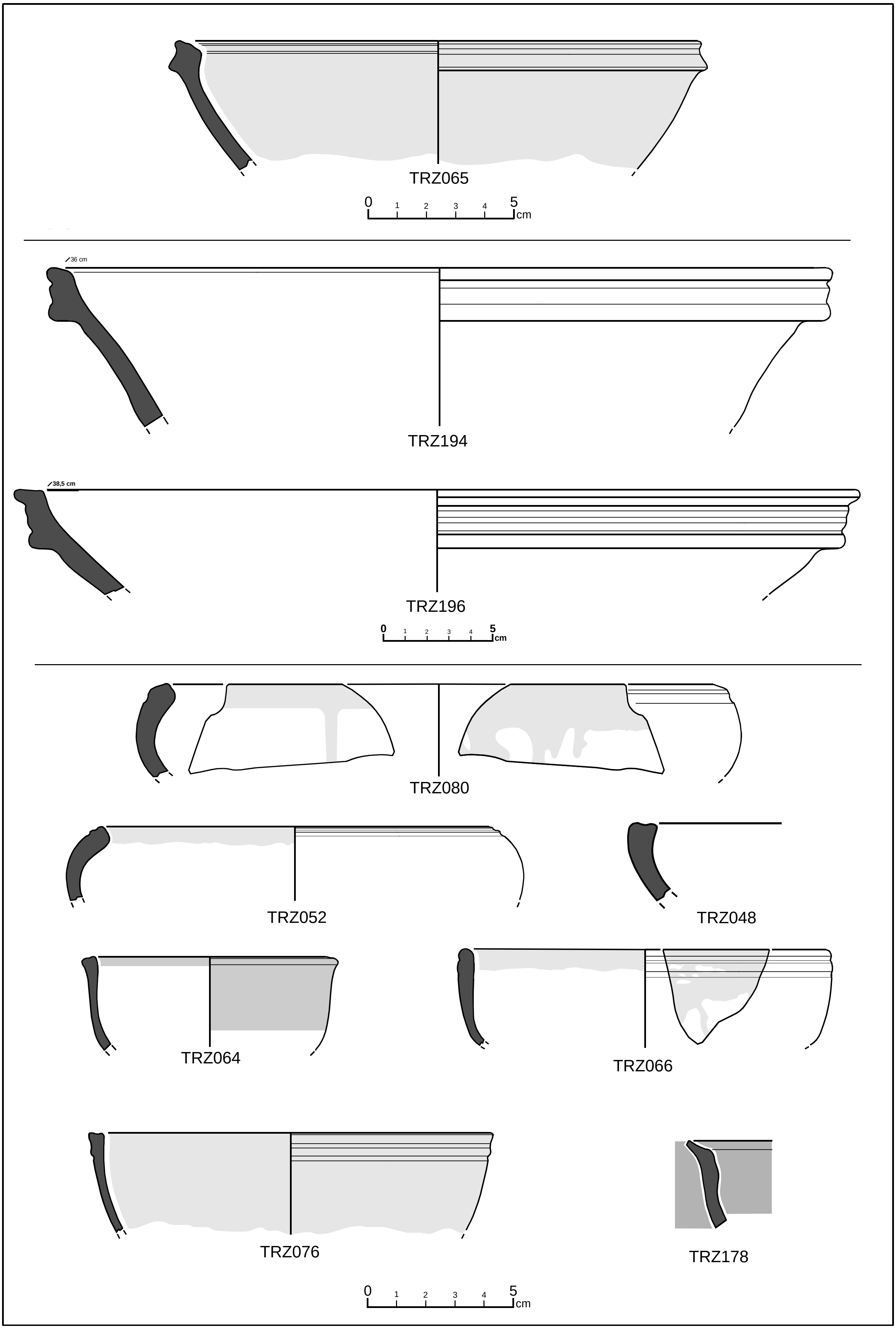

Figure 17: Typology of the group TRZ

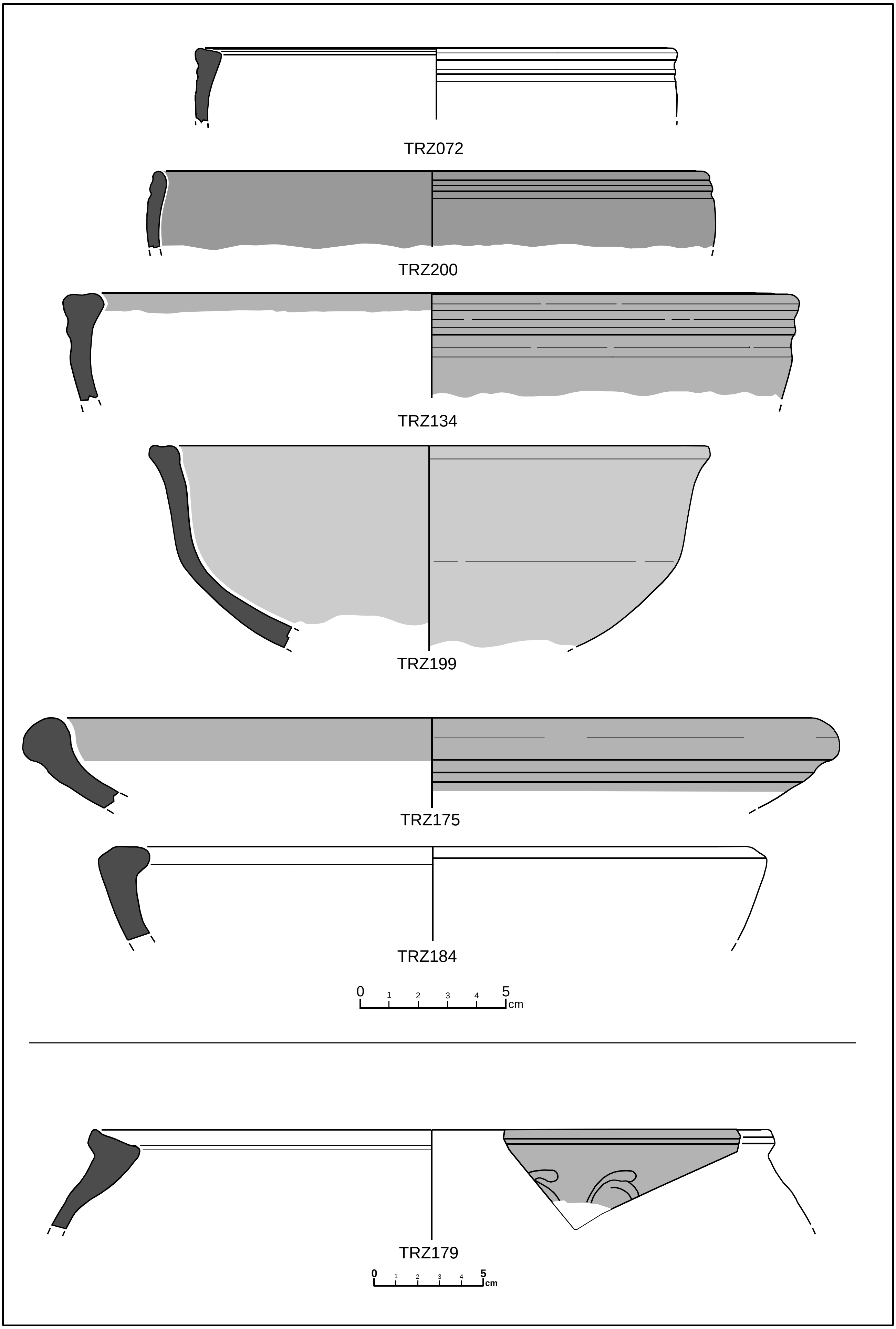

Figure 17: Typology of the group TRZ

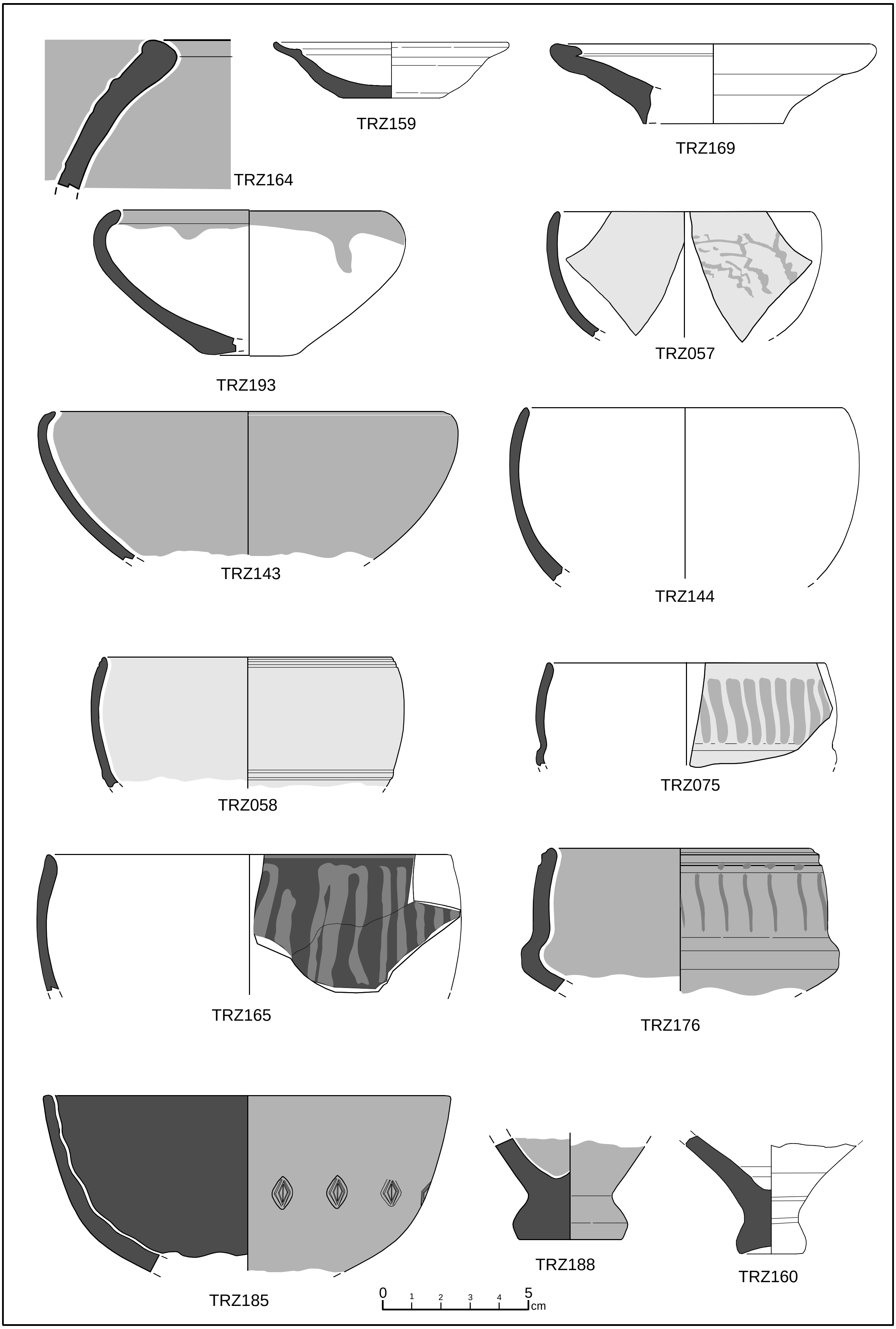

Figure 17: Typology of the group TRZ

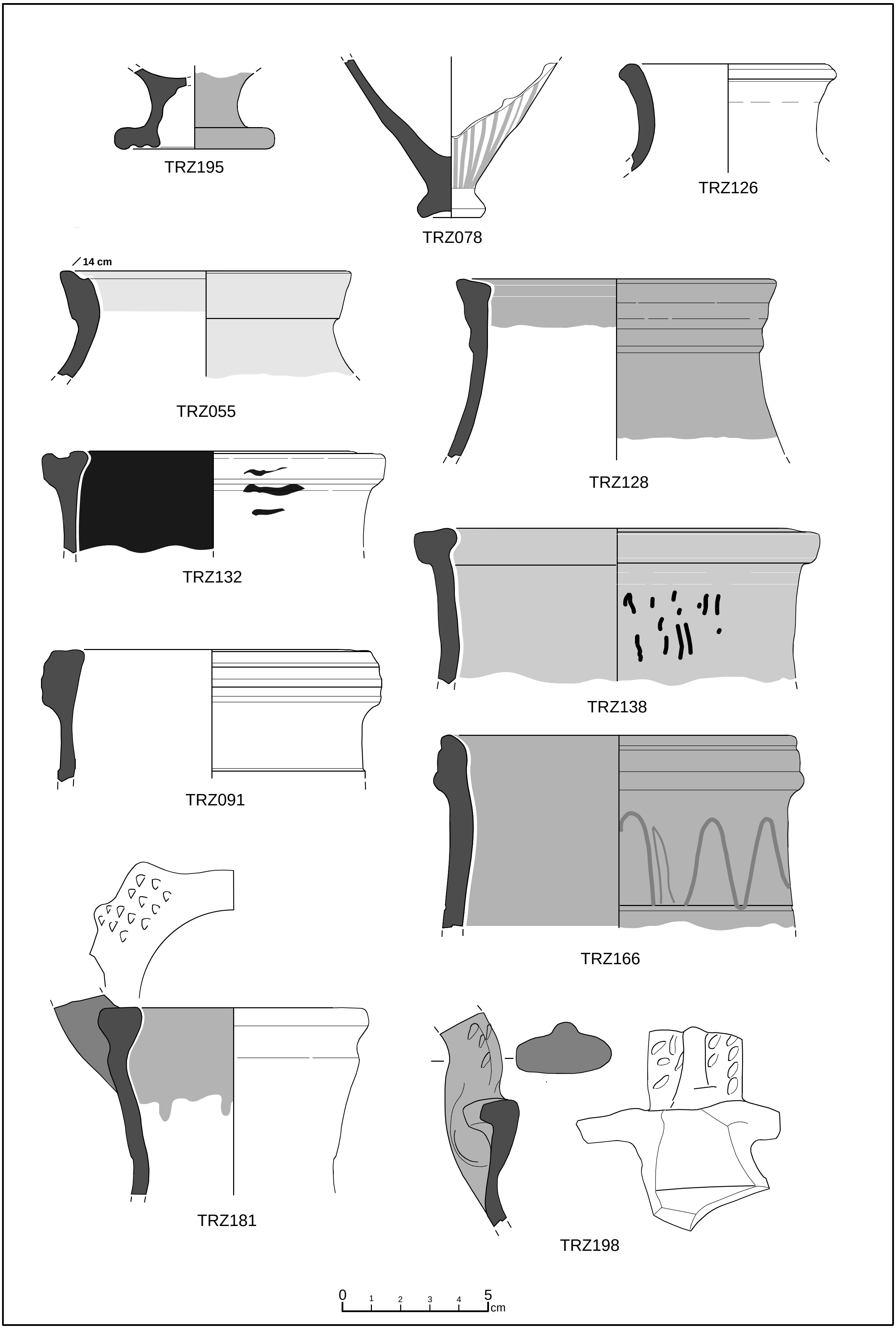

Figure 17: Typology of the group TRZ

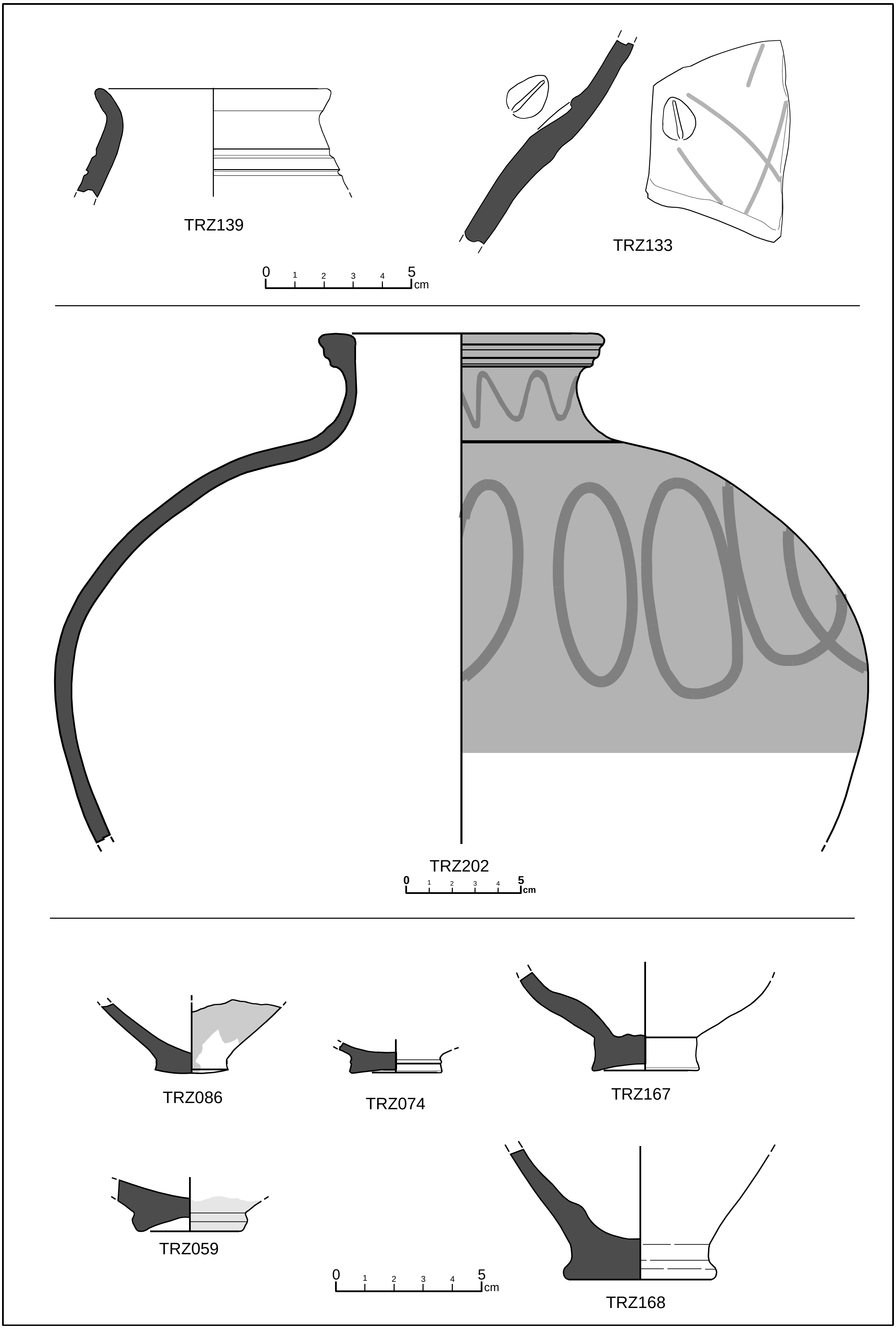

Figure 17: Typology of the group TRZ

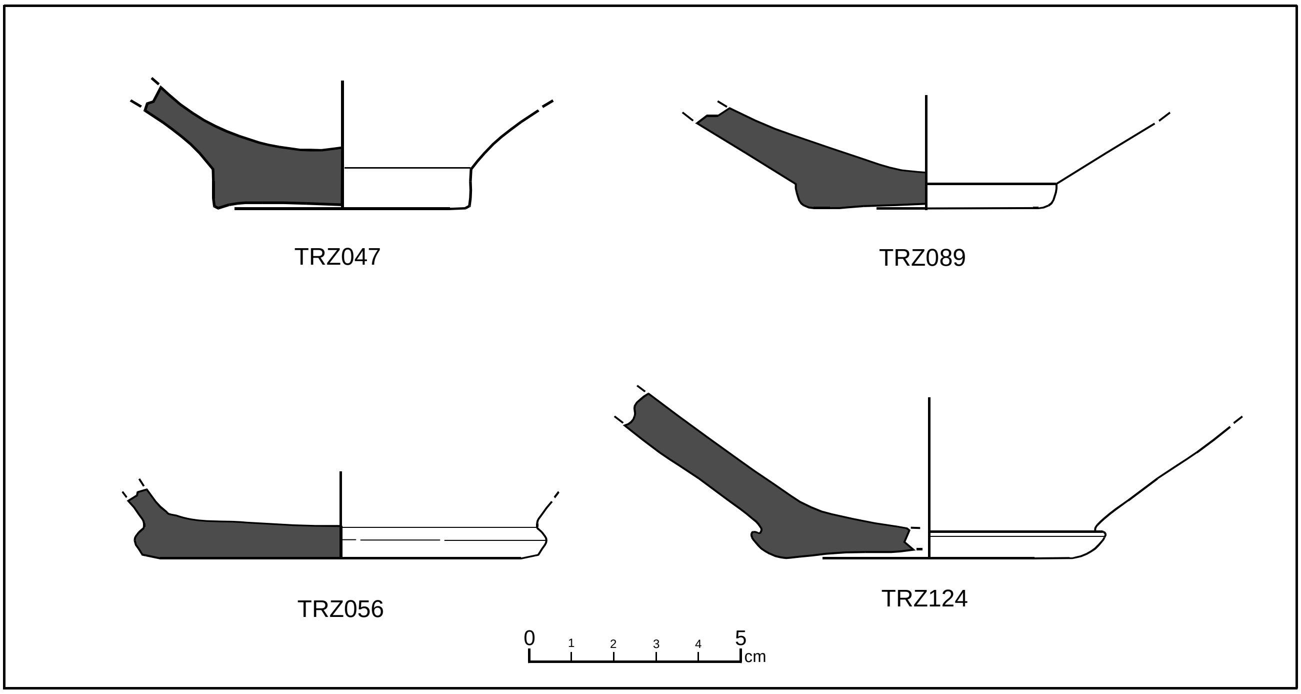

Figure 17: Typology of the group TRZ

Ten ceramics from TRZ group have been analysed by thin section and two different petrographical fabrics have been identified mainly due to the composition and frequency of non-plastic inclusions (Table 5). On the one hand, seven common wares can be grouped in a fine fabric with few non-plastic inclusions named TRZ-1(A) (Figure 18). One individual comes from the stratigraphical units of ***Kiln 1 from Kara Tepe*** (TRZ126), four from the ***Monasteries*** (TRZ132, TRZ133, TRZ138 and TRZ143) and two (TRZ065 and TRZ076) from RC grid from ***Tchinguiz Tepe***. All of them have a similar petrographical composition than ceramics of K2 kiln from ***Kara Tepe***. Groundmass is quite homogeneous; with a yellowish-brown colour under PPL. The optical activity of the groundmass is medium-low. Coarse fraction is rare, open-spaced and reflects a bimodal grain-size distribution. Granite (500µm long axis dimension), quartz-mica schist (300 to 600µm long axis dimension) fragments and chert are predominant (500µm). Other non-plastics inclusions of quartz (200-600µm) are dominants and plagioclase (200µm), amphibole (350µm), epidote, biotite (600µm) and mica-muscovite (300µm) are frequent. This fabric has few voids and vesicles are dominant.

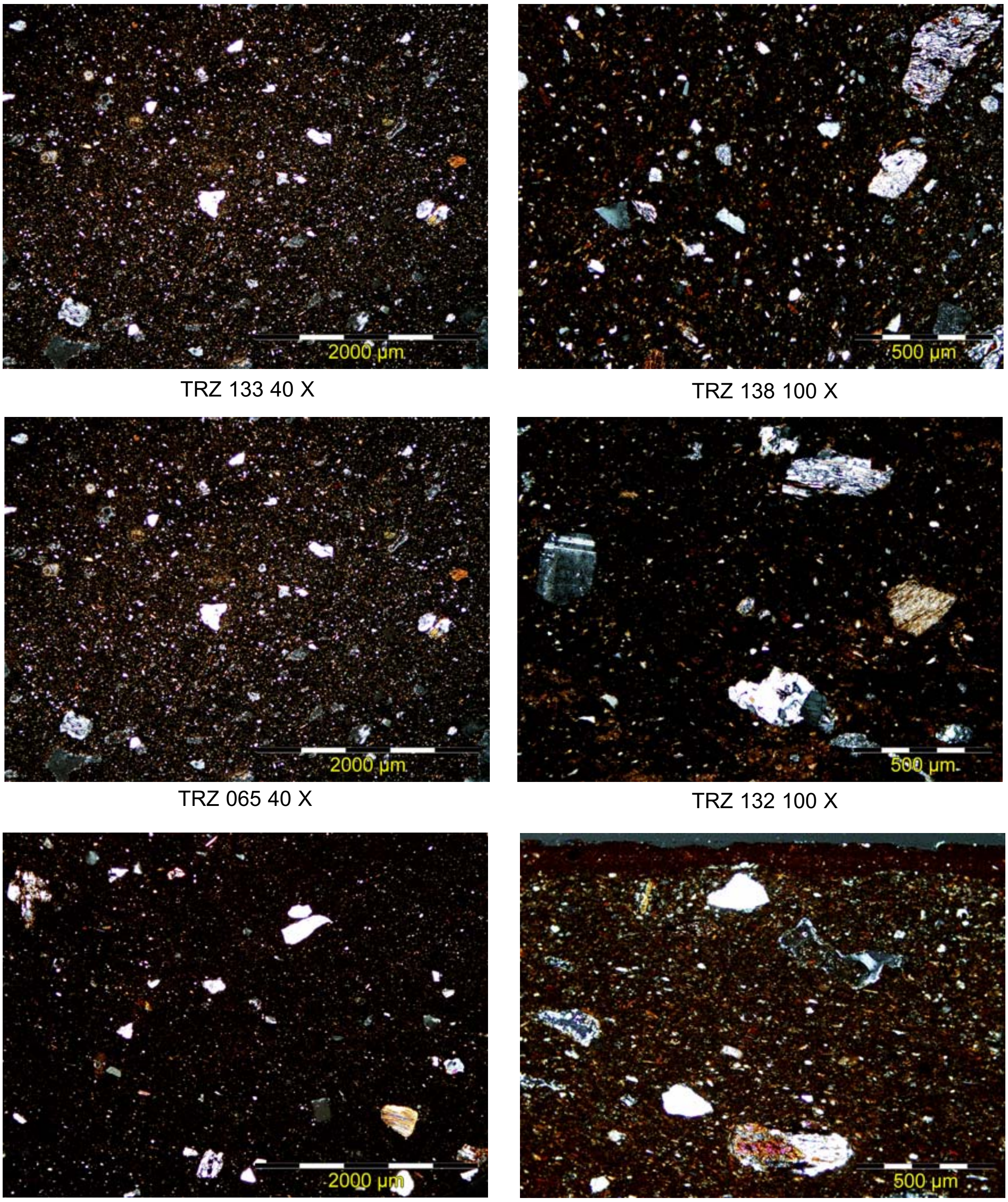

Figure 18: A microphotograph by crossed polars of the samples TRZ065, TRZ076, TRZ132, TRZ133, TRZ138 and TRZ143 from TRZ-1$_{(A)}$ fabric from the chemical group TRZ

On the other hand, the examination of the samples TRZ085, TRZ183 and TRZ188 suggests three different petrographic fabrics (Table 5). They are cooking wares and present differences in type, frequency and size of the non-plastic inclusions. TRZ085, from RC grid stratigraphy, can be considered a medium-coarse fabric (**TRZ-1$_{(B)}$**). The micromass is characterised by rich in iron oxides with few carbonate concentrations and it has an orange-brown colour under PPL. The matrix is only slightly optically active, suggesting a generally higher firing temperature for this sample (Figure 19). The coarse fraction of the non plastic inclusions is medium-well sorted, following a bimodal grain-size distribution and rock fragments are generally sub-angular. It includes frequents metamorphic fragments as quartz-mica schist. Some crystals correspond to isolated quartz, plagioclase and k-feldspar coming from granite rocks or gneiss. Amphibole and epidote are also presents as accessory minerals. Is evident that secondary component of this fabric contains calcareous crystals coming from macrofossils remains and shell fragments, some of them up to 2mm long axis dimension. Firing process has altered the calcareous component of microfossils, favouring the decomposition of primary calcite and the formation of secondary micritic calcite within the closed pores (Cau *et al*., 2002). Coarse fraction also presents other volcanic rocks, as basalt. Finally, fine fraction includes fine quartz crystals and mica-muscovite as a major component but also micritic calcite, k-feldspar, amphibole and epidote.

The groundmass in TRZ183 cooking ware (RC grid of ***Tchingiz Tepe***) is homogeneous and reddish-brown under PPL and (Figure 19). The clay is rich in iron oxides but includes rests of carbonates that can be the consequence of calcareous shell decomposition, latter altered to secondary micritic calcite (Cau *et al*., 2002). This suggests that firing temperature was high, and it is evidenced by the optically inactive micromass, the degree of alteration, the bloating suffered by non-plastic inclusions and the

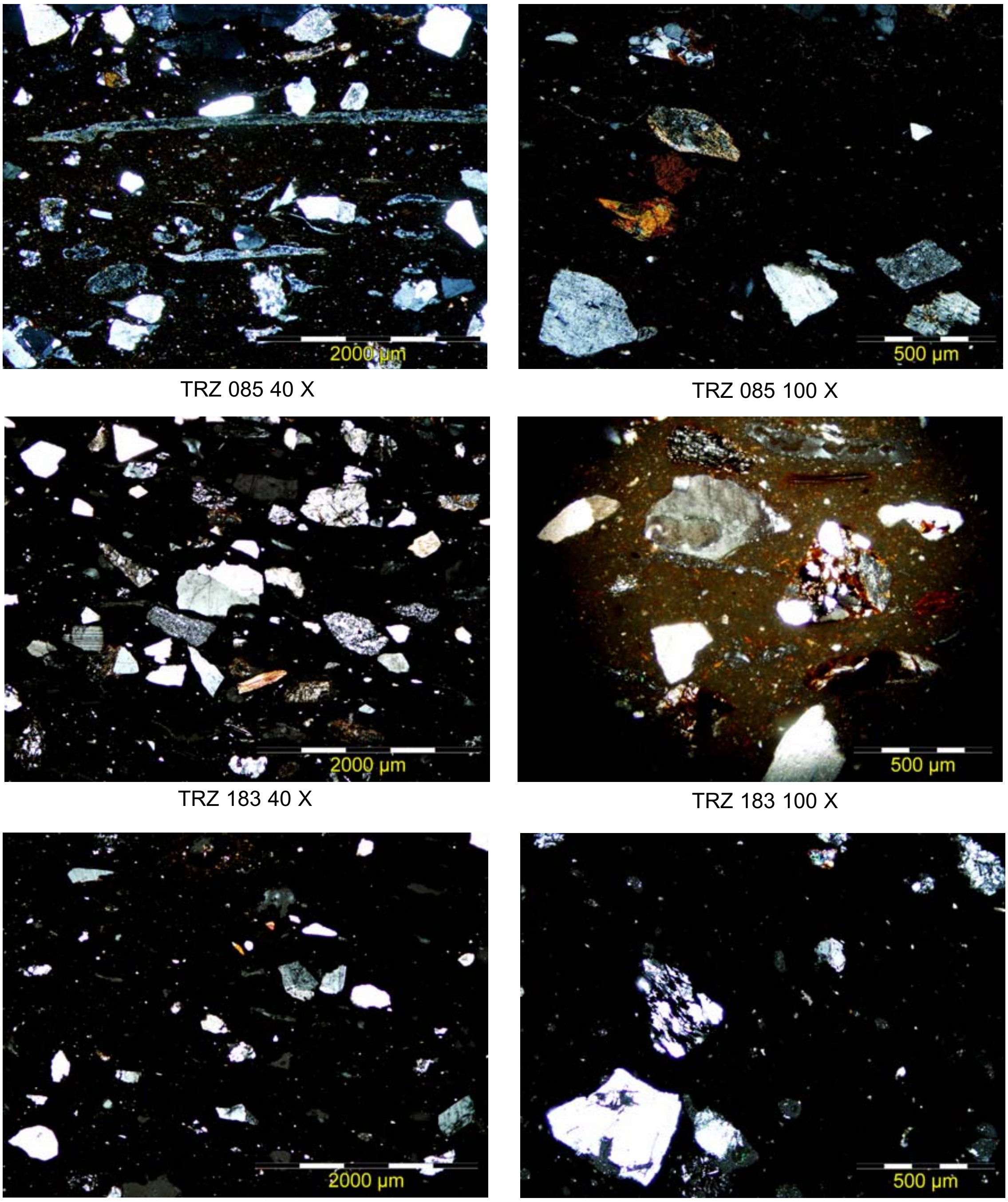

Figure 19: A microphotograph by crossed polars of the samples TRZ085, TRZ183 and TRZ188 belong to TRZ-$1_{(B)}$, TRZ-$1_{(C)}$ and TRZ-$1_{(D)}$ fabrics respectively

decomposition process suffered by the calcareous shell fragments. The inclusions of the coarse fraction relate this individual petrographically to TRZ085, but inclusions in TRZ183 are more frequent and coarser, ranging up to 1mm long axis dimension. For this reason it has been differentiated as **TRZ-1$_{(C)}$** fabric. A variety of rock inclusions can be observed in the coarse fraction. It includes quartz-mica schist (500µm), quartzite and chert (600µm) as dominant rocks together with monocrystalline (400µm) and polycrystalline quartz (800µm). Coarse fraction contains other isolated crystals as plagioclase (350µm), k-feldspar (300µm), amphiboles (200-400µm), epidotes, opaques (350µm), biotites (250 to 500µm) and mica-muscovite (450µm). There are also frequent microfossils, some of which have decomposed during the firing process. This fabric also contains few fragments of sedimentary rocks as sandstones. Fine fraction presents lot of mica-muscovite lames together with quartz fragments and opaques. This vessel is very porous with predominant mesovughs and macrovughs orientated parallel to the vessel margins.

Finally, TRZ188 cooking ware from the kiln found in RF grid has been defined as **TRZ-1$_{(D)}$** fabric. Inclusions are smaller and less frequent than in TRZ085 and TRZ183 but similar in size and frequency to the ones of **TRZ-1$_{(A)}$** fabric (Figure 19). Firing temperature was high as evidenced by the decomposition process suffered by the carbonate rocks and the degree of alteration of non-plastic inclusions. High firing temperature can be deduced by only slightly optically active matrix, also. The groundmass of yellowish-green colour under PPL is rich in carbonates and quite homogeneous. The optical activity of the groundmass is medium-low. The grains of the coarse fraction are frequent, open-spaced and reflect a bimodal grain-size distribution. Concerning the coarse fraction the inclusions are subangular and monocrystalline and polycrystalline quartz together with quartz-mica schist are dominants. Plagioclase, K-feldspar, biotite and mica-muscovite appear as isolated crystals. Chert is also present as accessory rock. Fine fraction includes few crystals of quartz and mica-muscovite. Voids are frequents, as vesicules and microvughs.

The individuals within **TRZ-F2** located outside of **F2** and **TRZ** in the dendrogram of Figure 13 are variants of these two productions sharing the same geological sources of raw materials but non of them can be clearly classified into these two identified productions although chemically they seem to be variants of broader local ceramic tradition.

Regarding the petrographical analysis, two individuals from ***Kara Tepe's K1***, a painted common ware (TRZ123) and an unpainted common ware (TRZ127) represent petrographical loners (Table 5). The groundmass of TRZ123 is rich in iron oxides, reddish-brown under PPL and presents medium optical activity, suggesting generally medium firing temperature for this sample. The coarse fraction of the non-plastic inclusions is well sorted, following a unimodal grain-size distribution and rock fragments are generally small (200-600 µm long axis dimension) and sub-rounded (Figure 20). Fragments of monocrystalline and polycrystalline quartz (300 to 600 µm), plagioclase (200µm), biotite (600µm) and mica-muscovite (350µm) are predominant. Amphiboles (200µm) and epidote (100µm) together with quartz-mica schist (550 µm), chert (300µm) and sandstones (500µm) appear as accessory minerals and rocks. The slip presents low state of vitrification and its 150 µm wide in the outer part and 45 µm in the inner part. TRZ127 corresponds to a individual with very fine fabric. It presents a heterogeneous micromass with evidence of clay mixing, which appears as streaks or clots with clear boundaries of mixed calcareous with red clay. Coarse fraction contains few non-plastic inclusions as quartz-mica schist (200 µm), quartz, plagioclase (200 µm) and mica-muscovite.

From ***Monasteries*** site of ***Kara Tepe***, the common ware TRZ142 represents another petrographical loner characterised by fine fabric. The groundmass is rich in iron oxide and in carbonates and it has a reddish-brown colour under PPL. Inclusions are moderately, 650µm as maximum long axis dimension (Figure 20). Quartz-mica schist fragments (500µm) together with isolated monocrystalline and polycrystalline quartz (400µm), plagioclase (550µm), k-feldspar (350µm), opaque, amphibole, biotite (400µm)

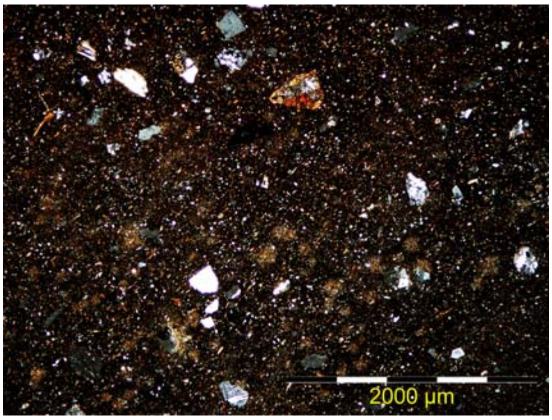

TRZ 142 40 X

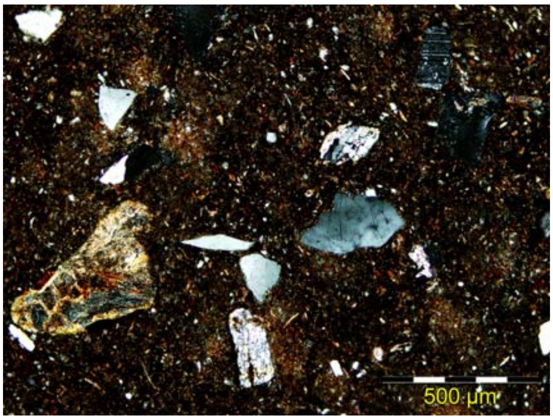

TRZ 142 100 X

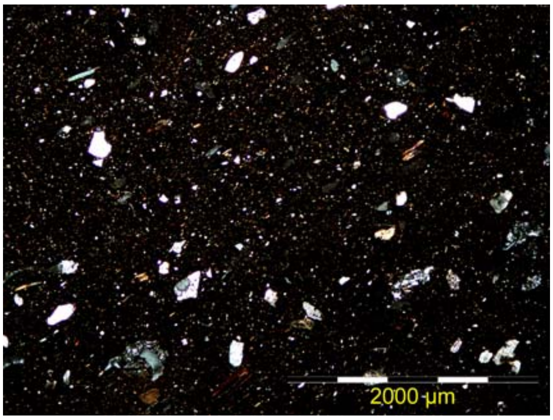

TRZ 123 40 X

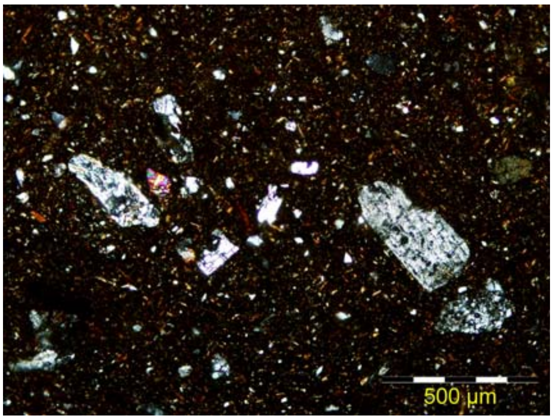

TRZ 123 100 X

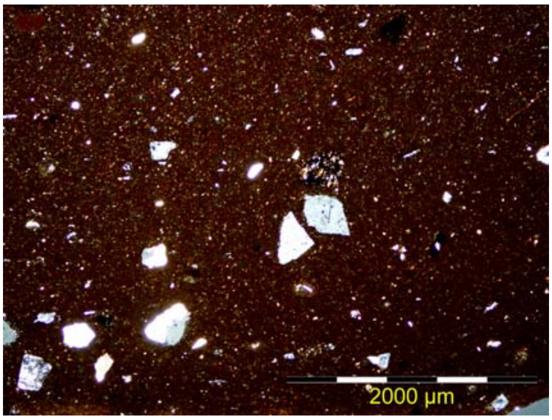

TRZ 068 40 X

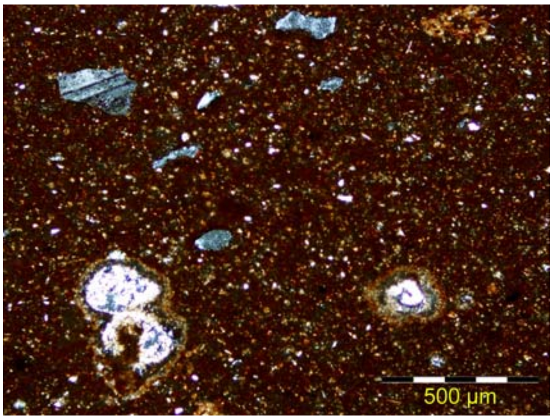

TRZ 068 100 X

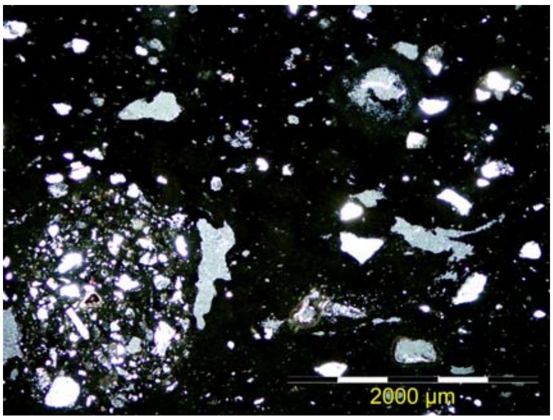

TRZ 067 40 X

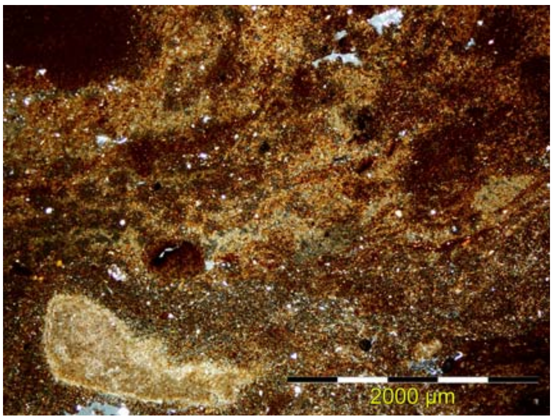

TRZ 127 40 X

Figure 20: A microphotograph by crossed polars of the outliers samples TRZ020, TRZ067, TRZ068, TRZ123, TRZ127 and TRZ142 from the broader TRZ-F2 chemical cluster

and big mica-muscovite (650μm) crystals form the coarse fraction. Secondary crystallisation of salt crystals is confirmed in this individual. Few micro vesicles are present.

Petrographical examination of TRZ067 and TRZ068 common wares from the prospection realised in RC and RF grids of ***Tchinguiz Tepe*** reveals two different fabrics (Figure 20). On the one hand, TRZ067 is noticeably over-fired and can be characterized as '*waster*'. The groundmass presents a dark green colour under PPL and the micromass of the totally fired matrix is optically inactive. The majority of inclusions show strong alteration due to the high temperature of firing. Monocrystalline and polycrystalline quartz (500-700μm long axis dimension), quartz-mica schist (400μm), sandstone, chert (400μm), isolated fragments of plagioclase (250μm) and few biotite (300μm) is contained the coarse fraction. Voids are dominant as micro and meso-vesicles and vughs. On the other hand, TRZ068 represents a fine fabric. The groundmass is rich in iron oxides with an elevated carbonate component formed by calcareous microfossils. These compounds seem to be present in the calcareous clay which was added and mixed with a ferric one. The colour under PPL is generally reddish-brown and inclusions present a open-spaced, well sorted, unimodal grain-size distribution. They are few, medium-sized and sub-rounded. Coarse fraction is mainly composed by granite, quartz and quart-mica schist fragments. Other isolated minerals as plagioclase, k-feldspar, amphibole, opaques are rares. Biotite and mica-muscovite are more abundant in the fine fraction. There are also frequent microfossils, some of which have decomposed during the firing process. In other cases, the calcareous component has become micritic calcite.

The multivariate analysis based both upon the calculation of the Square Euclidian Distances and the Mahalanobis Distances agrees on that the individuals included into the group ***AC*** do not belong to any of the above described groups. By looking at the chemical results it can be observed that AC presents certain differences in Th, Sr, Ga, Cu, Ni and Cr which, even though are not very high, they are significant enough to separate this group from **F2** and **TRZ**. Therefore **AC** is one single production or Paste Compositional Reference Unit (PCRU) and it represents the PCRU of the ***Antique Quarters*** as it formed exclusively by individuals sampled at this site, beside three (TRZ149, TRZ152 and TRZ156). The mean chemical composition and the standard deviation of each element of **AC** are given in Table 10 and in Figure 21 typology of this production is presented.

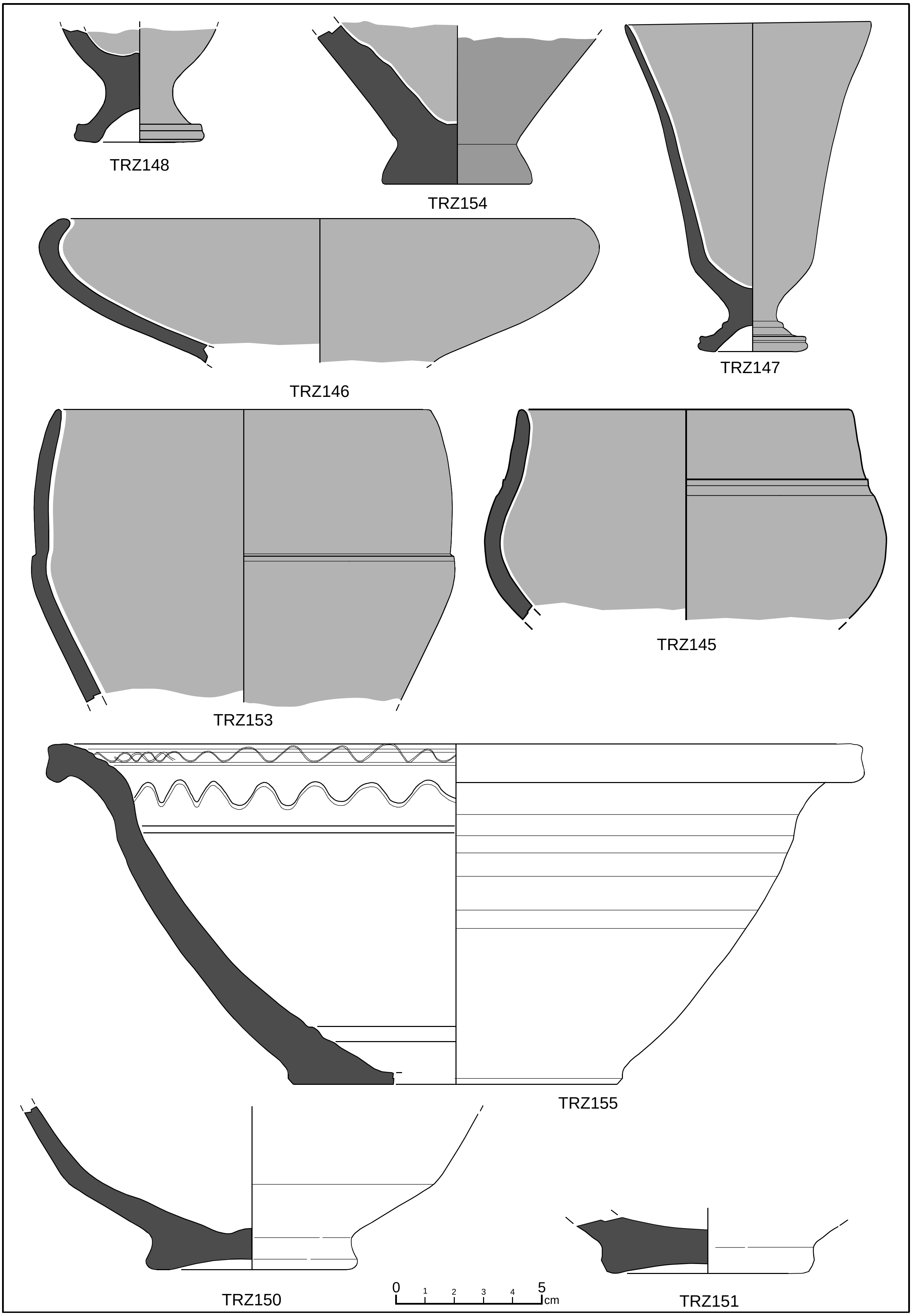

Figure 21: Typology of the group AC

AC (n=9)		
EL	Mean	St.dev
Fe2O3%	6,18	0,24
Al2O3%	15,41	0,63
TiO2%	0,67	0,02
MgO%	3,18	0,16
CaO%	8,63	1,08
Na2O%	1,12	0,16
K2O%	3,11	0,11
SiO2%	57,23	1,36
Ba ppm	636	50
Rb ppm	121	6
Th ppm	20	2
Nb ppm	14	0
Zr ppm	153	7
Y ppm	23	1
Sr ppm	394	40
Ce ppm	58	8
Ga ppm	18	1
V ppm	99	9
Zn ppm	94	7
Cu ppm	42	5
Ni ppm	52	4
Cr ppm	81	5

Table 10: Mean chemical composition and the standard deviation of each element of AC

The cooking ware TRZ156 from ***Antique Quarters*** has been examined by thin section analysis (Table 5). It corresponds to a coarse fraction (Figure 22) that share some petrographical similarities with **TRZ**$_{\mathbf{(B)}}$ (Figure 6) and **TRZ**$_{\mathbf{(D)}}$ (Figure 11) fabrics. The micromass is partially homogeneous with colour changes from orange-brown into yellowish under PPL. The inclusions are frequent, poorly-sorted and single-spaced, reflecting a bimodal grain-size distribution. The coarse fraction is formed by big fragments of 3mm maximum long axis dimension. Non plastic inclusions are frequent, elongated and subrounded and shell fragments together with sandstones (1.3mm) and siltstones (3.6mm) are the predominant inclusions. Sandstones are composed by small quartz, plagioclase, mica-muscovite and spathic calcite crystals mixed with iron oxide rich clay. Opaques are also dominants and only few quartz, biotite and mica-muscovite have been observed. Voids are mainly represented by frequent meso-channels and mesovughs orientated in a parallel axis to the vessel margins.

TRZ 156 40 X

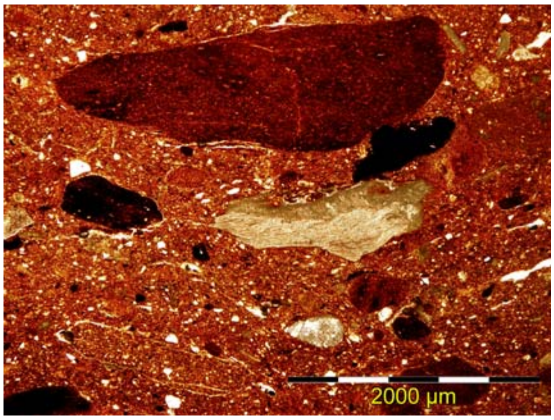

TRZ 156 100 X

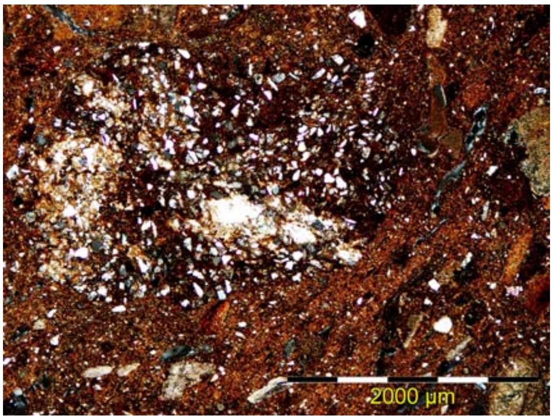

TRZ 156 40 X

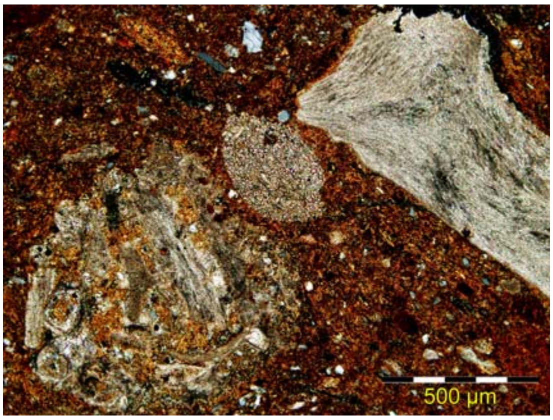

TRZ 156 100 X

Figure 22: A microphotograph by crossed polars of the sample loner TRZ156 from Antique Quarters (AC)

Finally, comparing the mean chemical composition of the three chemically identified groups (***Kara Tepe's RG***, **TRZ** and **AC**) which can be seen at the Tables 8, 9 and 10 the chemical differences are insignificant to indicate different geological raw material sources and petrography also indicates that the geological character of these productions is common. Therefore, our preliminary hypothesis, that the limited existence of adequate clay deposits in the area or the common geological character of these deposits leaded to a long lasting local ceramic tradition, where the exploded raw material recourses are the same, even though there are differences in the production processes, chronology and typology.

On the other hand, the individuals situated at the left and right side of these tree groups (Figure 13) (TRZ008, TRZ027, TRZ029, TRZ041, TRZ054, TRZ060, TRZ063, TRZ077, TRZ097, TRZ098, TRZ100, TRZ102, TRZ112, TRZ114, TRZ120, TRZ149, TRZ152 and TRZ159) can not be clearly classified into non of the above identified productions therefore even though the chemical similarities indicate a local/regional character they must be local/regional variants with certain chemical similarities with all three productions. Some of these chemical loners have been examined by thin section analysis (Table 5). The non plastic inclusions found in the coarse fraction of all these samples are compatible with the range of geological deposits in the broader local area, however clear differences in frequency and size of the inclusions can be observed between them (Figure 23). The common ware TRZ060 (TZ07-RC-10-10) from the stratigraphical unit 10 of RC grid from ***Tchinguiz Tepe*** corresponds to a fine fabric. The groundmass is reddish-brown under PPL, rich in iron oxides and it has medium optical activity, suggesting a generally higher firing temperature for this sample. Non plastic inclusions are generally small (200-500µm long axis dimension) and sub-rounded, well sorted and they follow a unimodal grain-size distribution. Quartz (200 to 500µm) and zoned plagioclase (350µm) fragments are dominants and biotite and mica-muscovite (360µm) are frequent in the coarse fraction and predominant in the fine fraction.

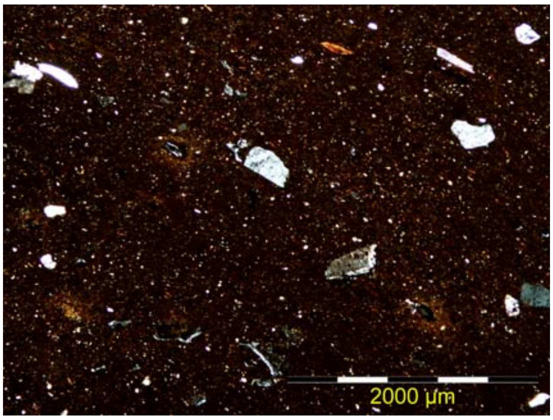

TRZ 060 40 X

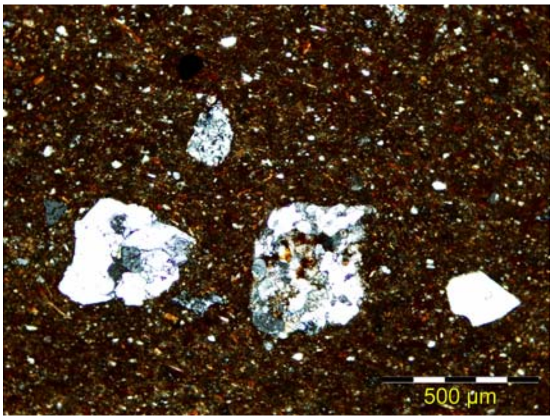

TRZ 060 100 X

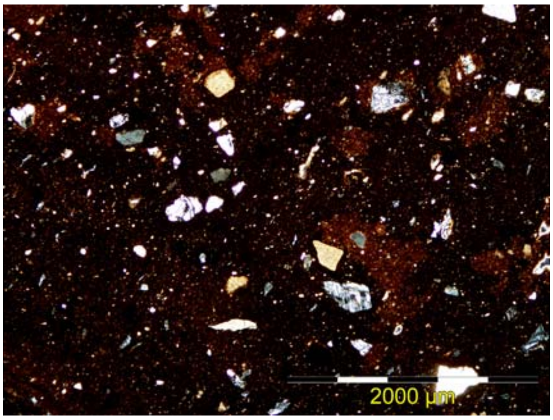

TRZ 098 40 X

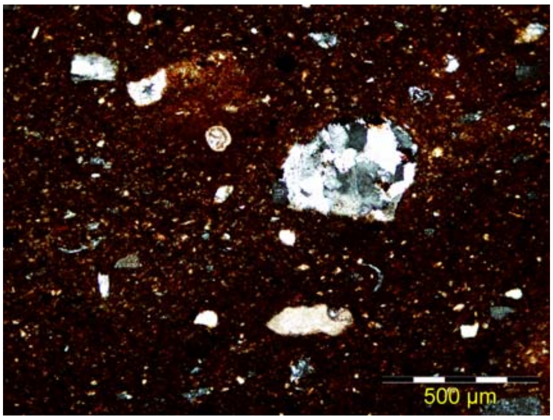

TRZ 098 100 X

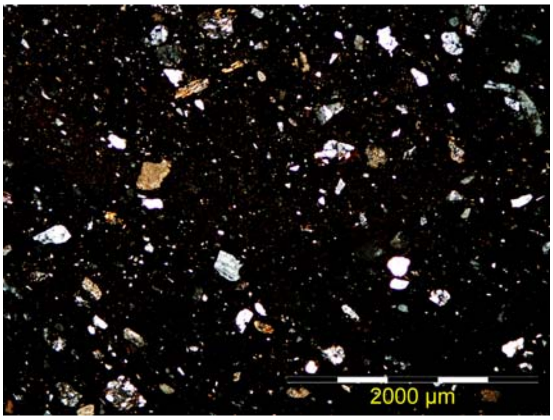

TRZ 112 40 X

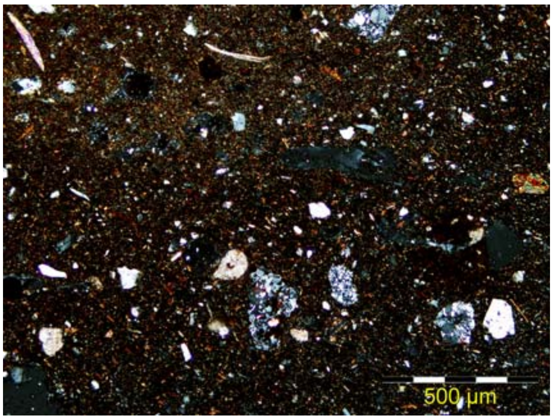

TRZ 112 100 X

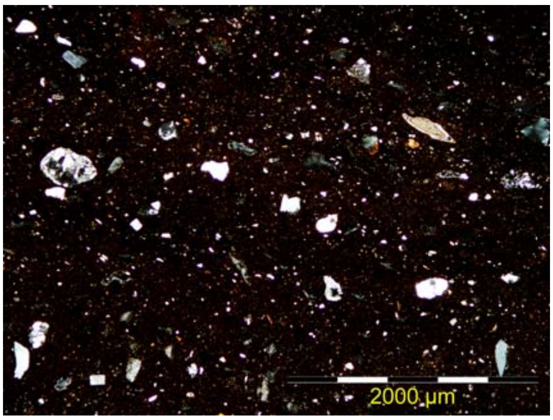

TRZ 114 40 X

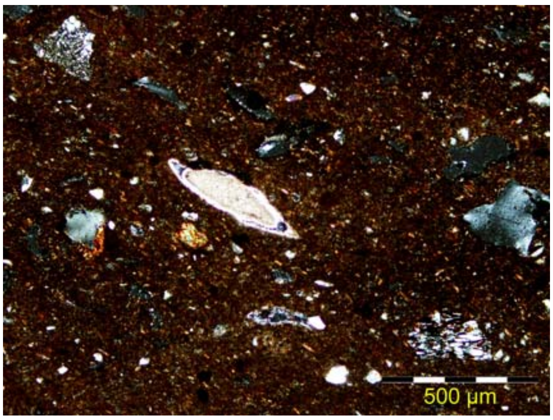

TRZ 114 100 X

Figure 23: A microphotograph by crossed polars of the outliers samples TRZ060, TRZ098, TRZ112 and TRZ114

The coarse fraction is also composed by a great variety of rocks as granites, phyllite, quartzite (350µm) and quart-mica schist (400µm). This individual includes few sedimentary rocks as sandstone (425µm) and chert (400µm). Amphiboles, opaques and k-feldspar appear as accessories minerals. Nodules of micritic calcite are few and, sometimes, voids are partially filled with secondary calcite.

From the ***Citadel***, three individuals have been examined by thin section analysis. All of them represent fine fabrics with similar inclusions as found in the above identified productions (Table 5). However, the micromass of TRZ098 (TZ07-4-48) is generally yellowish-brown under PPL and displays streaks of calcareous clay within the darker iron oxide rich clay matrix (Figure 23) that indicates the mixing of clays during the paste preparation process. The carbonate component possibly comes from this calcareous clay, where de presence of calcareous microfossils is evidenced. Coarse fraction contains few and small inclusions, sub-rounded and they follow a bimodal grain-size distribution. As in the above mentioned productions, there are granites and crystals detached of granites (quartz, plagioclase, k-feldspar, amphibole, biotite and mica-muscovite), quartz-mica schist and quartz-schist, carbonate sandstones and big nodules of micritic calcite. The fine fraction includes mica-muscovite, quartz, feldspar fragments and opaques and there are few micro-vesicles. TRZ112 contains more inclusions than the other loners but coarse fraction is medium size (< 600µm long axis dimension), well sorted, following a unimodal grain size distribution (Figure 23). The micromass is reddish-brown, rich in iron oxydes with a carbonate component. The coarse fraction is mainly formed by granites fragments and crystalls detached of these rocks, as quartz fragments, plagioclase, k-feldspars and big fragments of biotite and mica-muscovite. This pot includes frequent quartz-mica schist grains, few sandstone and other isolated minerals as opaques, amphiboles and epidote. Mica-muscovite is dominant in the fine fraction together with small grains of quartz, feldspars, amphiboles, opaques and epidotes. There are few voids in form of mesovughs. Finally, TRZ114 is similar to TRZ112 but micromass is more calcareous and is clear the presence of microfossils and shell fragments (Figure 23). Coarse fraction includes granite and crystals detached of these rocks as quartz (400µm), plagioclase, amphiboles (250µm), biotite and mica-muscovite. Quartz-mica schist fragments are also dominants (300µm) as well as chert. Sandstone appears as an accessory rock together with other isolated crystalls as epidote, opaques and few fragments of a volcanic rock.

Technological study of ceramics from Termez by XRD

The technological aspects of the analysed material have been studied by XRD analysis and the mineralogical aspects of the analysed ceramic are going to be described following the identified chemical groups.

Generally, it is important to mention from the beginning, that the majority of the analysed material is calcareous (CaO>5-6%). These CaO proportions are owed basically to the presence of calcium carbonates in the paste. Calcium carbonates facilitate the formation of calcosilicates and aluminosilicates (gehlenite, diopside, etc.) during the firing process and the development of a characteristic microstructure proportioning specific physical properties to the material (Maniatis *et al*., 1981; Tite *et al*., 1982). However, there is one no calcareous group (**$TRZ_{(A)}$**) identified in the present data set. In the no calcareous pottery instead the development of calcosilicates during firing the crystallisation of magnesiumsilicates takes place (spinel, enstatite, clinoenestatite) and the microstructure and mechanical properties of this ceramic products are totally different.

Firing temperature and mineralogical aspects of ceramics from TRZ(A) group

Each one of the two individuals represents a different mineralogical category corresponding to different Equivalent Firing Temperature (EFT). However, both correspond to very high fired ceramics. TRZ163 is characterised by the simultaneous presence of primary (illite-muscovite) and firing phases (spinel) which indicates relatively high firing temperature (Figure 24a). Despite of the presence of illite-muscovite in the difractogram of this individual the 10 Ǻ peak of this crystalline phase is already decomposed. The partial descomposition of illite-muscovite, which probably corresponds not only to the clay but also to micas (muscovite plates) in this case, as the peaks are too sharp to represent only the clay, and the obvious presence of spinel in the ceramic paste, under an advanced stage of development, indicates a EFT in the rang of 950/1000°C, that is because micas withstand relatively high temperatures. On the other hand, the total decomposition of illite-muscovite in the difractogram of TRZ170 (Figure 24b) and the even sharper peaks of spinel situate the EFT of this individual over 1000°C, possibly between 1050°C and 1100°C.

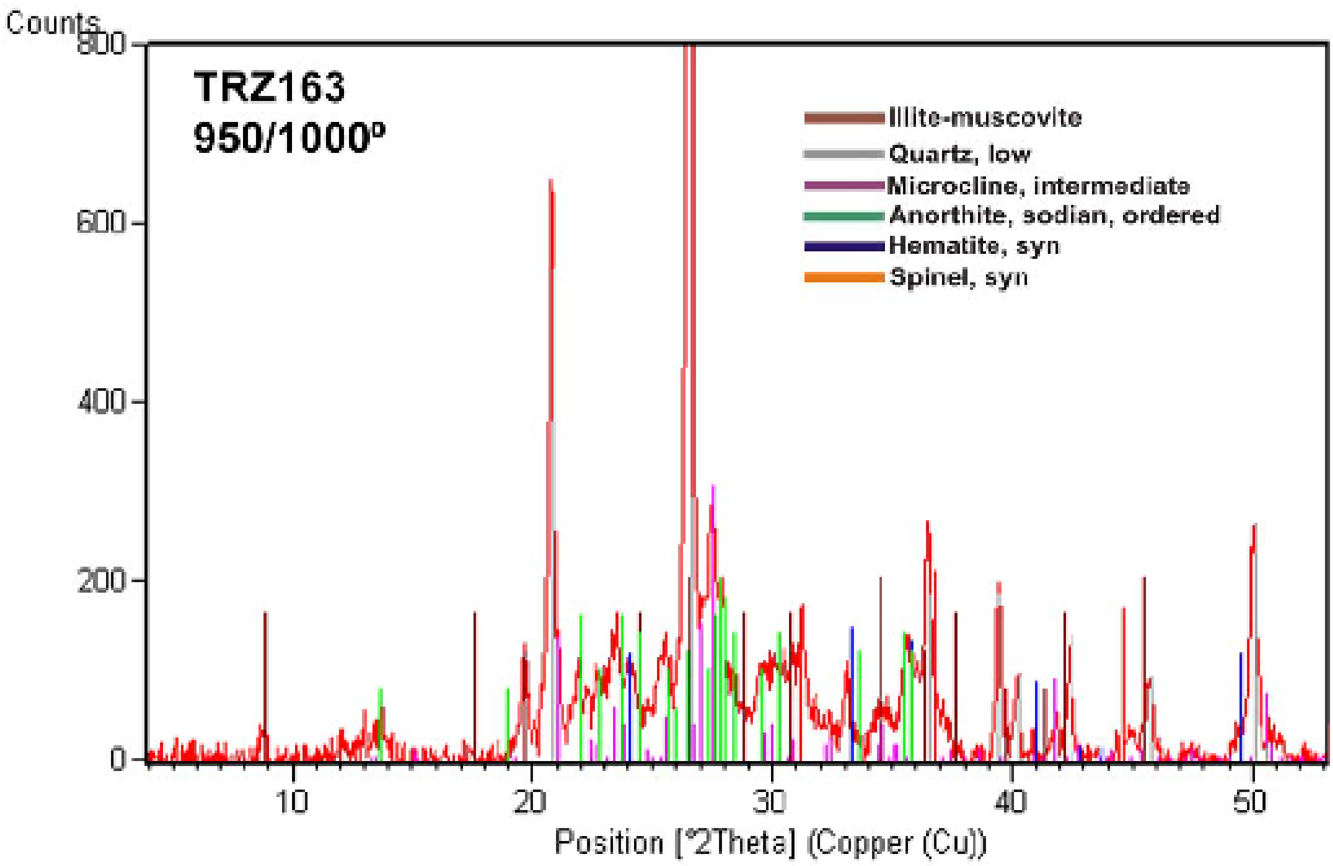

Figure 24a: Difractograms of the individuals TRZ163 and TRZ 170, representing the chemical group $TRZ_{(A)}$

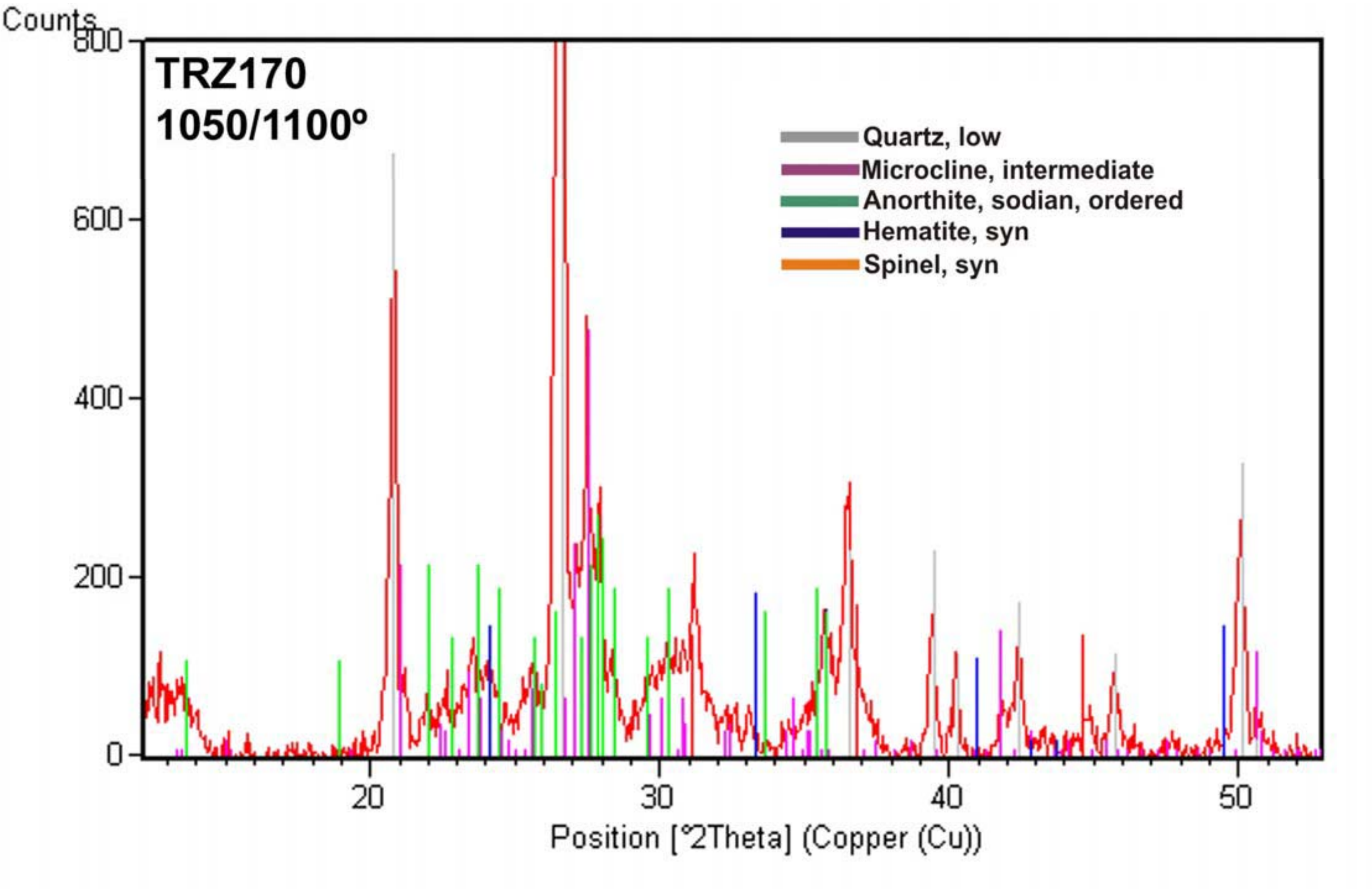

Figure 24b: Difractograms of the individuals TRZ163 and TRZ 170, representing the chemical group $TRZ_{(A)}$

Firing temperature and mineralogical aspects of ceramics from $TRZ_{(B)}$ **group**

The three individuals belong to this group correspond to two different mineralogical category associated to two different Equivalent Firing Temperature (EFT). TRZ172 (Figure 25) and TRZ187 both are characterised by the presence of clear primary (illite-muscovite, alkaline feldspars and according to petrography plagioclase here is primary) but not clear firing phases (gehlenite or pyroxene) which indicates low firing temperature. The EFT of both individuals can be estimated in the rang of 800/850°C. On the other hand, TRZ182 (Figure 25) difractogram shows the total decomposition of the illites-muscovite, which in these fabrics correspond mostly to micas, that decompose at higher temperature compared to the clay which decomposed at 950/1000°C and the sharp peaks of pyroxene with the additional absence of intermediate firing phases like gehlenite that has already decomposed, situate the EFT of this individual over 1000, possibly between 1050°C and 1100°C.

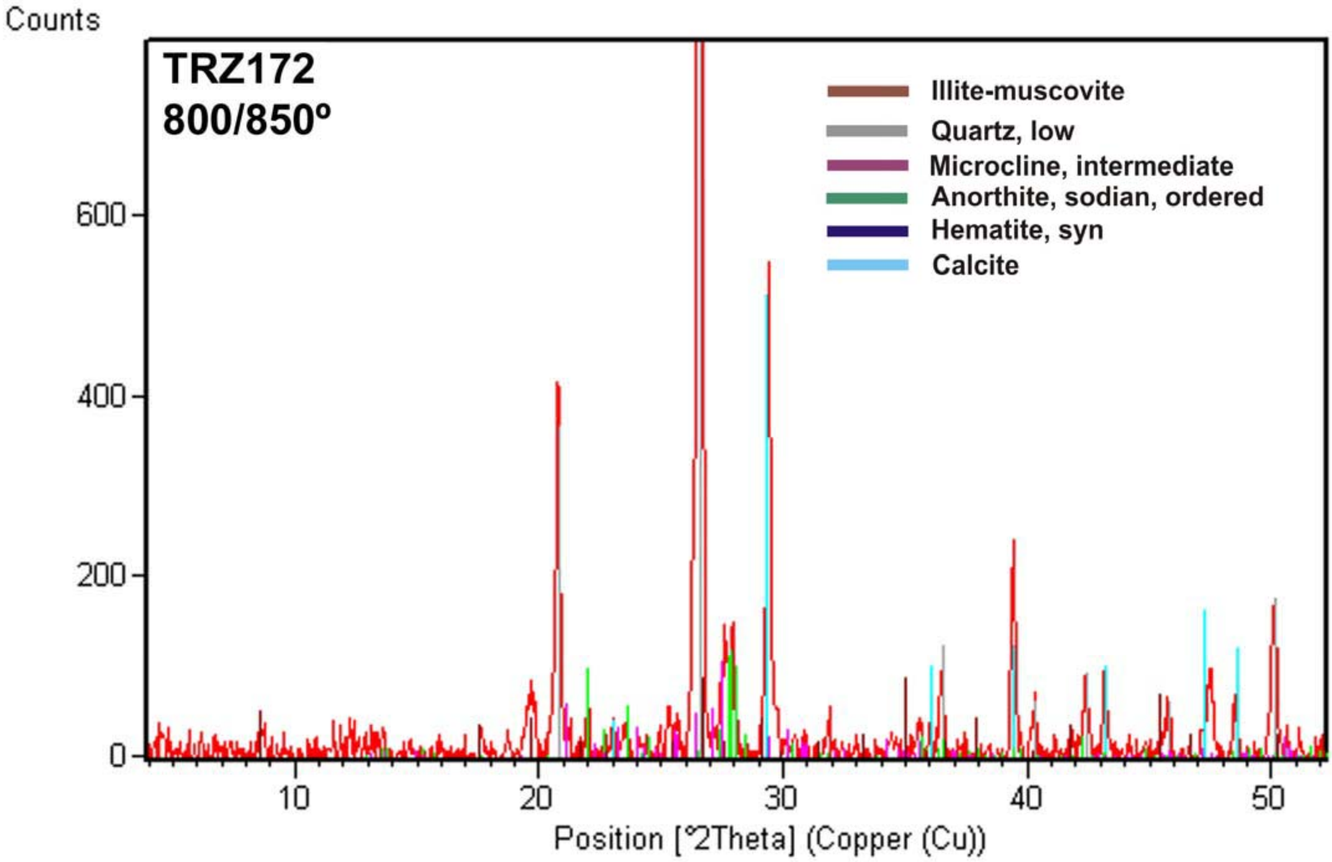

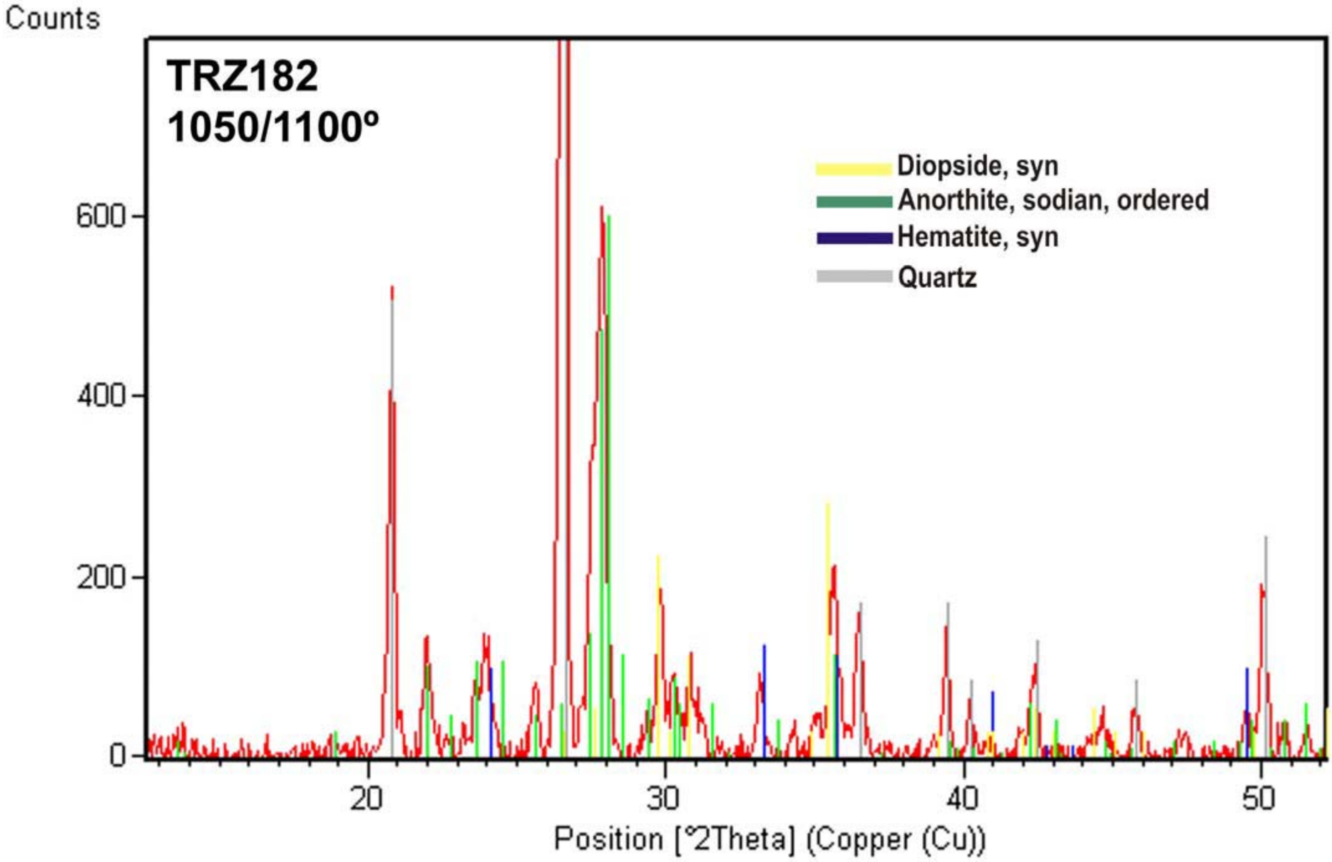

Figure 25: Difractograms of the individuals TRZ172 and TRZ 182, representing the chemical group TRZ$_{(B)}$

Firing temperature and mineralogical aspects of ceramics from AC group

The nine individuals that identified into **AC** represent three different EFT and mineralogical categories. In the difractogram of TRZ151 (Figure 26a), which represent only the 11% of AC, the presence of clear primary mineral phases (illite-muscovite, alkaline feldspars and plagioclase that according to petrography is primary) but not clear firing phases (gehlenite or pyroxene) can be observed . This indicates a firing temperature between 800°C and 850°C. On the other hand, TRZ147 (Figure 26b) and TRZ155 (22%) are both characterised by the simultaneous presence of primary (illite-muscovite) and firing phases (pyroxene and gehlenite), which indicates relatively high firing temperature. The obvious presence of gehlenite and mostly pyroxene as this last one is a crystalline phase which develops visibly under high temperatures in the ceramic paste indicates a EFT around 950/1000°C. The descomposition of illite-muscovite still did not take place because the illite-muscovite peaks in the difractograms of these individuals correspond mostly to micas. Finally the 67% of the individuals of AC (TRZ145, TRZ146, TRZ148, TRZ150, TRZ153 and TRZ154) correspond to overfired ceramics (Figure 26c) . The almost total decomposition of the illites-muscovites and the intense peaks of pyroxene with the additional absence of gehlenite, that has already decomposed, situate the EFT of these individuals over 1000 °C, possibly between 1050°C and 1100°C.

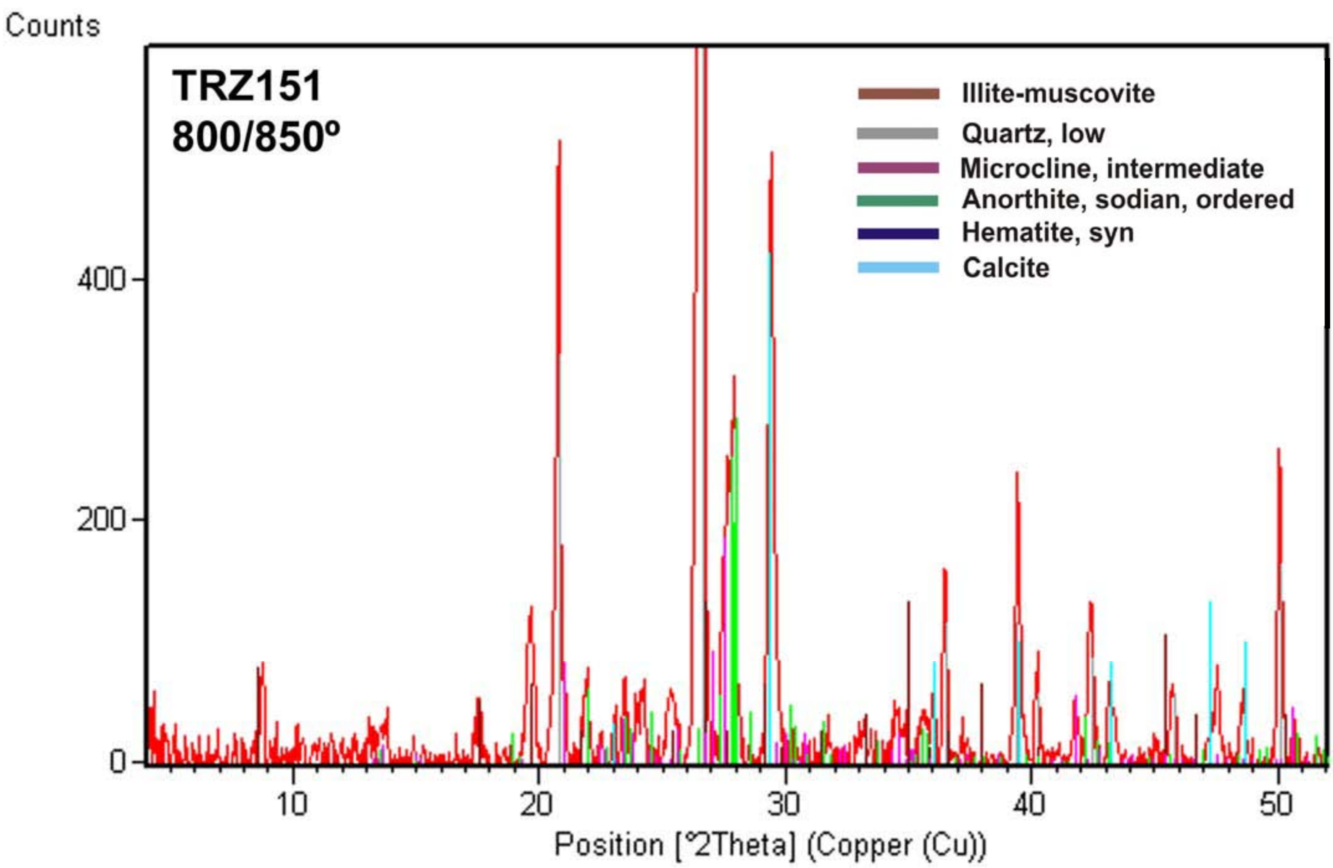

Figure 26a: Difractograms of the individuals TRZ151 TRZ147 and TRZ153, representing the chemical group AC

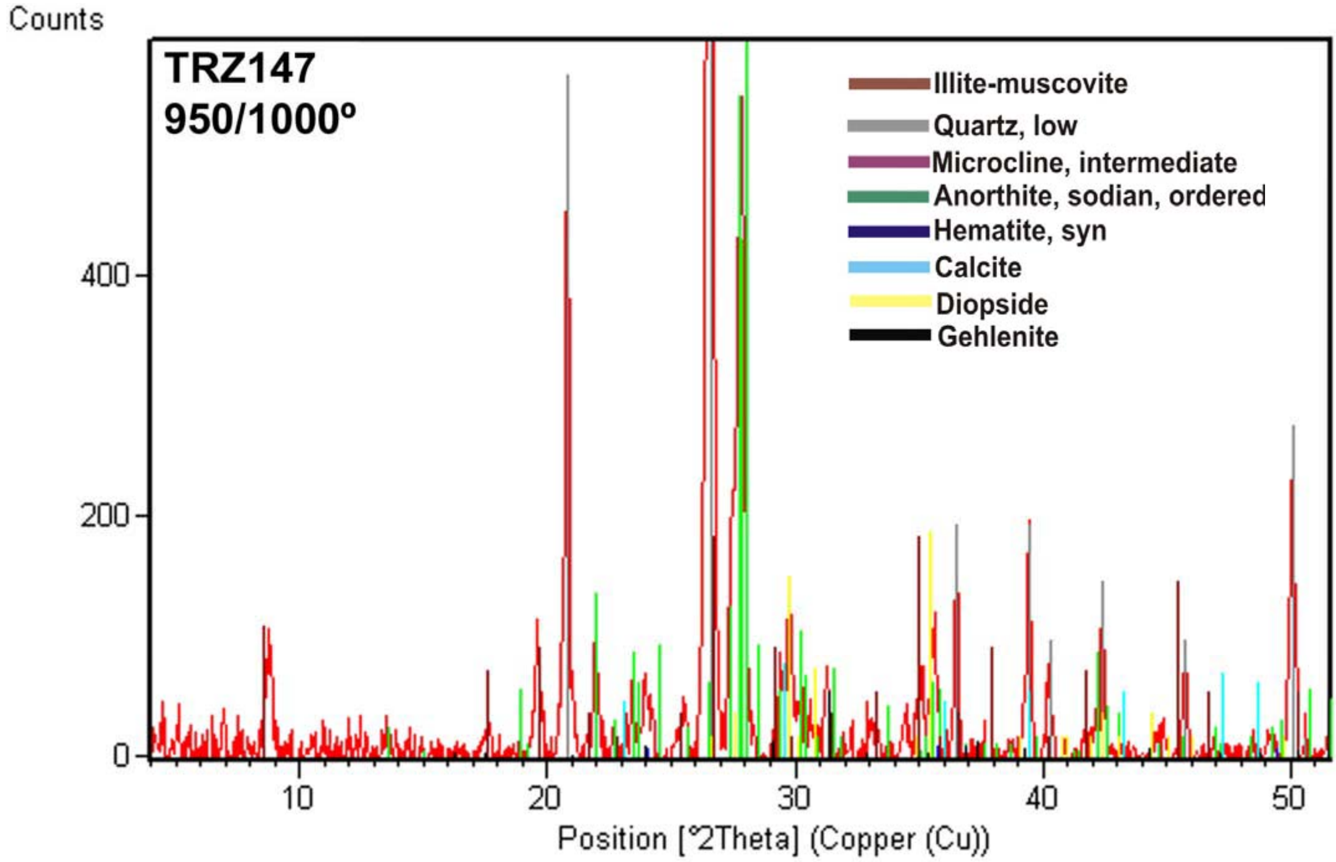

Figure 26b: Difractograms of the individuals TRZ151 TRZ147 and TRZ153, representing the chemical group AC

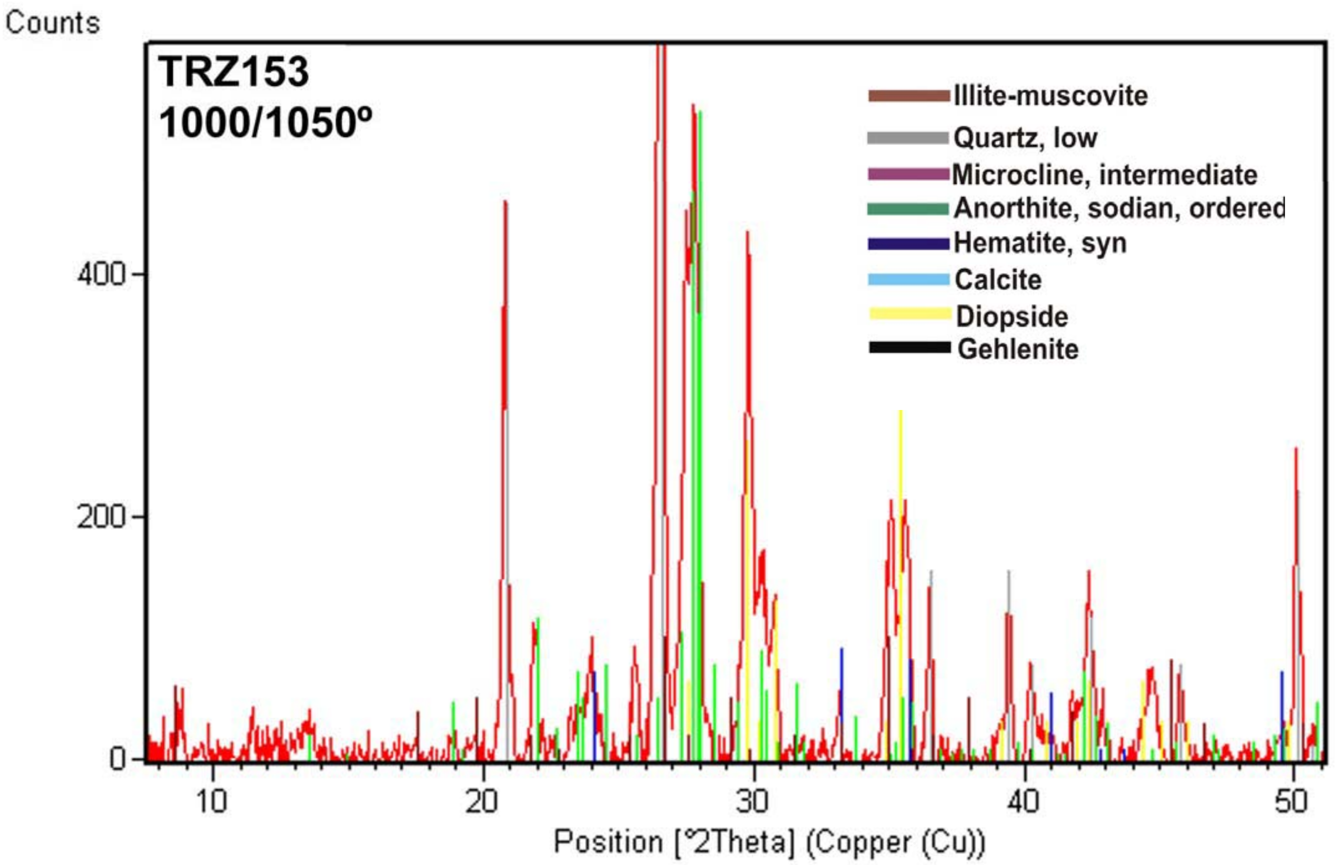

Figure 26c: Difractograms of the individuals TRZ151 TRZ147 and TRZ153, representing the chemical group AC

Firing temperature and mineralogical aspects of ceramics from Expanded F2 **group or Kara Tepe's Kilns RG**

According to the mineralogical analysis, the 36 individuals that configure **F2** or the RG of ***Kara Tepe's Kiln Site*** can be separate into three basic mineralogical fabrics. The first fabric that contains two individuals: TRZ039 and TRZ042 (Figure 27) is characterised by the presence of primary mineral phases and the total absence of clear firing phases. Therefore, the Equivalent Firing Temperature (EFT) estimated for this category is around the 800/850°C and it corresponds to a low fired material. In the second fabric the coexistence of primary phases, like illite-muscovite and alkaline feldspars, and clear firing phases, like gehlenite and pyroxenes can be observed. Therefore, the individuals that belong to this fabric are: TRZ013, TRZ022, TRZ023 (Figure 27), TRZ024, and TRZ031. the EFT estimated for this fabric is between 950°C and 1000°C. Finally, the last mineralogical category is characterised by the

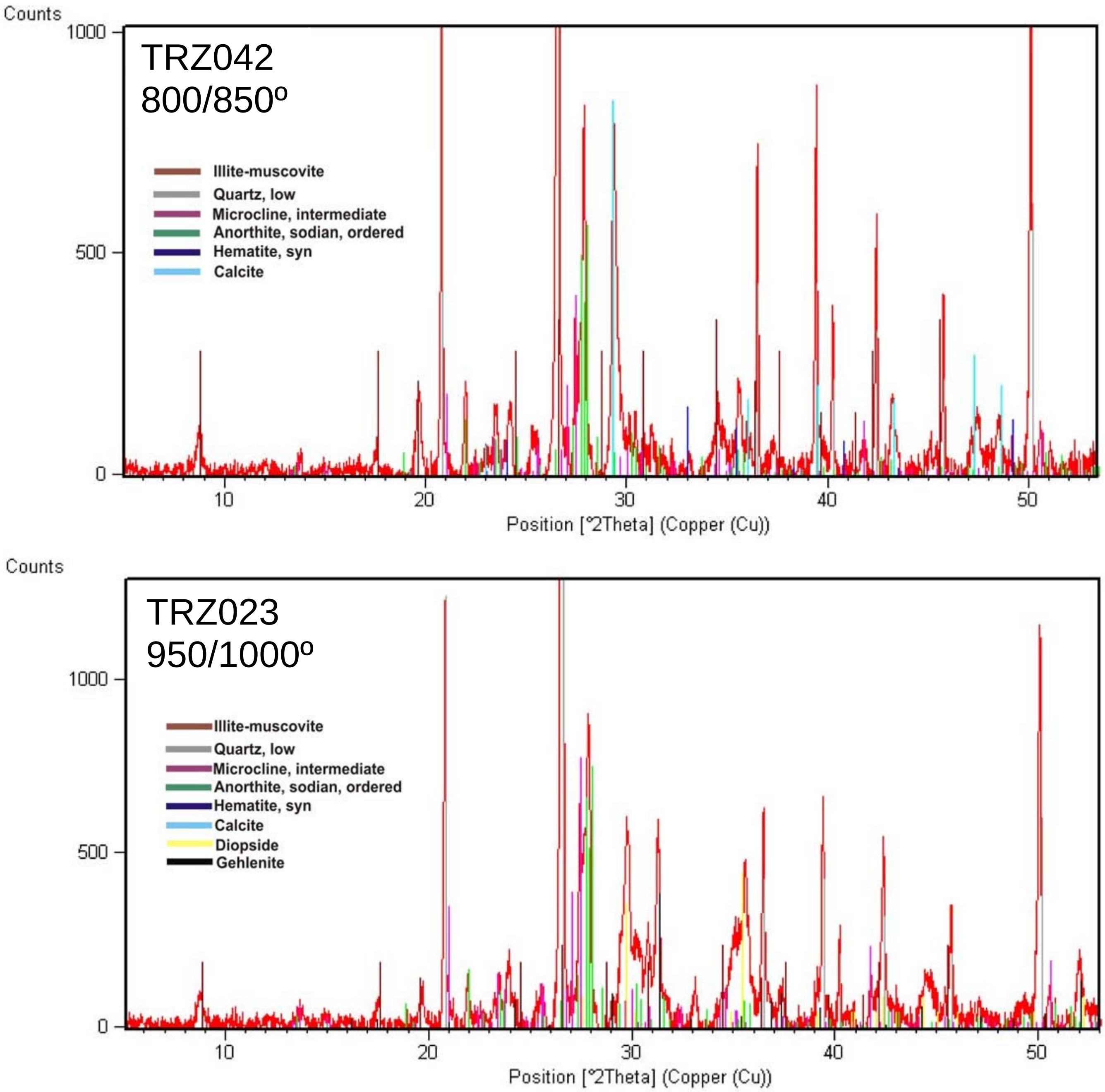

Figure 27: Difractograms of the individuals TRZ042 and TRZ023, representing the chemical group F2

advanced decomposition of illite-muscovite and gehlenite and the total decomposition of calcite with the parallel clear increment of the pyroxenes as a firing phases of a high temperature. Consequently, this fabric represents over fired ceramics, its ETF can be estimated in the rang of 1050/1110°C and it includes TRZ001, TRZ003, TRZ008, TRZ009, TRZ012, TRZ014, TRZ015, TRZ016, TRZ017, TRZ018, TRZ021, TRZ025, TRZ026, TRZ029 (Figure 28), TRZ030, TRZ031, TRZ032, TRZ033, TRZ034, TRZ035, TRZ036, TRZ037, TRZ038, TRZ040 and TRZ041. Two of them, TRZ033 and TRZ037 (Figure 28) present also analcime in their difractogram. Analcyme is a zeolith which forms as a result of a post-depositional alteration and/or contamination in the pores of a normally high/over fired calcareous ceramics. The presence of analcime justifies the lower concentrations of K_2O and Rb and higher concentrations of Na_2O in these two individuals.

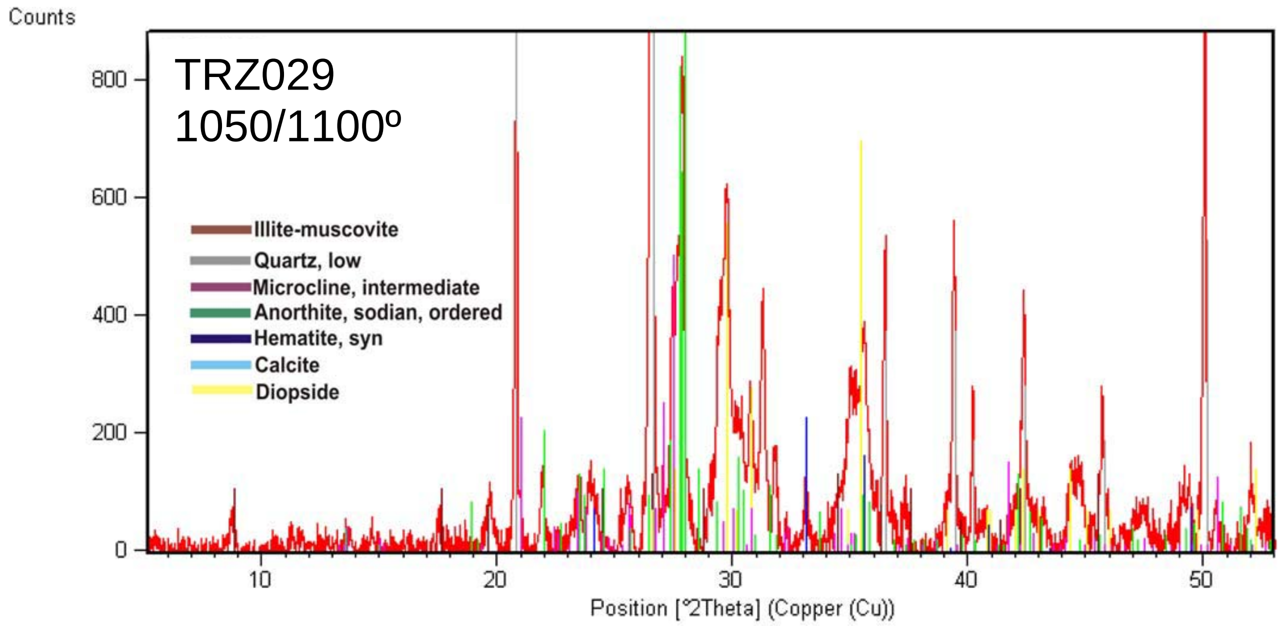

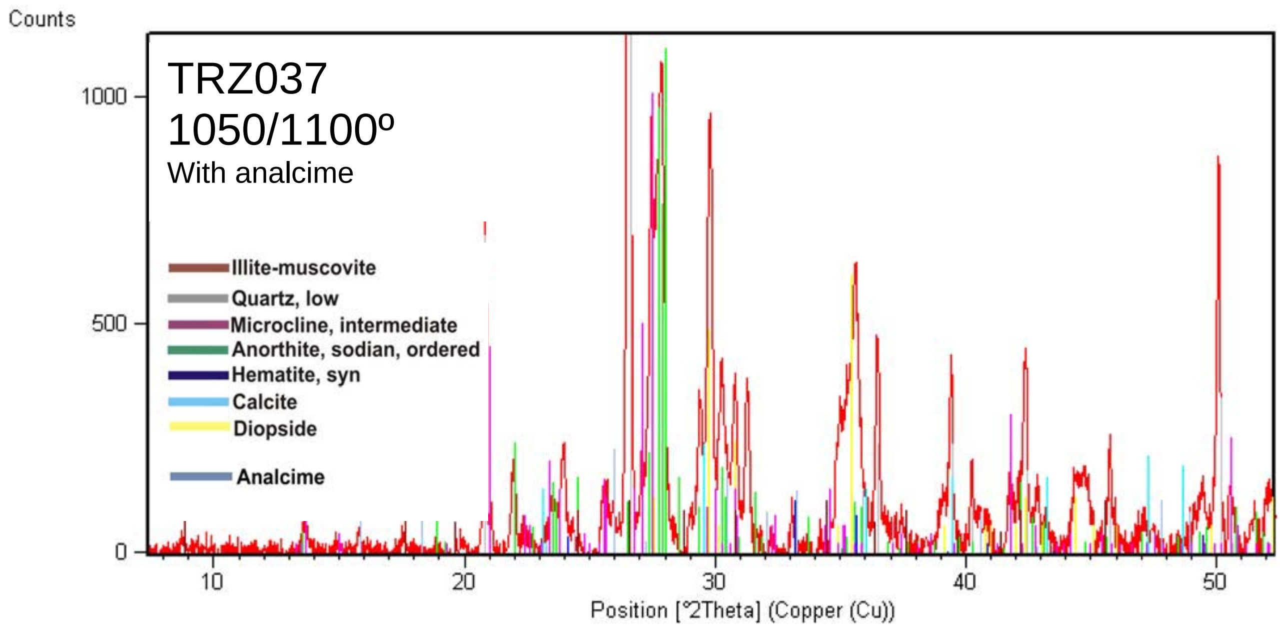

Figure 28: Difractograms of the individuals TRZ029 and TRZ037, representing the chemical group F2

It is important to mention that in all the mineralogical fabrics the presence of hematite is obvious. Hematite is an iron oxide which develops under preferably oxidising atmospheres. Another observation can be made is that during firing in ancient kilns the firing temperature in the laboratory can vary ±150°C depending on the position of the ceramic. Specifically, the temperature is always higher in the central part of the kiln than in the sites. Thus, an EFT estimated in between approximately 850°C and 1000°C, can represent the same firing procedure. That is why, in the case of the Kushan ceramic analysed sampled at the kiln site of ***Kara Tepe***, we can say that even though, there are three different mineralogical fabrics determined according to the mineral phases identified, the process of manufacture of this ceramics is very constant and generally they represent a high fired ceramic material.

Firing temperature and mineralogical aspects of ceramics from TRZ **group**

According to the mineralogical analysis, the 99 individuals representing the group **TRZ** can be divided into four mineralogical categories. The first contains the individuals: TRZ080, TRZ089, TRZ166 (Figure 29), TRZ179, TRZ184 and TRZ202 and it is characterised by the presence of primary mineral phases and the total absence of clear firing phases. The EFT estimated for this category is 800/850°C, wich corresponds to a low firing temperature. In the second category, the coexistence of primary phases, like illite-muscovite and alkaline feldspars, and firing phases in the initial phase of development, like gehlenite and pyroxenes can be observed. Therefore, the EFT of this category is around 850/950°C. This category is configured by TRZ051, TRZ052, TRZ055, TRZ064, TRZ085, TRZ086, TRZ103, TRZ105, TRZ138, TRZ141 TRZ144 TRZ160 TRZ164 (Figure 29), TRZ169 and TRZ178. In the third category, the development of the firing phases is much more advanced but the existence of illite-muscovite in the difractograms of the individuals in this category indicate a EFT between 950°C and 1000°C.The individuals that belong to this fabric are: TRZ053, TRZ065, TRZ066, TRZ070,TRZ078, TRZ092, TRZ093, TRZ126, TRZ128, TRZ129, TRZ130, TRZ133, TRZ143, TRZ157, TRZ158, TRZ173, TRZ174, TRZ175, TRZ181 (Figure 30), TRZ190, TRZ192, TRZ193, TRZ195, TRZ196, TRZ197, TRZ198, TRZ199 and TRZ201. Finally, the last mineralogical category is characterised by the advanced decomposition of illite-muscovite and gehlenite and the total decomposition of calcite with the parallel clear increment of the pyroxenes as a firing phase of a high temperature. Consequently, this fabric represents over fired ceramics, its ETF can be estimated in the rang of 1050/1110°C and it includes TRZ044, TRZ047, TRZ048, TRZ056, TRZ059, TRZ071, TRZ072, TRZ073, TRZ074, TRZ075, TRZ076, TRZ079, TRZ082, TRZ083, TRZ090, TRZ091, TRZ094, TRZ095, TRZ101, TRZ117, TRZ119, TRZ121, TRZ124, TRZ128, TRZ132, TRZ134, TRZ136, TRZ139, TRZ141, TRZ165, TRZ167 (Figure 31), TRZ168, TRZ176, TRZ177, TRZ183 (Figure 31), TRZ185, TRZ188 (reduction atmosphere), TRZ194 and TRZ200. Moreover, TRZ056, TRZ071, TRZ079, TRZ083, TRZ119, TRZ183 and TRZ200 present also analcime in their difractogram.

To conclude, the same way that in the case of **F2**, the process of manufacture of these ceramics is very constant and they represent a generally high fired ceramic material. A firing predominantly under oxidising atmosphere can be identified on the base of the mineralogical study.